Technische Universität München

Wissenschaftszentrum Weihenstephan für Ernährung, Landnutzung und Umwelt

Fachgebiet Biotechnologie gartenbaulicher Kulturen

Characterization of the AMP1 regulatory network in the control of shoot meristem function in Arabidopsis

Saiqi Yang

Vollständiger Abdruck der von der Fakultät Wissenschaftszentrum Weihenstephan für Ernährung, Landnutzung und Umwelt der Technischen Universität München zur Erlangung des akademischen Grades eines

Doktors der Naturwissenschaften

genehmigten Dissertation.

Vorsitzende(r): Prof. Dr. Kay H. Schneitz

Prüfer der Dissertation:

1. Prof. Dr. Brigitte Poppenberger-Sieberer
2. apl. Prof. Dr. Ramón A. Torres Ruiz

Die Dissertation wurde am 31.08.2017 bei der Technischen Universität München eingereicht und durch die Fakultät Wissenschaftszentrum Weihenstephan für Ernährung, Landnutzung und Umwelt am 14.11.2017 angenommen.

Abstract

In plants, new organs are repeatedly initiated during postembryonic development, due to self-renewing division and differentiation of stem cells. The stem cells responsible for shoot growth reside in the shoot apical meristem (SAM). Correct SAM organization requires the maintenance of a stem cell population in the central zone of the meristem, and coordinated differentiation of stem cell descendants in the meristem periphery. In Arabidopsis, the putative carboxypeptidase ALTERED MERISTEM PROGRAM1 (AMP1) is required for radial SAM organization by suppressing stem cell identity in the meristem periphery. AMP1 has been shown to mediate the translational repression of miRNA targets. Such targets include Class III Homeodomain Leucine Zipper (HD-ZIP III) transcription factors, which determine SAM identity and organization.

The first part of this work analysed whether the *amp1*-related defects in SAM organization are mediated by an increased translation of HD-ZIP III family members. Consistent with enhanced HD-ZIP III activity the direct target *LITTLE ZIPPER3* (*ZPR3)* was upregulated in *amp1*. Ubiquitous increase of HD-ZIP III activity in *zpr3 zpr4* caused peripheral stem cell formation as in *amp1*. Moreover, *zpr3 zpr4* and *amp1* genetically interacted in a strong synergistic manner in respect to SAM malformation, whereas reduction of HD-ZIP III activity by *ZPR3* overexpression could partially suppress these defects in *amp1*. By monitoring the tissue-specific expression of YFP-tagged HD-ZIP III members, an increase of HD-ZIP III protein abundance in *amp1* was observed, however without a significant alteration in their spatial distribution, which is specified by miRNAs 165/166. These results suggest that AMP1 controls SAM organization by limiting HD-ZIP III expression in a quantitative but not spatial manner.

The second part of this study showed that AMP1 also functionally interacts with the AP2/ERF transcription factor RAP2.6L. *RAP2.6L* transcription was increased in *amp1* and overexpression of *RAP2.6L* in wild type caused *amp1*-related SAM phenotypes and SAM marker misexpression. Conversely, perturbation of *RAP2.6L* function in *amp1* suppressed the SAM hypertrophy, accelerated leaf initiation as well as the increased shoot regeneration capacity of the mutant. Moreover, AMP1 appears to control SAM activity by limiting *RAP2.6L* expression in a HD-ZIP III-dependent manner. Taken together, the work identified and characterized two components, which act downstream of AMP1 in the control of SAM activity.

Zusammenfassung

Die kontinuierliche Teilung und Differenzierung von Stammzellen ermöglicht Pflanzen die fortlaufende Ausbildung neue Organe nach der Keimung. Die Stammzellen für die Entwicklung von Sprossorganen befinden sich im Sprossapikalmeristem (SAM). Zur korrekten Funktion des SAMs muss einerseits eine Stammzellpopulation in der zentralen Zone des Meristems beibehalten werden und andererseits eine kritische Anzahl an Tochterzellen in der Meristem-Peripherie differenzieren. In Arabidopsis unterdrückt die vermeintliche Karboxypeptidase ALTERED MERISTEM PROGRAM1 (AMP1) Stammzellidentität in der Meristem-Peripherie und trägt somit zur radialen Organisation des Meristems bei. Auf biochemisch noch nicht geklärte Weise vermittelt AMP1 die Translationshemmung von miRNA-bindenden Transkripten. Dazu gehören mRNAs der Class III Homeodomain Leucine Zipper (HD-ZIP III) Transkriptionsfaktor-Familie, die eine zentrale Rolle in der Bildung und Organisation von Sprossmeristemen spielen.

Im ersten Teil dieser Arbeit wurde analysiert, ob die SAM-Defekte der *amp1*-Mutante durch die erhöhte Translationsrate von HD-ZIP III Proteinen verursacht werden. Übereinstimmend mit einer vermehrten Aktivität dieser Transkriptionsfaktoren war die Expression des HD-ZIP III-regulierten *LITTLE ZIPPER3 (ZPR3)* Gens in *amp1* induziert. Eine generelle Steigerung der HD-ZIP III Proteinfunktion durch Inaktivierung von *ZPR3* und *ZPR4* führte zu einer Re-Etablierung von Stammzellidentität in der Meristem-Peripherie wie in der *amp1* Mutante. Außerdem zeigten *zpr3 zpr4* und *amp1* eine starke genetische Interaktion bezüglich Missbildung des SAMs, wohingegen eine Senkung der HD-ZIP III Aktivität durch *ZPR3* Überexpression diesen Defekt abschwächte. Durch mikroskopische Analyse eines YFP-markierten HD-ZIP III Proteins konnte dessen gewebsspezifische Expression in *amp1* bestimmt werden. Die Reporterexpression war in der Mutante erhöht jedoch kam es zu keiner räumlichen Ausbreitung der Expressionsdomäne, die durch die miRNAs 165/165 definiert ist. Diese Analysen weisen darauf hin, dass AMP1 die SAM-Organisation durch quantitative aber nicht räumliche Einschränkung der HD-ZIP III Expressionsstärke beeinflusst.

Im zweiten Teil dieser Studie konnte eine funktionelle Wechselwirkung zwischen AMP1 und dem AP2/ERF Transkriptionsfaktor RAP2.6L nachgewiesen werden. *RAP2.6L* zeigte eine erhöhte Transkription in *amp1* und Überexpression dieses

Faktors in Wildtyp führte zu *amp1*-artigen SAM-Phänotypen und einer veränderten Expression von SAM-Markern. Hingegen unterdrückte eine Einschränkung der RAP2.6L Funktion die SAM-Hypertrophie, die beschleunigte Blattbildungsrate als auch die erhöhte Sprossregenerationsrate der *amp1* Mutante. Zudem scheint die verstärkte *RAP2.6L* Expression in *amp1* durch die erhöhte HD-ZIP III Aktivität in der Mutante zustande zukommen. Zusammenfassend führte diese Arbeit zur Identifizierung und Charakterisierung zweier Komponenten, die unterhalb von AMP1 in der Kontrolle der SAM-Aktivität agieren.

List of figures

Abbreviations

35S	35S promoter from Cauliflower Mosaic Virus
ABA	abscisic acid
AGO1	ARGONAUTE 1
AGO10, PINHEAD/ZWILLE	ARGONAUTE 10
AHK2/4	ARABIDOPSIS HISTIDINE KINASE 2/4
AMP1	ALTERED MERISTEM PROGRAM 1
AP2/ERF	APETALA 2/ETHYLENE RESPONSE FACTOR
ARR	ARABIDOPSIS RESPONSE REGULATOR
cDNA	complementary DNA
CIM	callus induction medium
CK	cytokinin
CLV1	CLAVATA 1
CLV3	CLAVATA 3
CNA	CORONA
Col-0	Columbia-0; ecotype of Arabidopsis thaliana
CUC1/2	CUP-SHAPED COTYLEDON 1/2
CZ	central zone
d	day
DAG	days after germination
de novo	anew; from the beginning
e.g.	exempli gratia = for example
EBE	ERF BUD ENHANCER
ER	endoplasmic reticulum
et al.	et alterni = and others
etc.	et cetera = and so on
g	gram
GUS	β-glucoronidase
h	hour
HD-ZIP III	class III Homeodomain Leucine Zipper
HsGCPII	human glutamate carboxypeptidase II
i.e.	id est = that is
JA	jasmonic acid
L	liter
LAMP1	LIKE AMP1
Ler	Landsberg erecta; ecotype of Arabidopsis thaliana
miRNA	micro RNA

mM	millimolar
MP	MONOPTEROS
mRNA	messenger RNA
MS	Murashige and Skoog medium
NAAG	N-acetyl-L-aspartyl-L-glutamate
NAALADase	N-acetylated-alpha-linked acidic dipeptidase
nm	nanometer
OC	organizing center
PCR	polymerase chain reaction
PHB	PHABULOSA
PHV	PHAVOLUTA
PLT	PLETHORA
PSMA	prostate specific membrane antigen
PZ	peripheral zone
qPCR	quantitative real-time PCR
REV	REVOLUTA
RISC	RNA-induced silencing complex
RZ	rib zone
SDS	sodium dodecyl sulfate
SAM	shoot apical meristem
SEM	scanning electron microscope
SIM	shoot induction medium
STM	SHOOTMERISTEMLESS
WIND	WOUND INDUCED DEDIFFERENTIATION
WT	wild type
WUS	WUSCHEL
ZPR	LITTLE ZIPPER
µl	microliter
µM	micromolar
µm	micrometer

I. Introduction

1. Structure and function of the shoot apical meristem

In higher plants, meristems are small domains of undifferentiated cells in the shoot or root apices, which contain pluripotent stem cells that are committed to form new organs reiteratively. In the eudicot model plant *Arabidopsis thaliana*, the meristem located in the central region of the shoot apex is called shoot apical meristem (SAM). It is formed during embryo development and except for the cotyledons and hypocotyl, the SAM is responsible for all the above ground tissues including leaves, stems and flowers throughout post-embryonic growth.

There are three anatomically distinct cell layers in the SAM (L1-L3; Figure 1). The L1 and L2 are single layers of cells and divide in an anticlinal manner in parallel with the meristem surface. The L3 layer includes the rest of the meristem and cells within this layer divide into all directions (Barton, 2010; Galli and Gallavotti, 2016).

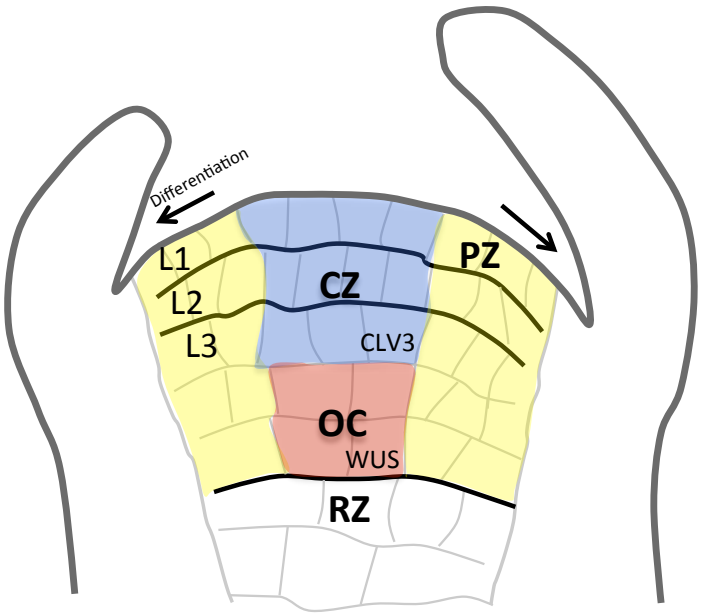

Figure 1. Schematic structure of Arabidopsis shoot apical meristem

The Arabidopsis shoot apical meristem (SAM) consists of three distinct cellular layers (L1-L3). Cells in L1 and L2 only divide anticlinally, while L3 cells divide into all directions. According to divergent gene expression patterns and functions, the SAM can be divided into four developmental zones, including a stem-cell-containing central zone (CZ, blue) marked by CLV3 expression, a WUS-expressing organizing center (OC, red) responsible for maintaining stem cell identity in the CZ, a lateral-organ-initiating peripheral zone (PZ, yellow) and a rib zone (RZ) responsible for forming internal tissues.

Functionally, the SAM can also be divided into different areas including central zone (CZ), organizing center (OC), peripheral zone (PZ) and rib zone (RZ) (Figure 1). The CZ contains the stem cell pool and lies in the top central area of the meristem. The stem cells in the CZ divide infrequently, and the generated progeny cells are either recruited to the PZ, where they proliferate and form lateral primordia, or displaced into the RZ to give rise to the internal tissues (Meyerowitz, 1997; Heidstra and Sabatini, 2014; Soyars et al., 2016). At a later stage of plant growth, additional axillary meristems (AM) are initiated in Arabidopsis. These laterally located, post-embryonically formed meristems are responsible for the formation of secondary rosettes. Furthermore, along with the phase transition from vegetative growth to reproductive growth, the SAM converts into the inflorescence meristem (IM) which gives rise to floral tissues (Galli and Gallavotti, 2016).

1.1 Control of the stem cell pool size

Since the SAM is of great significance to the adaptive growth and development of plants, the meristem size is stably maintained via a sophisticated control of cell division. On the one hand, the stem cells need to divide and sustain a certain size of the stem cell pool so that the SAM does not loose its proliferative potency prematurely; on the other hand, the stem cells also need to differentiate continuously in adaption to the requirement of plant growth and environment change. The maintenance of this delicate balance between proliferation and differentiation relies on intercellular communication between OC and CZ and one important regulatory pathway controlling this process is the WUSCHEL/CLAVATA (WUS/CLV) feedback regulation loop.

The *WUS* gene encodes a homeodomain transcription factor that is important for promoting stem cell identity. Although expressed in the OC, WUS is able to migrate to the CZ through plasmodesmata, and activates CLV3 expression in the CZ in a non-cell-autonomous manner (Yadav et al., 2011). The secreted CLV3 protein is modified to the small CLV3p peptide and diffuses to the OC, where it is perceived by the extracellular domain of the leucine-rich repeat kinase receptors (LRR-RKs) CLV1 and CLV2. Then an intracellular signal cascade is triggered and in turn represses *WUS* expression in the OC (Mayer et al., 1998; Brand et al., 2000; Schoof et al., 2000; Yadav et al., 2011; Daum et al., 2014). Consistent with their roles in SAM

maintenance, the most severe *wus* mutant failed to develop any post-embryonic organ (Mayer et al., 1998), whereas *clv* mutants exhibit enlarged SAM sizes (Brand et al., 2000).

The understanding of this feedback loop was deepened by characterization of other components that contribute to this pathway. Recently, it was found that multiple HAIRY MERISTEM (HAM) transcriptional regulators interact with WUS and function as cofactors in regulating many downstream genes and promoting stem cell proliferation in the SAM (Zhou et al., 2015). Besides CLV1/CLV2, more receptors were found to be involved in the perception of CLV3 peptide. The putative receptor-like kinase CORYNE associates with CLV2 and functions as a co-receptor (Müller et al., 2008). BARELY MERISTEM (BAM) 1, 2 and 3 are CLV1-related receptor kinases that function partially redundant to CLV1 (Nimchuk et al., 2015). In parallel to CLV1/CLV2, RECEPTOR-LIKE PROTEIN KINASE 2 (RPK2) is also involved in transmitting CLV3 signal in Arabidopsis (Kinoshita et al., 2010).

Maintenance of the stem pool size also requires the control of bHLH transcription factor HECATE1 (HEC1) (Schuster et al., 2014). As a direct target of WUS, HEC1 expression is present in the SAM while specifically excluded from the OC area probably by WUS function. In association with another bHLH protein SPATULA, HEC1 promotes stem cell proliferation and functions antagonistically to CLV3. Interestingly, HEC1 also reversely interferes with WUS expression in the OC via controlling the response of the phytohormone cytokinin, indicating a highly complicated regulatory framework in SAM regulation by these two transcription factors.

1.2 Positioning of the stem cell pool in the shoot apical meristem

The plant hormone cytokinin (CK) plays a vital role in SAM maintenance. In Arabidopsis, CK biosynthesis in the meristem is enhanced by the Class I KNOTTED1-like homeobox (KNOX) transcription factor SHOOTMERISTEMLESS (STM) and its close homologs via activation of *ISOPENTENYLTRANSFERASE (IPT)* genes, which in turn promote stem cell proliferation (Jasinski et al., 2005; Yanai et al., 2005). This mechanism was supported by the characterization of a cytokinin-activating enzyme LONELY GUY (LOG) in rice, which expresses specifically in the top cell layers of shoot meristem. The local activation of CK by

LOG is required for SAM maintenance since impaired LOG function caused SAM size reduction in the vegetative phase as well as premature termination of floral meristem (Kurakawa et al., 2007).

The role of CK in controlling SAM maintenance is largely associated with the key meristem regulator WUS. Type-A ARABIDOPSIS RESPONSE REGULATORs (ARRs) are negative CK response regulators (To et al., 2004) and WUS maintains stem cell pool activity by directly repressing the type-A ARRs in the SAM (Leibfried et al., 2005). Consistently, uncoupling the suppression of these negative CK regulators by WUS leads to the arrested SAM in the seedling. On the other hand, enhanced CK activity also promotes WUS function in the SAM. Exogenous CK treatment significantly represses *CLV1* expression (Lindsay et al., 2006; Gordon et al., 2009), and simultaneously promotes WUS activity by increasing its transcription level as well as broadening its expression domain in the meristem, in a CK receptor ARABIDOPSIS HISTIDINE KINASE 4 (AHK4)/AHK2-dependent manner (Gordon et al., 2009; Chickarmane et al., 2012). Moreover, it was shown that the HEC1-activated type-A ARR7 and ARR15 can function as mobile signals in restricting WUS expression in the OC, implying a highly dynamic role of CK in controlling meristem activity (Schuster et al., 2014).

Recently it was shown that the miRNA394 plays a vital role in SAM maintenance (Knauer et al., 2013). In the meristem, miRNA394 functions as a mobile signal, since these miRNAs are solely produced in the protoderm (L1) layer cells by the *miR394B* gene, while their localization expand inwardly to the L2 and L3 layers. The authors demonstrated that in the meristem the repression of the F box protein LEAF CURLING RESPONSIVENESS (LCR) by miRNA394 is essential for WUS to promote stem cell identity, although the function of LCR protein remains elusive.

1.3 Radial organization of the shoot apical meristem

Besides the correct positioning of the central stem cell niche, the maintenance of the meristem architecture also requires the suppression of the pluripotency in the periphery. Early study showed that ablation of the CZ in the meristem causes ectopic WUS expression as well as formation of stem cell niche in the PZ (Reinhardt et al., 2003), implying that there might be a persisting mechanism that confines OC localization in the meristem, and this mechanism can be eliminated by the absence of

the stem cell pool which leads to the reestablishment of stem cell niche in the PZ.

Factors in chromatin assembly or remodeling contribute largely in keeping this radial organization of the SAM by regulating *WUS* expression (Gaillochet and Lohmann, 2015). The SNF2-type chromatin-remodeling ATPase SPLAYED (SYD) (Kwon et al., 2005) and the Type IB DNA Topoisomerase MGOUN1 (MGO1) (Graf et al., 2010) are required for *WUS* transcription; whereas the BRUSHY1 (Takeda et al., 2004) and BRCA1-associated ring domain 1 protein (BARD1) (Han et al., 2008) were shown to confine WUS expression area within the OC. However, it is still not clear yet how the alteration on the chromatin structure controls the CZ/PZ tissue-specific patterning and reestablishment of the stem cell niche.

On the other hand, it is also vital to keep the meristem periphery cells in a undifferentiated status. A recent study indicated that besides migrating to the CZ to promote stem cell identity, the OC marker WUS is also responsible for preventing the premature cell differentiation in the PZ by transcriptional repression (Yadav et al., 2013). WUS directly binds to the promoters of the previously identified organ polarity patterning regulators e.g. *KANADI1/2* and *YABBY3* and represses their local expression. This is consistent with the computational model and live imaging observations, whereas how WUS exerts this non-cell-autonomous repression in the PZ that differs from its promoting role in the CZ still remains elusive. Conversely, the expression of YABBY proteins especially YABBY3 and FIL in the differentiating organ primordia is also required for correct SAM organization, by restricting the expression areas of WUS and CLV3 in the meristem (Goldshmidt et al., 2008).

1.4 HD-ZIP III proteins determine the radial organization of the SAM

Class III Homeodomain Leucine Zipper (HD-ZIP III) proteins are important regulators that function in many developmental processes, including embryo shoot-root polarity patterning, meristem organization, lateral organ adaxial-abaxial/dorsal-ventral polarity establishment and vasculature development. In Arabidopsis, there are five members in the HD-ZIP III subfamily: REVOLUTA (REV), PHAVOLUTA (PHV/ATHB 9), PHABULOSA (PHB/ATHB 14), CORONA (CNA/ATHB15/INCURVATA 4) and ATHB8.

During embryogenesis, HD-ZIP III proteins function in specifying the shoot/apical identity in an antagonistic manner to the basal/root identity master regulators

PLETHORA1/2 (PLT) (Smith and Long, 2010). Starting from the heart stage, these transcription factors are activated in the apical domain of the embryo and show an adaxialized expression pattern (Prigge et al., 2005; Williams, 2005; Smith and Long, 2010), which is required for limiting *PLT1/2* expression in the shoot apical domain. Conversely, together with miRNA165/166, PLT1/2 also excludes HD-ZIP III expression from the root meristem. In extreme cases, when *HD-ZIP III* genes are missexpressed in the basal part, a second shoot pole is induced instead of the root pole. Moreover, when REV is misexpressed in the basal domain of the embryo, the OC marker gene *WUS* and the cotyledon primordia marker gene *AINTEGUMENTA (ANT)* are also induced in the presumptive second shoot position, supporting a precedent role of HD-ZIP III genes over these two marker genes in shoot development. Consistently, high order HD-ZIP III mutants showed highly defective shoot architecture, in most severe cases only formed a radialized pin-like structure that lacks meristem and cotyledon formation (Prigge et al., 2005). Therefore, a role of HD-ZIP IIIs in determining shoot meristem specification is supported, whereas the underlying molecular mechanism only begins to become clear.

A recent study showed that in the *in vitro* tissue culture process, HD-ZIP III proteins directly interact with the cytokinin positive regulators B-type ARRs and co-activate *WUS* expression in the SAM progenitor cells (Zhang et al., 2017). However, whether HD-ZIP IIIs controls shoot meristem organization via the same pathway still needs to be tested. Alternatively, HD-ZIP III proteins, especially REV, are also involved in the establishment of the axillary meristems by directly upregulating *STM* expression level in leaf axil meristematic cells (Shi et al., 2016).

1.5 HD-ZIP III proteins control diverse patterning processes

HD-ZIP III proteins promote the specification of the adaxial side in leaf primordia, which is the side close to the meristem and later differentiates into the upper part of the leaf. In Arabidopsis, the adaxial side of the leaf is dark-green and trichome-rich while the abaxial side shows lighter color and less trichomes. The *PHV* and *PHB* gain of function dominant mutants exhibit adaxial characters in the abaxial side of the leaf, and in extreme cases, the leaves are pod-like or trumpet-like shaped (McConnell and Barton, 1998; McConnell et al., 2001). Further studies showed that HD-ZIP III proteins also promote xylem proliferation in the vascular bundle and cotyledon, and

these functions are antagonistically regulated by the GARP transcription factors KANADI (Emery et al., 2003). A recent study indicated that this antagonistic effect of these two families of transcription factors is likely due their opposite roles in auxin accumulation, distribution and responses, especially in embryo development (Huang et al., 2014). Additionally, the YABBY transcription regulators (Bowman, 2000; Sarojam et al., 2010) and the ASYMMETRIC LEAVES 1/2 (Xu et al., 2003; Li et al., 2005) are also involved in determining the leaf polarity fate.

1.6 HD-ZIP III activity is controlled at different regulatory levels

HD-ZIP III proteins contain three major domains, a HD-ZIP domain for DNA binding and protein-protein interaction, a START domain that putatively binds lipids or sterols and a MEKHLA/PAS domain. In line with the protein structure, the activity of HD-ZIP III is tightly modulated by several pathways.

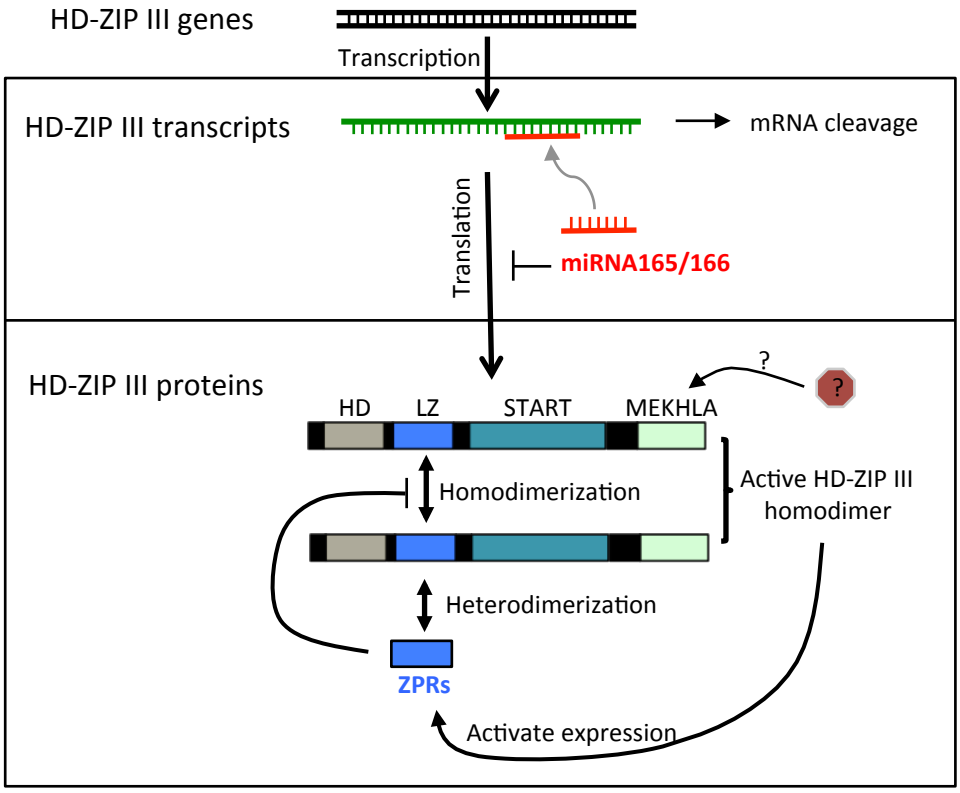

Figure 2. Simplified schematic representation of mechanisms controlling HD-ZIP III activity

On the post-transcription level, miRNA165/166 inhibit HD-ZIP III expression via mRNA cleavage as well as translation inhibition. HD-ZIP IIIs and ZPRs form a feedback regulation loop. HD-ZIP III proteins activate *ZPR* expression, while ZPR proteins block the homodimerization of HD-ZIP III protein monomers via forming non-functional heterodimers. The MEKHLA domain is also important for HD-ZIP III activity, yet the component aiming for this domain is not known.

1.6.1 HD-ZIP III transcription is restricted by miRNA165/166

Early miRNA binding site prediction analysis suggested that *HD-ZIP IIIs* are targets of miRNA165/166 (Rhoades et al., 2002). Later studies indicated that HD-ZIP III genes were indeed regulated by a miRNA-related pathway, since a silent mutation, which changed the mRNA sequence but not the protein sequence, could already cause the adaxialization phenotypes (Emery et al., 2003). Further study confirmed this result and indicated that similar to the animals, the 5' part of the miRNA165/166 contains the core sequences for pairing to *HD-ZIP III* mRNAs (Mallory et al., 2004). Interestingly, a recent study showed that in association with HD-ZIPII proteins, HD-ZIP III proteins also directly suppress the expression of *MIR165/166* genes in the adaxial side of the leaf primordia, therefore forming a bidirectional repressing circuit in controlling leaf polarity patterning (Merelo et al., 2016).

The transcript cleavage function of miRNAs requires the formation of the RNA-induced silencing complexes (RISCs), and one important factor is the PAZ domain protein ARGONAUTE1 (AGO1) (Kidner and Martienssen, 2004). A previous study indicated that AGO1 is also required for the abaxial distribution of the miRNA165 transcripts (Lynn et al., 1999). *ago1* mutant shows radialized localization of both miRNA165 and *HD-ZIP III* transcripts resulting in severe adaxialized leaves and in extreme cases radialized organs, which are reminiscent of the miRNA-insensitive *phb-d* or *phv-d* seedlings.

In contrast to AGO1, another closely related AGO protein, AGO10 (PINHEAD/ZWILLE), was shown to express in the overlapping domains with *HD-ZIP III* genes in the embryo and leaf primordia (Lynn et al., 1999). AGO10 competitively binds miRNA165/166 in these domains, and prevent the miRNA165/166 from loading to the AGO1 RISC, leading to de-repression of *HD-ZIP IIIs* (Zhu et al., 2011). Consistently, *ago10* leaves are slightly abaxialized. Moreover, it was shown that REV also directly promotes *AGO10* expression and therefore forms a positive feedback regulation loop (Brandt et al., 2013; Reinhart et al., 2013).

Interestingly, the miRNA166 gain of function mutants *jabba1-D* (Williams, 2005) and *men1* (Kim et al., 2005) showed an enlarged meristem size along with enhanced WUS/CLV3 activities. In these two mutants, *PHB*, *PHV* and *CNA* mRNAs are preferentially cleaved, while *REV* and *ATHB8* are less affected or even increased. This is consistent with the finding that these HD-ZIP III members show distinct or

even antagonistic roles in certain circumstances (Prigge et al., 2005), and further indicated that miRNA166 may serve as a regulator in fine-tuning HD-ZIP III activities.

1.6.2 HD-ZIP III proteins are directly regulated by LITTLE ZIPPER proteins via forming a feedback loop

HD-ZIP III proteins contain a leucine zipper domain immediately behind the DNA-binding homeodomain, and this domain was known to have a tendency in forming homo- or heterodimers. Unlike the animal homeodomain proteins, the dimerization of HD-ZIP III monomers not only serves as a way of modulating the protein function, but was also identified to be as a prerequisite for their DNA binding activity (Sessa et al., 1998). By analyzing ChIP-seq experiments, REV was identified to bind with the sequence motif AT[G/C]AT (Brandt et al., 2012), which is consistent with the core palindromic sequences of the previously identified *in vitro* binding site of HD-ZIP III proteins (Sessa et al., 1998).

A group of LITTLE ZIPPER (ZPR) proteins that contain similar leucine zipper domain were found to form a feedback loop regulation module with HD-ZIP IIIs: HD-ZIP III proteins promote *ZPR* expression, the resulting accumulating ZPR proteins then reversely dampen the HD-ZIP III protein activity by forming nonfunctional heterodimers (Wenkel et al., 2007; Kim et al., 2008; Reinhart et al., 2013). A recent stoichiometry study with *in planta* single-molecule pull-down assay indicated that HD-ZIP III and ZPR proteins form a tetrameric complex consists of two HD-ZIP III and two ZPR monomers, rather than the presumptive dimeric heterodimers (Husbands et al., 2016).

There are four *ZPR* genes in Arabidopsis, they are all upregulated in the *35S:GR-REVd* lines when induced with dexamethasone, yet the increase of *ZPR3* and *ZPR4* transcription was prominently higher than that of *ZPR1* and *ZPR2* (Wenkel et al., 2007). *ZPR3* is only expressed in the central domains and the leaf adaxial side due to the local HD-ZIP III activity. Overexpression of *ZPR3* results in downwardly curling leaves, which is considered to be an abaxialized phenotype. In extreme cases only a rod-like leaf is formed in the shoot apex with terminated SAM. In contrast, *zpr3 zpr4* did not show clear leaf polarity patterning defects. However, due to potential de-repressed HD-ZIP III activity, this mutant shows clear growth alteration

including disturbed leaf phyllotaxy, cotyledon number increase and inflorescence stem fasciation (Wenkel et al., 2007; Kim et al., 2008). Moreover, *zpr3 zpr4* develops a protrusion in the center of the shoot apex surrounded by SAM-like tissues, with enhanced expression of SAM marker genes *WUS* and *CLV3* (Kim et al., 2008).

1.6.3 The MEKHLA domain is required for fine-tuning HD-ZIP III activity

The HD-ZIP III C-terminal MEKHLA domain contains a subregion that shares significant similarity to the PAS domain, which is known to function as a sensory module in respond to various of physical and chemical stimuli (Mukherjee, 2006). A later study specifically investigated the role of the MEKHLA domain in HD-ZIP III regulation. Overexpression of the truncated REV lacking the MEKHLA domain (REV-ΔMEKHLA) leads to an upwardly curling leaf phenotype, which is not present in the full-length REV overexpression lines. Then in the yeast two-hybrid and split-YFP assays it was shown that MEKHLA domain is able to block the homodimerization of the REV monomers. Therefore, the MEKHLA domain may serve as a steric mask for restraining REV function via inhibiting dimerization of the REV monomers, however, the certain ligand for unveiling this mask still remains elusive (Magnani and Barton, 2011).

The importance of the MEKHLA domain in HD-ZIP III function was supported by the characterization of the *hoc* mutant, which bears a point mutation in the MEKHLA domain of CNA (Catterou et al., 2002; Duclercq et al., 2011a). The *hoc* mutant shows versatile phenotypes including bushy shoot architecture with multiplied rosettes, axillary meristems and branches, shortened stature, strongly elevated shoot de novo formation ability and constitutive skotomorphogenesis, which were considered to be caused by the enhanced endogenous cytokinin accumulation in this mutant (Catterou et al., 2002; Duclercq et al., 2011a).

2. Shoot apical meristem respecification from differentiated tissue

Compared to animals, plant cells possess a high regenerative potential (De Klerk et al., 1997; Gaillochet and Lohmann, 2015). This allowed the establishment of plant *in vitro* tissue culture procedures aiming for shoot *de novo* formation, which had been

proven to be crucial for both plant biotechnology and fundamental biological studies.

2.1 Developmental phases of *de novo* shoot formation

Exogenous application of phytohormones, i.e. cytokinin and auxin, can induce *de novo* organ formation from various explants *in vitro* (Duclercq et al., 2011b; Ikeuchi et al., 2016). The morphogenetic outcome can be simply manipulated by altering the ratio of cytokinin and auxin in the medium: high cytokinin-to-auxin ratio triggers shoot regeneration and high auxin-to-cytokinin ratio leads to root regeneration (Skoog and Miller, 1957). In the canonical Arabidopsis tissue culture protocol, initially the intended tissues, are cultured on the auxin-rich callus induction medium (CIM) to facilitate cell dedifferentiation and competence acquisition. Then the cultured explants are transferred to the cytokinin-rich shoot induction medium (SIM) to promote shoot regeneration (Che et al., 2002; Che et al., 2006). Various plant tissues had been utilized as explants for inducing shoot *de novo* formation, and root is one of the most frequently used explants. The root pericycle is a layer of xylem-surrounding meristematic cells which is responsible for regenerating shoots from root and hypocotyl explants (Parizot et al., 2008; Atta et al., 2009). It had been proposed that the de novo shoot formation process resembles the initiation of lateral roots, since both of these two processes are originated from the pericycle cells and share the same genetic control in initiating the division of pericycle-like cells (Sugimoto et al., 2010; Duclercq et al., 2011b).

2.2 Molecular basis of de novo shoot formation

Since the shoot *de novo* formation requires reestablishment of the SAM, naturally many key SAM regulators are also dynamically controlled in this process. The spatiotemporal expression patterns of these genes are well characterized using live imaging approaches and reporter lines (Cary et al., 2002; Gordon et al., 2007; Chatfield et al., 2013; Zhang et al., 2017). During callus induction on CIM, the *CUP-SHAPED COTYLEDON 1 (CUC1)* and *CUC2* which function in SAM formation and organ boundary specification (Bilsborough et al., 2011; Hasson et al., 2011), are widely expressed in the induced callus (Gordon et al., 2007).

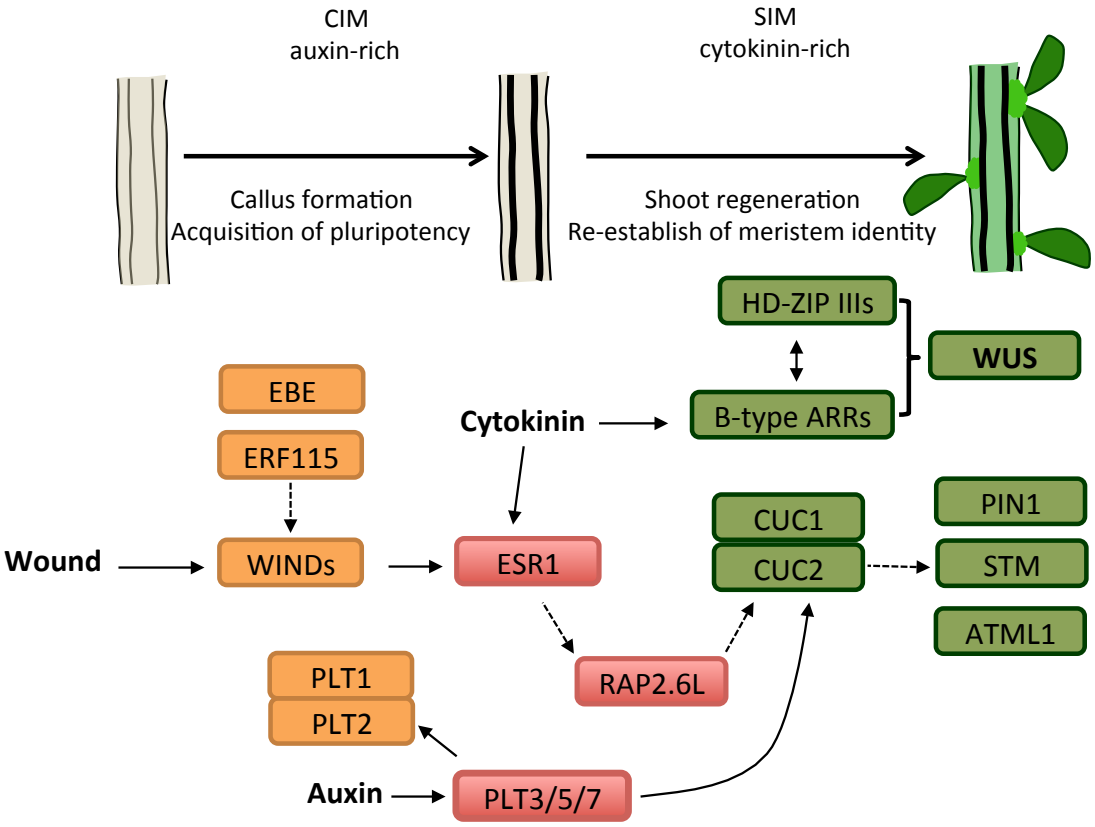

Figure 3. Schematic diagram showing the simplified molecular basis of plant shoot *de novo* formation

The shoot *de novo* formation procedure activates key meristem regulators including WUS, CUC1/2, PIN1, STM and ATML1. In a cytokinin rich environment, HD-ZIP IIIs interact with B-type ARRs and co-activate *WUS* expression. A couple of AP2/ERF proteins contribute to the shoot de novo formation either by promoting callus formation e.g. EBE, ERF115, WINDs (induced by wounding) and PLT1/2, or by triggering shoot regeneration e.g. ESR1 and RAP2.6L. The expression of PLT3/5/7 are activated by auxin-rich CIM, these AP2/ERF proteins then triggers PLT1/2 and CUC1/2 to establish shoot fate. Figure was adapted from Ikeuchi et al., 2016.

As a key regulator of stem cell specification and SAM maintenance, WUS plays an important role in the shoot de novo formation process on the SIM (Gordon et al., 2007; Chatfield et al., 2013). Explants from *wus* mutant can barely regenerate any shoots. A recent study proposed a two-step model for the activation of WUS expression in shoot regeneration (Zhang et al., 2017). In the callus cells, initially a CK rich environment is required for scavenging the epigenetically repressing histone mark H3K27me3 on the *WUS* promoter. Then the CK positive regulators B-type ARRs directly interact with HD-ZIP III proteins and co-activate *WUS* expression in the SAM progenitor cells. Additionally, another meristem marker gene *STM* (Jasinski et al., 2005; Yanai et al., 2005) is also activated in the meristem progenitor cells (Gordon et al., 2007).

During the shoot initiation process, the HD-ZIP class IV gene *ARABIDOPSIS THALIANA MERISTEM L1 LAYER (ATML1)* which marks the L1 layer in SAM (Lu et al., 1996; Takada et al., 2013) is activated to define the L1 cell layer in the promeristem.

Besides these known key SAM regulators, many APETALA2/ETHYLENE RESPONSE FACTOR (AP2/ERF) transcription factors were shown to function in the tissue culture process (Ikeuchi et al., 2016). When overexpressed, both *DRN/ESR1* and its closely related homolog *DRN-LIKE (DRNL)/ESR2/BOLITA,* can readily induce shoot de novo formation from root explants without application of exogenous hormones, and the regeneration efficiency can be further enhanced by cytokinin treatment (Banno et al., 2001; Ikeda et al., 2006; Marsch-Martinez et al., 2006). *RAP2.6L* expression level is specifically upregulated in the shoot regeneration process, and mutation of this gene leads to a significant reduce in the shoot de novo formation capacity (Che et al., 2006). Close homolog of *RAP2.6L*, *ERF BUD ENHANCER (EBE,* also known as *ERF114)* was strongly upregulated in the callus formation process, and the overexpression lines showed enhanced cell proliferation during callus growth (Mehrnia et al., 2013). PLETHORA (PLT) 3, PLT5 and PLT7 together render the shoot de novo formation capacity via a two-step mechanism (Kareem et al., 2015). In the callus formation process, these AP2/ERF proteins activate their close homologs *PLT1/PLT2* to promote the proliferation of shoot progenitor cells, and then in the regeneration process, CUC2 is activated to initiate shoot *de novo* formation.

Similar to *in vitro* tissue culture, in plants the wounding-induced organ regeneration also undergoes dedifferentiation of somatic cells and subsequent organ regeneration. Another group of AP2/ERF proteins, WOUND INDUCED DEDIFFERENTIATION (WINDs) function in promoting the dedifferentiation of somatic cells after wounding by regulating B-type ARR-mediated cytokinin responses (Iwase et al., 2011).

Conversely, there is increasing evidence that these AP2/ERF proteins also cooperate with each other. As previously mentioned, PLT3/5/7 are able to activate *PLT1/PLT2* expression (Kareem et al., 2015). ERF115 was shown to promote stem cell replenishment and tissue regeneration, in correlation with upregulation of *WIND1* (Heyman et al., 2016). Interestingly, a recent study indicated that WIND1 also directly activates *DRN/ESR1* expression (Iwase et al., 2017). RAP2.6L might also be part of this transcription network, since knocking out DRN/ESR1 function also impaired the activation of *RAP2.6L* in shoot regeneration process (Iwase et al., 2017).

2.3 The AP2/ERF transcription factor RAP2.6L is required for de novo shoot organization

RAP2.6L (At5g13330) belongs to group X of the ERF subfamily (Nakano et al., 2006). As mentioned above, RAP2.6L is known as key regulator for shoot regeneration in the tissue culture process (Che et al., 2006). RAP2.6L was isolated due to its specific upregulation in the early shoot regeneration process. A T-DNA insertion mutant *rap2.6l-2* demonstrated strongly attenuated *de novo* shoot formation capacity together with significantly reduced *CUC2* expression, an important SAM formation regulator. On the other hand, in the incised stem, *RAP2.6L* is specifically upregulated in the lower part of the wound, and functions in promoting the tissue reunion (Asahina et al., 2011; Pitaksaringkarn et al., 2014). The depletion of auxin and subsequently accumulation of jasmonic acid (JA) in this area is considered to be responsible for the activation of *RAP2.6L*.

Like some reported AP2/ERF transcription factors, RAP2.6L was also found to enhance stress tolerance in response to several stress-involved hormones, yet a clear characterization of the molecular mechanism is still missing (Nakano et al., 2006; Krishnaswamy et al., 2011). One study proposed that RAP2.6L promotes waterlogging resistance via activating abscisic acid (ABA) responses (Liu et al., 2012), and this is supported by studies on the RAP2.6L close homolog, AP2-like ABA repressor 1 (ABR1/ERF111). *ABR1* was shown to be activated by ABA and abiotic stresses including cold, salinity and drought, and the enhanced ABR1 in turn negatively feedback regulates ABA response (Pandey et al., 2005; Li et al., 2016).

The knowledge concerning the role of RAP2.6L in plant development is limited. RAP2.6L promoter GUS fusion reporter line showed broad staining in the vasculature of young seedlings. In the young leaves this reporter showed a staining intensity front which reminiscent of the leaf maturation process (Che et al., 2006). On the other hand, the promoter GUS reporter line of RAP2.6L in another study displayed a flower and young silique specific staining (Krishnaswamy et al., 2011). Both mutation and overexpression of RAP2.6L was described to only cause minor effects on plant development except early flowering. Conversely, the dominant negative line showed a compact seedling architecture with closed cotyledons and curled true leaves (Che et al., 2006; Krishnaswamy et al., 2011).

Including RAP2.6L, EBE and ABR1, within the group X of the ERF subfamily there are eight members (The Arabidopsis Genome Initiative, 2000; Nakano et al., 2006). Although the role of RAP2.6L in plant development is not clear yet, functions of two RAP2.6L homologs were characterized. In addition to its role in promoting callus formation, EBE is also involved in regulating shoot architecture. Under short-day condition, overexpression of *EBE* results in a bushy phenotype including increased leaf initiation rate and enhanced shoot branching, which is in association with increased SAM size and ectopic formation of axillary meristems (Mehrnia et al., 2013). Another group X AP2/ERF transcription factor, ERF115 also promotes stem cell fate in the root. In response to brassinosteroids, ERF115 facilitates cell division in the root quiescent center (Heyman et al., 2013). A later study further indicated that ubiquitous expression of both ERF115 and the GRAS protein PAT1 was able to trigger ectopic stem cell pool formation in the root, and co-activation of these two proteins was required for the reestablishment of stem cell identity when losing root meristem (Heyman et al., 2016).

Similar to EBE and ERF115, other AP2/ERF transcription factors that promote tissue regeneration capacity were also shown to be involved in controlling meristem activity. The activation tagged mutant *drn-D* displayed arrested SAM development and severely radialized leaves (Kirch et al., 2003), while the *drn drnl* double mutant displayed a high-frequency of defective embryo patterning and subsequent disturbed cotyledon development (Chandler et al., 2007). Intriguingly, in line with these polarity patterning and meristem development phenotypes, it was shown that the AP2 domains of the DRN and DRNL interact with the C-terminal PAS-like domain of HD-ZIP III proteins (Chandler et al., 2007). PLT1 and PLT2 are key root development regulators (Aida et al., 2004; Galinha et al., 2007), and function in an antagonistic manner to HD-ZIP IIIs in defining shoot-root identity of the embryo (Smith and Long, 2010). Conversely, high order mutant of *AINTEGUMENTA, PLT3* and *PLT7* failed to maintain shoot meristem after developing a few leaves (Mudunkothge and Krizek, 2012; Horstman et al., 2014).

3. The putative glutamate carboxypeptidase AMP1 controls shoot apical meristem organization and regeneration

3.1 AMP1 deficiency prominently affects shoot apical meristem organization and activity

The key aim of this work was to further characterize the function of ALTERED MERISTEM PROGRAM 1 (AMP1, AT3G54720), a putative glutamate carboxypeptidase, since AMP1 loss-of-function mutants demonstrate drastically altered SAM organization and activity (Helliwell et al., 2001). Starting from the embryo stage, *amp1* shows a strongly enlarged SAM size, a high frequency of extra cotyledon formation and premature leaf primordia initiation before germination (Vidaurre et al., 2007).

A recent study indicated that *amp1* shows high ratio of twin embryo formation, which originated from the transdifferentiation of synergids to supernumerary egg cells (Kong et al., 2015). Intriguingly, an AMP1-dependent signal derived from the surrounding sporophytic tissues is sufficient to suppress the transition of synergid to the supernumerary egg (Kong et al., 2015), indicating that in early ovule development stages AMP1 is required to keep the non-gametic synergid cell fate, and this AMP1-dependent signal acts in a non-cell-autonomous manner.

In the vegetative growth phase, in line with the hypertrophic SAM size, *amp1* shows highly accelerated leaf initiation rate with altered phyllotaxy (Chaudhury et al., 1993; Nogué et al., 2000a). Several studies on AMP1 orthologs showed that the SAM-related mutant phenotypes of *amp1* are conserved in maize, rice and *Lotus japonicus* (Suzuki et al., 2008; Kawakatsu et al., 2009; Suzaki et al., 2013).

By histological and reporter line analysis, a recent study demonstrated that along with size enlargement, *amp1* forms extra stem cell niches within the meristem, and the increased leaf formation rate is at least partially caused by this meristem defect (Huang et al., 2015). The Arabidopsis genome contains a *AMP1* homolog, named *LIKE AMP1* (*LAMP1,* At5g19740). Although *lamp1* single mutant barely shows any notable phenotype, LAMP1 is considered to function in a partially redundant manner to AMP1, since the *amp1* phenotype including the formation of ectopic stem cell niche is drastically enhanced in *amp1 lamp1* double mutant (Huang et al., 2015).

In line with its enhanced meristem activity, *amp1* also shows strongly increased shoot regeneration efficiency in tissue culture (Nogué et al., 2000a). Additionally, mutation in *AMP1* also causes other notable phenotypes in seemingly unrelated processes including enhanced capacity in somatic embryogenesis (Mordhorst et al., 1998), de-etiolation in the dark (Chaudhury et al., 1993; Chin-Atkins et al., 1996) and ecotype-dependent precocious flowering time (Lee, 2009).

3.2 AMP1 belongs to the M28 peptidase family

Structurally, AMP1 is a zinc-dependent metalloprotease (MEROPS ID: M28.007), which belongs to the subfamily B of the M28 peptidase family. The members of this family had been identified in several organisms, and typically these proteins consist of an N-terminal transmembrane domain, a protease-associated domain, a M28 peptidase motif and a transferrin receptor-like dimerization domain (Helliwell et al., 2001; Suzaki et al., 2013; Poretska et al., 2016). The N-terminal trans-membrane domain is indispensable for AMP1 function, since the truncated protein lacking this domain failed to rescue the *amp1* mutant (Shi et al., 2013b).

An in-depth analysis of the AMP1 enzymatic activity is still missing until now, whereas its homolog human glutamate carboxypeptidase II (HsGCPII) had been well characterized. HsGCPII has 28% amino acid sequence identity to AMP1 (Poretska et al., 2016). In the nervous system, HsGCPII can cleave the N-acetyl-L-aspartyl-L-glutamate (NAAG) into N-acetyl-L-aspartate and L-glutamate, and the latter is a potent excitatory neurotransmitter. Due to this function, the HsGCPII is also named as N-acetylated-alpha-linked acidic dipeptidase (NAALADase) (Robinson et al., 1987; Klusák et al., 2009). Excessive glutamate in the nervous system causes neuronal dysfunction, also known as glutamate excitotoxicity, which is considered to be the cause of several neuronal diseases including stroke, Alzheimer's dementia and Parkinson's disease. In contrast to glutamate, NAAG is considered to be neuroprotective (Bařinka et al., 2012). Therefore, restraining GCPII function might be effective for relieving the glutamate excitotoxicity. Many compounds that aiming for the specific inhibition of GCPII activity had been developed, and utility of these inhibitors on several animal diseases that links to enhanced glutamate transmission had been performed (Bařinka et al., 2012).

Apart from brain tissues, HsGCPII is highly expressed in human prostatic tissues, and the expression level is further promoted in prostate carcinoma tissues. Hence, GCPII is also used as the marker for imaging of and therapy for prostate cancer. Therefore, GCPII is also named as prostate specific membrane antigen (PSMA) (Bařinka et al., 2012).

In small intestine, GCPII is known as folate hydrolase 1 (FOLH1) (O'Keefe et al., 1998) and considered to be responsible for the uptake of folates, which is crucial for replication of the rapidly dividing cells. However, the dietary folates are mixed varieties of folyl-poly-γ-L-glutamic acids ($FolGlu_n$) and are not able to pass through the cell membrane. With its folate hydrolase activity, GCPII hydrolyzes the $FolGlu_n$ and releases the absorbable γ-linked L-glutamates (Bařinka et al., 2012; Navrátil et al., 2014).

In Arabidopsis, GCPII is not able to complement AMP1 function, since overexpressing GCPII protein in *amp1* failed to rescue the *amp1* phenotype (Poretska et al., 2016). On the other hand, GCPII is considered to locate on the plasma membrane and the major portion of the protein orients to a extracellular milieu (Bařinka et al., 2012), while AMP1 had been shown to localize in the endoplasmic reticulum (ER) (Vidaurre et al., 2007; Li et al., 2013). Together with the fact that these two proteins share low amino acid sequence identity (28%), especially with the amino acids defining the substrate-binding activity (27%), this might imply that AMP1 exerts a divergent function to GCPII (Poretska et al., 2016).

3.3 Interaction of AMP1 with established determinants of SAM organization and activity

The ectopic SAM formation phenotypes of *amp1* suggest the connection between AMP1 and WUS/CLV feedback loop. Consistent with the enlarged SAM size of *amp1*, in this mutant WUS and CLV reporter activities are both active in a broader range in the shoot apex. Close-up analyses revealed that the *amp1* SAM forms secondary stem cell niches between leaf primordia. Furthermore, although the *wus amp1* double mutant showed cessation of SAM activity during floral transition, knocking out WUS function in *amp1* mutant neither inhibited the formation of ectopic stem cell niches nor rescued the accelerated leaf formation rate of *amp1* during the vegetative growth phase. Therefore, it is rather unlikely that *amp1* phenotypes are

direct consequences of WUS/CLV feedback loop malfunction (Huang et al., 2015).

One of the most prominent molecular changes in *amp1* is the ectopic accumulation of CK, which is caused by enhanced endogenous CK biosynthesis (Huang et al., 2015). In the *amp1* mutant, the expression of the CK biosynthetic gene *IPT3* was upregulated in the vascular tissues, which is further supported by the promoted *ARR5* activity. Moreover, consistent with multiple stem cell niches in the SAM of *amp1*, multiple CK response maxima were identified (Huang et al., 2015). In early studies, AMP1 was considered to function through controlling endogenous CK level (Chaudhury et al., 1993; Helliwell et al., 2001). Indeed, seedlings with high endogenous CK level demonstrate many phenotypes resembling *amp1*, including enlargement of SAM size (Saibo et al., 2007; Huang et al., 2015), increased shoot regeneration efficiency (Nogué et al., 2000a), promoted shoot branching (Aguilar-Martínez et al., 2007) and enhanced tolerance against nitric oxide (Liu et al., 2013). However, an in-depth study revealed that applying exogenous CK or promoting endogenous CK biosynthesis equally augmented the SAM size in both wild-type and *amp1* mutant background. In contrast, multiple SAM-related phenotypes of *amp1* including increased leaf formation rate and ectopic stem cell niche formation remained largely unaffected by reducing CK levels or depleting the CK perception. Hence, the increased CK accumulation in *amp1* is much likely a consequence of ectopic SAM activity rather than a cause of the abnormal SAM phenotypes in *amp1* (Huang et al., 2015).

Previous studies revealed that AMP1 is also connected with other plant hormonal pathways. The *amp1* mutant is less sensitive to gibberellin and ethylene treatment in the process of hypocotyl elongation (Saibo et al., 2007). The effect of *amp1* is epistatic over the mutation in auxin response factor *MONOPTEROS (MP/ARF5)* gene, since most of the embryo and early meristem development defects of *mp* can be significantly restored by knocking-down AMP1 function (Vidaurre et al., 2007). Furthermore, AMP1 seems to negatively modulate freezing and drought stress responses via suppressing abscisic acid (ABA) biosynthesis and signaling (Shi et al., 2013a; Shi et al., 2013b; Yao et al., 2014). Moreover, it was shown that *amp1* mutants displayed an ecotype-dependent variation in seed dormancy acquisition and maintenance, which is also related to the alteration of ABA content in the freshly harvested dry seeds (Griffiths et al., 2011; Shi et al., 2013a).

In a recent study, AMP1 was identified to function in the miRNA-related translation inhibition, in association with AGO1 protein (Li et al., 2013). It was shown that the

protein abundance of the miRNA-targets was increased in *amp1* while the transcription level remained to be unaffected. The authors also showed that AMP1 is an integral membrane protein and preferentially associates with the rough endoplasmic reticulum. Correspondingly, AMP1 was shown to specifically block the association of the miRNA target transcripts to the membrane-bound polysomes, while the association to the total polysomes is not affected. Among these miRNA targets there are the HD-ZIP III transcription factors, which are known as important SAM regulators. However, whether and to which extent this effect indeed evokes the *amp1*-related SAM phenotypes has not been tested yet.

4. Aim of this study

This study focused on the characterization of AMP1 and its interaction with two potential downstream components HD-ZIP IIIs and RAP2.6L.

1. To analyze whether the increased HD-ZIP III abundance/activity in *amp1* caused the SAM malformation, and further investigate how AMP1 controls the tissue-specific expression of these proteins.

2. To test whether and to what extent the upregulation of RAP2.6L contributes to *amp1* phenotype including SAM hypertrophy, accelerated leaf initiation as well as the increased shoot regeneration capacity.

II. Materials and methods

Plant materials and growth conditions

Arabidopsis thaliana ecotypes Columbia (Col-0) and Landsberg *erecta* (L*er*) were used in this study. *amp1-1* (Col-0; N8324), *amp1-13* (Col-0; N522988), *pt* (L*er*; N235), *lamp1-2* (Col-0; SM_3.22750), *rap2.6-2* (N863006), *rap2.6l-1* (N656482), *erf112-1* (N563727) and *phb-1d* (N3761) were ordered from the Nottingham Arabidopsis Stock Centre (http://www.arabidopsis.info). The *35S::RAP2.6L* lines (C23, C28 and C31; named *RAP2.6L-OX* throughout this study) and *pRAP2.6L::RAP2.6L:GUS* were kindly donated by Nat Kav (Krishnaswamy et al., 2011). Of the RAP2.6L overexpression lines, C28 was used throughout this study if not indicated otherwise. *35S::FLAG-ZPR3, pZPR3::ZPR3:GUS, zpr3-1* (N686368), *zpr4-1* (N508069) and *rev-10d* were kindly provided by Stephan Wenkel. *CycB1;1::CycB1;1-GUS* (in Col-0) was provided by John Celenza (DiDonato et al., 2004), *pCLV3::GUS* and *pWUS::GUS* (in Ler) were received from Thomas Laux (Gross-Hardt et al., 2002) and *pKLU::GUS* (in Col-0) was obtained from Michael Lenhard (Anastasiou et al., 2007). 35S::AMP1 line was a kind gift from Thomas Berleth (Vidaurre et al., 2007).

Combinations of mutants and reporter lines were generated by crossing individual lines and genotypes were verified phenotypically and by PCR genotyping.

Arabidopsis seeds were surface sterilized with 70% ethanol containing 0.05% sodium dodecyl sulfate (SDS) for 3 min and rinsed with 96% ethanol for 1 min.

The seeds were plated on half strength MS medium (Duchefa) with 0.7% (w/v) agar (Duchefa) and 1% (w/v) sucrose or in soil. After Stratification (4 °C for 48 h) seeds were transferred to the incubator set at long day condition (16 h of 80 µmol s^{-1} m^{-2} light/ 8 h dark) or short day condition (8 h of 80 µmol s^{-1} m^{-2} light/16 h dark).

Gene constructs and transformation

PCR was performed with proofreading thermostable polymerase, and all clones were confirmed by sequencing.

To create 35S::PHV-MYC (PHV-MYC), 35S::PHB-MYC (PHB-MYC), 35S::PHV-YFP (PHV-YFP) and 35S::PHB-YFP (PHB-YFP), the *PHV* and *PHB* ORF

were amplified from cDNA (Col-0 seedlings) by PCR with primers PHV ORF F (*Eco*RV), PHV ORF R (*Not*I), PHB ORF F (*Eco*RV) and PHB ORF R (*Not*I), respectively. The fragments were subcloned into pGEM-T Easy (Promega). Subsequently, the *PHV* and *PHB* ORF were transferred via *Eco*RV and *Not*I into the pGWR8 (Rozhon et al., 2010) backbone to generate p35S::PHV and p35S::PHB. The YFP ORF (from pGWR8-YFP) and 6xMYC-tag (from pGWR8-MYC) sequences were subcloned into the *Not*I sites of p35S::PHV and p35S::PHB to create PHV-MYC, PHB-MYC, PHV-YFP and PHB-YFP, respectively.

To create 35S::RAP2.6L-MYC-SRDX (RAP2.6L-SX) and 35S::EBE-MYC-SRDX (EBE-SX), the RAP2.6L and EBE open reading frames (ORFs) were amplified from cDNA (Col-0) by PCR with primer pairs RAP2.6L ORF F (EcoRV)/ RAP2.6L ORF R (NotI) and EBE ORF F (EcoRV)/ EBE ORF R (NotI), respectively. The fragment was subcloned into pGEM-T Easy (Promega). Subsequently, in a previously created pGWR8-CES-MYC-SRDX (Poppenberger et al., 2011) the CES ORF was removed by a double digestion with EcoRV and NotI to generate the pGWR8-MYC-SRDX backbone. The RAP2.6L and EBE ORFs were then transferred via EcoRV and NotI into pGWR8-MYC-SRDX to generate RAP2.6L-SX and EBE-SX, respectively.

To create pZPR3::GUS, a 3132-bp genomic sequence upstream of the ZPR3 ORF was amplified with primers pZPR3F(PstI) and pZPR3R-2(BamHI) and subcloned into pGEM-T Easy (Promega). The fragment was excised via PstI and BamHI and ligated into pPZP-GUS-1 (Diener et al., 2000), resulting in pZPR3::GUS.

To create pRAP2.6L::GUS, a 1487-bp genomic sequence upstream of the RAP2.6L ORF was amplified with primers AP2.6proF(PstI) and AP2.6proR(BamHI) and subcloned into pGEM-T Easy (Promega). The fragment was excised via PstI and BamHI and ligated into pPZP-GUS-1, resulting in pRAP2.6L::GUS.

Using the floral dip method, Col-0 plants were transformed with PHV-MYC, PHB-MYC, PHV-YFP, PHB-YFP, pZPR3::GUS, RAP2.6L-SX, EBE-SX and pRAP2.6L::GUS, respectively. At least 10 independent transformants were generated for each line and the resulting T2 lines were confirmed for single transgene insertion sites based on the 3:1 segregation of the selection marker and propagated for further analysis.

Primers

Table 1. Primers used in this study

Name	Sequence 5'-3'
AMP1F	TATCAGTGGCTGGAATTTGG
AMP1R	GCTCTCTGAATCGCTCTTGC
amp1.1F	TATCAGTGGCTGGAATTTGA
LBb1.3	ATTTTGCCGATTTCGGAAC
LP amp1-13	CGAAGAAAGTATTTGTCCTTT
RP amp1-13	AACGCAGATCCATTGTTTCAC
amr1.3 LP	AGCAAACAACCAACTCCATTG
amr1.3 RP	TAACAGTTTCCCCCTGAAACC
DSPM	TACGAATAAGAGCGTCCATTTTAGAGTGA
pt gen F	TGCATGGACATATGGAGCTG
pt gen R	TCTTCAATCCATTCAGTTGATCC
ZPR3F(G)	ACGTGAGTTTTCTCGACATGC
ZPR3R(G+RT)	TGTCCAGAAGCAGAGCTTGA
ZPR4F(G)	AAAGATCCTTTGCTCGTACCG
ZPR4R(G+RT)	CCAGAAGCAGAGCTTGATGA
PHV ORF F (EcoRV)	CCGATATCATGATGGCTCATCACTCCATGG
PHV ORF R (NotI)	ACGCGGCCGCTAACAAACGACCAACTAACGAGG
PHB ORF F (EcoRV)	CCGATATCATGATGATGGTCCATTCGATGA
PHB ORF R (NotI)	ACGCGGCCGCTAACGAACGACCAATTCACGAAC
pZPR3F(PstI)	AACTGCAGCGTGAGCGTCGATATTTATCCA
pZPR3R-2(BamHI)	CGGGATCCTTCTGCTTTCTTGCTACAAGT
qZPR3_1 F	TCTGCTTCTCAACACTCCTTCCC
qZPR3_1R	CAACAAACAGCTTCGAGTTTAGCC
qYFP F	TGGCCCACCCTCGTGACCACCT
qYFP R	CGGGTCTTGTAGTTGCCGTCGTC
qPCR PHV_1 F	ACTTGATGACTCTGGTCGTAGAGC
qPCR PHV_1 R	CGGAAGATTCGCATATCCCTGCTG
PHV mid F	GCAACTGCAGTGGAATAGCA
PHV mid R	GTGGAACCATCTAGGGACGA
PHB mid F	TTGGCATAGTCGCTATTTCG
PHB mid R	AGCTTGACGTGTGGATCCTT
RAP2.6L F-1	GCATAACACTGCTGCCAAAA
RAP2.6L R	GGAACATGCGTGGTCAAAAT
RAP2.6 F	ATGTGAACGCACGTTTTTGA
RAP2.6 R	TCGAAGACATATCTAAGAAGGCAAT
RAP2.6 R(CDS)	CGGGGAAATTAAGCTTTGCT
AtERF112 Forward	GACACCACCTAGTCCACCTC

AtERF112 Reverse	CGTTTCATATGCAGACTGTTACC
AP2.6proF(Pst I)	AACTGCAGTTGTTCTTCCTTGGTTTT
AP2.6proR(BamHI)	CGGGATCCGGCGGTGACATCAGTCTC
EBE ORF F (EcoRV)	CCAGATATATGTATGGGAAGAGGCCTTTTG
EBE ORF R (NotI)	AAGCGGCCGCTATATCCCGAATGAGGAGAGG
RAP2.6L ORF F (EcoRV)	CCAGATATATGGTCTCCGCTCTCAGCCGTG
RAP2.6L ORF R (NotI)	AAGCGGCCGCTTTCTCTTGGGTAGTTATAATAAT
qRap2_1 F	ACCAGACCAAGATCAACCAAGAAG
qRap2_1 R	GATTTCTGCCGCCCATTTACCC
qRAP2.6 f	CCATTGATTACCGGTTCAGCTGTG
qRAP2.6 r	ATACACGTGTCGCCTTGTGTGG
qERF112 f	AGATTCGTGACCCGAACAAGGC
qERF112 r	TAAGGCGGCTTCTTCTGCAGTG
qERF115 f	GCTCCTCCAACTCAAGATCAAGGG
qERF115 r	TTTGCGGATCCCGAATTTCAGC
qEBE f	AGAACTTGTTCCCGGTCTTCTCG
qEBE r	AGTCAAGGCCGAGACCATAACAC
UBCF	TCAAATGGACCGCTCTTATC
UBCR	CACAGACTGAAGCGTCCAAG

Microorganisms

Table 2. Microorganism lines used in this study

Microorganism lines		Reference
Escherichia coli	XL1-blue	Bullock, 1987
Agrobacterium tumefaciens	GV3101 (pSoup)	Hellens et al., 2000

Antibiotics

Table 3. Antibiotics used in this study

Antibiotic	Concentration (1000x stock)
Kanamycin	30 mg/ml in H_2O
Ampicillin	100 mg/ml in H_2O
Spectinomycin	100 mg/ml in H_2O
Hygromycin	15 mg/ml in H_2O
BASTA	5 mg/ml in H_2O
Rifampicin	20 mg/ml in methanol
Gentamycin	50 mg/ml in H_2O
Tetracycline	5 mg/ml in ethanol

GUS staining

Seedlings were put into the freshly made GUS staining buffer [100 mM sodium phosphate buffer (pH 7.0), 10 mM EDTA (pH 8.0), 0.5 mM $K_3[Fe(CN)_6]$, 0.5 mM $K_4[Fe(CN)_6]$, Triton X-100 (0.1% v/v) and 1 mM 5-bromo-4-chloro-3-indolyl-β-D-GlcA. The seedlings were incubated at 37 °C for a duration of time depending on the reporter strength. After staining the seedlings were dehydrated with 70% ethanol. Seedlings were analyzed using a stereomicroscope (SZX10; Olympus) equipped with a digital camera (DP26; Olympus).

Histology

The histological analysis was performed as previously described (De Smet et al., 2004). Seedlings were grown under long day condition for 8 days or short day condition for 18 days and fixed overnight at 4°C in FAA [5% (v/v) formaldehyde, 5% (v/v) acetic acid, and 50% (v/v) ethanol]. After fixation, samples were dehydrated in a graded ethanol series (2 h each in 30, 50, 70 and 96% ethanol) and embedded with Technovit 7100 (Heraus Kulzer) according to the manufacturer's instructions. A series of 5-7 mm thick longitudinal sections was made with a Leica RM 2065 microtome. Sections were transferred to microscopic slides (Marienfeld), stained for 5 min in 0.02% aqueous Toluidine blue O (Sigma-Aldrich) and rinsed with water. Subsequently, the stained sections were analyzed with a microscope (BX-61; Olympus).

Scanning electron microscopy

Seedlings were fixed in FAA (50% ethanol, 10% acetic acid, 5% formaldehyde) overnight at 4°C and then dehydrated through a graded ethanol series up to 96% ethanol and supercritical point-dried (CPD300; Leica Microsystems). Dried seedlings were dissected and mounted on conductive adhesive tabs (PLANO) under a stereomicroscope (SZX10; Olympus). Samples were subsequently examined using a T-3000 tabletop scanning electron microscope (Hitachi).

Vibratome sections

Shoot and root from 10-d-old seedlings were freshly embedded into 7% agarose

(Agarose Low Melt, Roth), and 100~200 μm transverse sections prepared with a vibratome (Compresstome VF-200, Precisionary).

Confocal laser scanning microscopy

YFP fluorescence of root from 10-d-old seedlings or vibratome sections was visualized using a confocal laser scanning microscope (FluoView 1000, Olympus).

Leaf Number Analysis

The shoot apex area of seedlings was examined under the stereomicroscope (2X magnification) at the indicated developmental stages and the number of visible leaves was recorded.

Regeneration capacity assay

The regeneration capacity assay was performed based on a previous protocol (Che et al., 2006). Briefly, Arabidopsis seedlings were grown for 7 d on 1/2 MS medium under long day condition. Root segments of 1-1.5 cm were cut, transferred to Gamborg's B5 medium (Sigma-Aldrich) supplemented with 0.5 g/L MES, 2.2 μM 2,4-dichlorophenoxyacetic acid, 0.2 μM kinetin and 0.8% agarose (callus induction medium) and incubated under constant light for 4 d. The root explants were then transferred to shoot induction medium (Gamborg's B5 medium containing 0.5 g/L MES, 5.0 μM isopentenyladenine, 0.9 μM indole acetic acid and 0.8% agarose) and incubated under constant light for 18 d. Regenerated shoots were counted and the number of regenerated shoots per cm explant was calculated.

Quantitative real-time PCR (qPCR)

About 50 mg of seedling material was collected, shock-frozen in liquid nitrogen and homogenized with a Retsch mill (Verder Scientific). The total RNA was extracted with the E.N.Z.A. Plant RNA Mini Kit (OMEGA Bio-Tek) and treated with DNase I (Thermo Fisher Scientific). The first-strand cDNA was synthesized using the extracted RNA as template with the RevertAid first-strand cDNA synthesis kit (Thermo Fisher Scientific). qPCR was performed with an Eppendorf Realplex

Mastercycler using SensiFAST SYBR Lo-ROX Mix (Bioline) and specific primers for the mRNAs of interest. Data were normalized to *UBC* (*AT5G25760*) and measured in at least three technical replicates.

Protein extraction and immunoblotting

Plant material (50 mg) was shock-frozen in liquid nitrogen and homogenized with a Retsch mill (Verder Scientific, Newtown, PA). 200 µL extraction buffer (62.5 mM TRIS pH 6.8, 125 mM DTT, 2.5% SDS, 12.5% glycerol, 0.003% bromophenol blue) was added to the samples, mixed thoroughly and incubated at 95°C for 2 min. The samples were centrifuged at 14,000g for 5 min and 10 µL of the supernatant was separated by SDS-PAGE (10% gel) and semi-dry-blotted onto a polyvinylidene difluoride membrane (Millipore, Billerica, MA). The membrane was blocked with blocking buffer (5% skim milk powder dissolved in 0.05% Tween 20, 150 mM NaCl, and 10 mM TRIS/HCl, pH 8.0). For PHV-YFP and PHB-YFP detection, the membrane was probed with a mouse anti-GFP-horseradish peroxidase antibody (1:5000; Miltenyi Biotec, Bergisch Gladbach, Germany) and signals were detected using the ECL Select Detection Reagent (GE Healthcare, Marlborough, MA). For PHV-MYC and PHB-MYC detection, membranes were probed with a mouse anti-Myc antibody (1:5000; Santa Cruz Biotechnology, Santa Cruz, CA). Alkaline phosphatase-conjugated goat anti-mouse IgG (Sigma-Aldrich) diluted 1:5000 with blocking buffer was employed as a secondary antibody. For detection, the CDP-Star detection reagent (GE Healthcare) was used.

Commercial kits and enzymes

Table 4. Commercial kits and enzymes used in this study

Name	Company
GoTaq DNA Polymerase	Promega, Manheim, Germany
GoTaq green buffer	Promega, Manheim, Germany
DNase I, RNase-free	Thermo Fisher Scientific, Braunschweig, Germany
RevertAid RT Reverse Transcription Kit	Thermo Scientific, Waltham, USA
GeneRuler DNA ladder	Thermo Fisher Scientific, Braunschweig, Germany
Protein ladder	Thermo Fisher Scientific, Braunschweig, Germany
T4 DNA ligase	Thermo Fisher Scientific, Braunschweig, Germany
Restriction enzymes	Thermo Fisher Scientific, Braunschweig, Germany

SensiFAST SYBR® Lo-ROX Kit	Bioline, London, UK
E.Z.N.A.® Plant RNA Kit	Omega Bio-Tek, Norcross, USA
E.Z.N.A® Gel Extraction Kit	Omega Bio-Tek, Norcross, USA
E.Z.N.A.® Plasmid DNA Mini Kit I	Omega Bio-Tek, Norcross, USA
JETstar Plasmid Purification Kit	GENOMED, Löhne, Germany
Phusion® DNA Polymerase	Thermo Fisher Scientific, Braunschweig, Germany

III. Results

1. AMP1 controls SAM integrity by limiting HD-ZIP III transcription factor activity

1.1 The HD-ZIP III direct target ZPR3 is upregulated in *amp1*

Based on the analysis of overexpressed transgenes, it has been reported that HD-ZIP III proteins over accumulate in *amp1* and *amp1 lamp1* in a miRNA-dependent manner (Li et al., 2013). To investigate whether this observed effect also results in a higher activity of these transcription factors, the expression level of the HD-ZIP III direct target *ZPR3* was analyzed in *amp1*. Accordingly, in a previously performed transcriptomic analysis (Poretska et al., 2016) *ZPR3* was found to be five-fold upregulated in *amp1-13*. By quantitative real-time PCR the enhanced expression of *ZPR3* in *amp1-13* was confirmed and an even higher induction of *ZPR3* transcription in the double mutant *amp1 lamp1* was detected (Figure 4A).

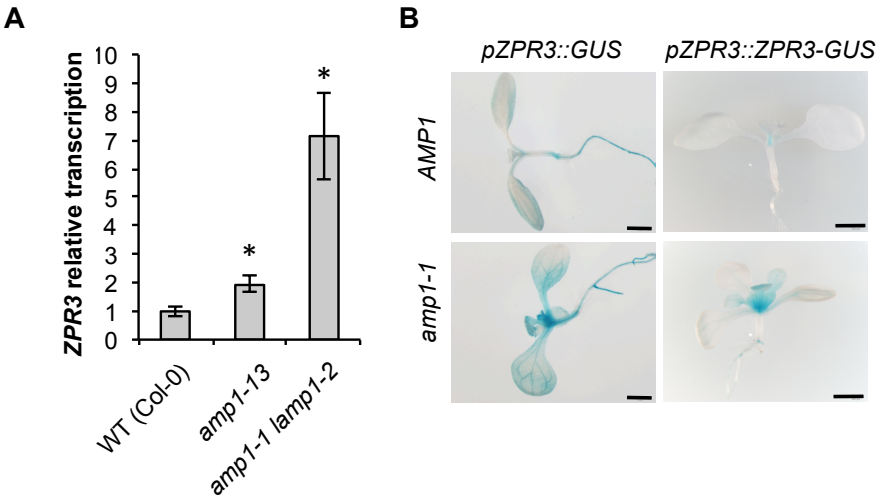

Figure 4. *ZPR3* expression is upregulated in *amp1*

(A) qPCR analysis of *ZPR3* expression in 8-d-old seedlings of the indicated genotypes. *UBC* was used as an internal control. The relative expression level of *ZPR3* was normalized to that of wild type Col-0. The SE was calculated from three biological replicates. Asterisks indicate significant difference ($p < 0.05$) as assessed by Student's 2-tailed t-test. (B) GUS activity of 8-d-old *pZPR3::GUS* and 9-d-old *pZPR3::ZPR3-GUS* seedlings in wild type Col-0 (*AMP1*) or *amp1-1*. Size bars: 1 mm.

To better understand the changes of *ZPR3* expression at the tissue-specific level a transcriptional GUS reporter *pZPR3::GUS* was generated. Analysis of this reporter further supported that *ZPR3* transcription is enhanced in *amp1-1*, particularly in the shoot apex and vascular-associated tissues (Figure 4B). Similarly, the translational GUS reporter *pZPR3::ZPR3-GUS* (Wenkel et al., 2007) showed a broadened and enhanced staining pattern in the shoot apex and young leaf primordia of *amp1-1* seedlings (Figure 4B). Hence, enhanced ZPR3 expression in *amp1* and *amp1 lamp1* indicates that endogenous HD-ZIP III activities are under control of these putative proteases.

1.2 Plants with enhanced HD-ZIP III activity show phenotypic similarities to *amp1*

To further investigate a possible hyperactivity of this class of homeodomain transcription factors in *amp1* and its causal contribution to the mutant developmental defects, the level of phenotypic overlap between *amp1* and *zpr3-1 zpr4-1* was assessed. As direct suppressors of HD-ZIP III activity, absence of ZPR3 and its close homolog ZPR4 results in a general de-repression of HD-ZIP III function at the post-translational level (Wenkel et al., 2007; Kim et al., 2008), a scenario also expected in *amp1*, based on its anticipated role in miRNA-dependent translation control. As previously described for plants with enhanced HD-ZIP III activity (Huang et al., 2014, Wenkel et al., 2007, Kim et al., 2007), *zpr3-1 zpr4-1* seedlings showed tricot formation and these defect happened at an even higher frequency than in *amp1-1* (Figure 5A). Moreover, both in *zpr3-1 zpr4-1* and *amp1-1* a simultaneous outgrowth of three first true leaves with an angle of 120° was observed instead of two separated by 180° in wild type (Figure 5A). However, whereas *amp1-1* showed a strongly accelerated leaf formation rate, this process was delayed in *zpr3-1 zpr4-1* (Figure 5A and B). The SAM organization of *zpr3-1 zpr4-1* and *amp1* also showed a clear phenotypic overlap. SAM size of *zpr3-1 zpr4-1* increased massively at a similar extent to *amp1-1* (Figure 5A and C).

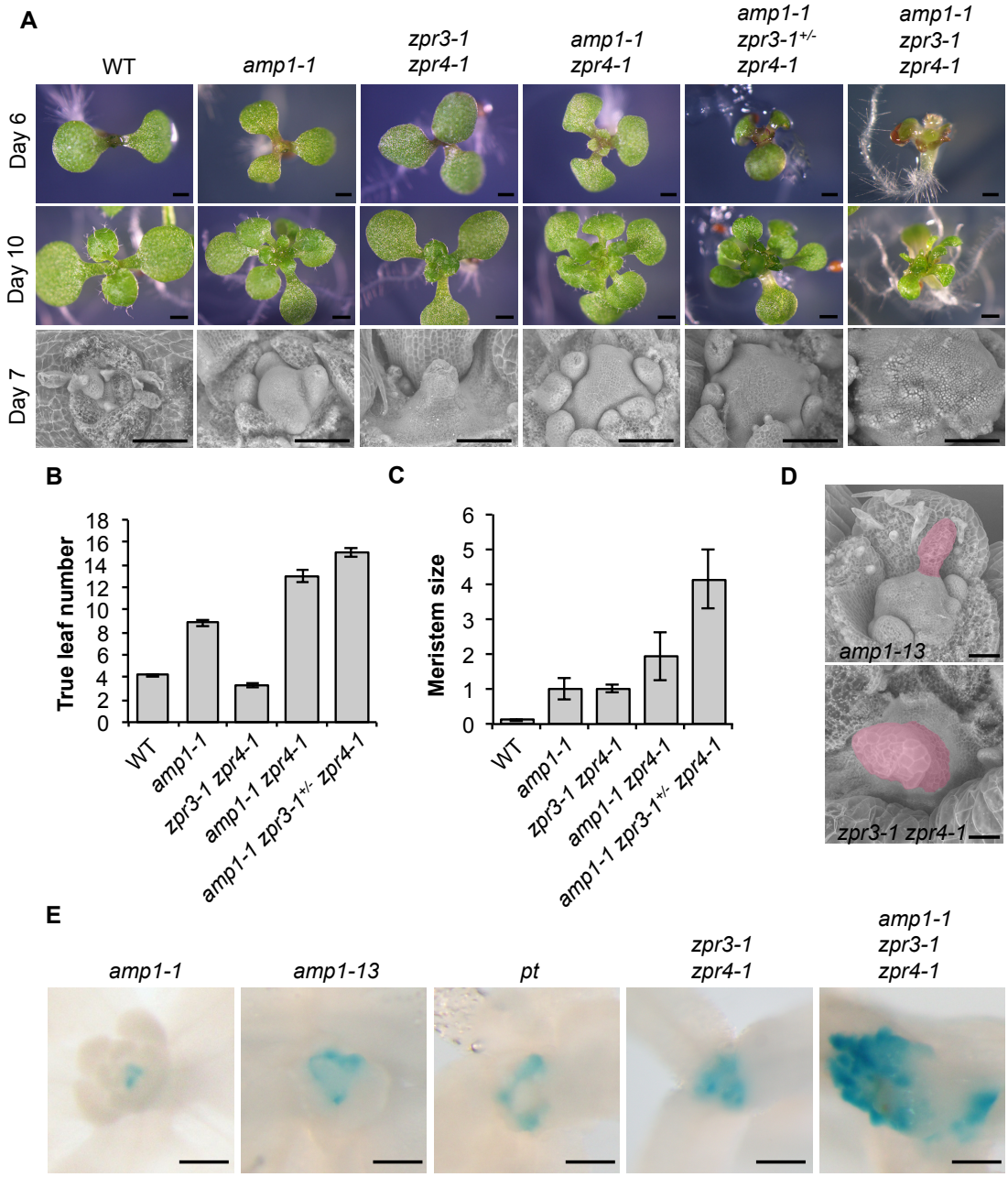

Figure 5. Increased HD-ZIP III activity causes *amp1*-related phenotypes

(A) Phenotypes of wild type Col-0 (WT), *amp1-1*, *zpr3-1 zpr4-1, amp1-1 zpr4-1, amp1-1 zpr3-1*$^{+/-}$ *zpr4-1* and *amp1-1 zpr3-1 zpr4-1* seedlings at 6 DAG (upper panel) and 10 DAG (middle panel). Scanning electron micrographs of SAMs from 7-d-old seedlings (lower panel). Scale bars: 500 µm (upper panel), 1 mm (middle panel) and 100 µm (lower panel). (B) True leaf number quantification of indicated genotypes at 8 DAG (means ± SE of the mean; n ≥ 9). (C) Meristem size quantification of 7-d-old seedlings (means ± SE of the mean; n ≥ 4). The meristem size was normalized to that of *amp1-1*. (D) Scanning electron micrographs of shoot meristems from 6-d-old *amp1-13* and 12-d-old *zpr3-1 zpr4-1* seedlings showing radial outgrowths from the center of the SAM (labeled in red). Scale bars: 50 µm. (E) Comparison of *pWUS::GUS* activities in 8-d-old *amp1-13, pt, amp1-1, zpr3-1 zpr4-1* and *amp1-1 zpr3-1 zpr4-1* seedlings. Scale bars: 250 µm.

Moreover, *zpr3-1 zpr4-1* seedlings formed a radialized organ-like bulge at a central apical position of the SAM (Figure 5A and D; Kim et al., 2007), which could be also observed in strong *amp1* alleles such as *amp1-13* (Figure 5D). Based on the related phyllotaxy and meristem organization pattern, the expression of the OC-Marker *pWUS::GUS* was analyzed. In strong *amp1* alleles and *zpr3-1 zpr4-1,* a central non-staining WUS-negative area was observed from where the outgrowth of these differentiated structures took place. These structures were surrounded by distinct WUS expression domains positioned in a concentric manner (Figure 5E). Therefore, this morphological defect of the meristem might be caused by ectopic stem cell pool formation in the shoot apex, creating a central organogenic area able to produce adaxialized leaf-like protrusions. Although *amp1-1* also produces ectopic OCs in the primary shoot apex, the number, size or distance of them appear to be too small to allow this central organ formation (Figure 5E; Huang et al., 2016).

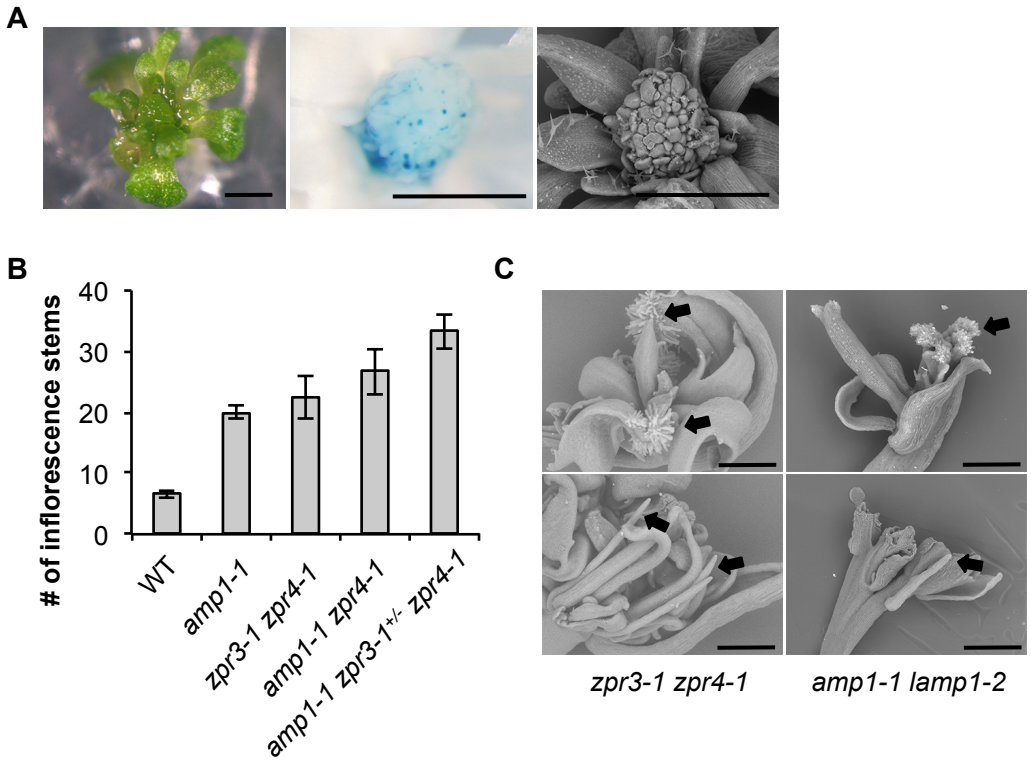

Figure 6. Genetic interaction between *amp1* and *zpr3 zpr4* at later developmental stages

(A) Meristem characteristics of *amp1-1 zpr3-1 zpr4-1 pWUS::GUS* seedlings at 12 DAG. From left to right: images of a representative seedling before and after staining, and analyzed by scanning electron microscopy. Scale bars: 1 mm. (B) Total inflorescence stem number of the indicated genotypes at 75 DAG. (C) Scanning electron micrographs of flowers from *zpr3-1 zpr4-1* and *amp1-1 lamp1-2* plants. Arrows mark carpelloid floral organs (upper panel) and pin-like stamens lacking anthers (lower panel). Scale bars: 500 µm.

The spectrum of overlapping developmental defects between *amp1* and *zpr3-1 zpr4-1* is not restricted to the vegetative growth phase. The inflorescence number is significantly enhanced in *zpr3-1 zpr4-1* causing a comparable increase as found in *amp1-1* (Figure 6B). Since *zpr3-1 zpr4-1* plants are fully sterile like *amp1-1 lamp1-2,* their flower morphology was also analyzed. Both lines showed drastic defects in flower organ development including homeotic transformation of sepals to carpeloid-like organs and the formation of pin-shaped stamens without anthers (Figure 6C).

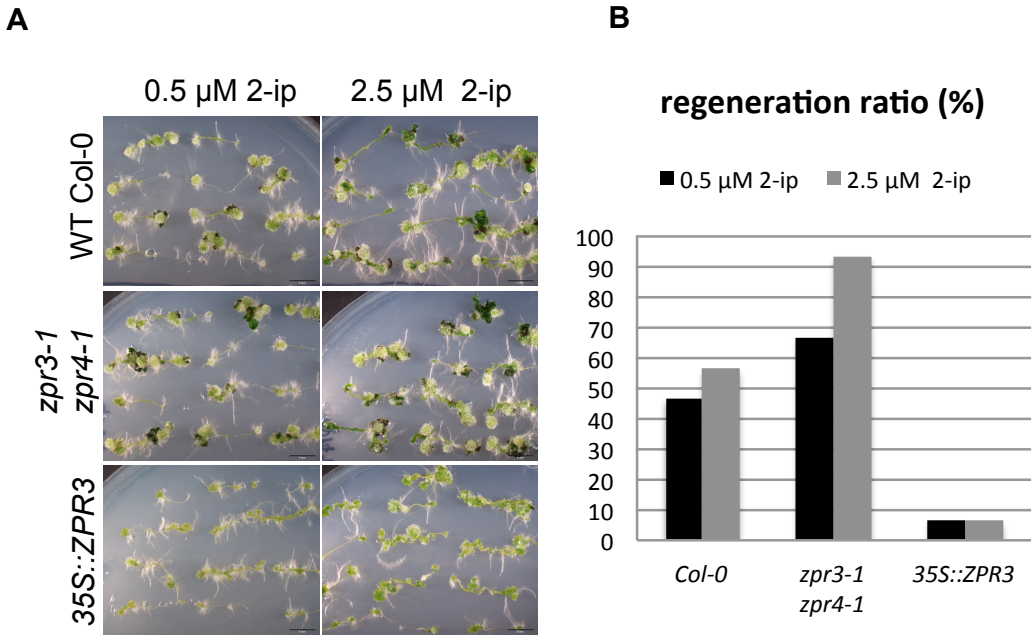

Figure 7. Enhanced HD-ZIP III activity promotes shoot *de novo* formation similar to *amp1*

(A) Comparison of the shoot regeneration capacity of wild type Col-0, *zpr3-1 zpr4-1* and *35S::ZPR3*. The root segments (approximately 1-1.5 cm) of 7-d-old Arabidopsis seedlings were grown on the SIM supplemented with 0.5 µM (left panel) or 2.5 µM (left panel) 2-ip, respectively. (B) Quantification of the regeneration ratio ($n \geq 15$).

The enhanced potential for shoot stem cell pool re-specification of *amp1* is also reflected in its increased shoot regeneration capacity in tissue culture (Chaudhury et al., 1993). Similar to *amp1*, *zpr3-1 zpr4-1* significantly promoted the shoot regeneration ability of root explants on shoot induction media (SIM) with different cytokinin concentrations (Figure 7A and B). In contrast, overexpressing *ZPR3* in

35S::ZPR3 nearly abrogated the shoot de novo formation capacity (Figure 7A and B).

Taken together, a number of analogous shoot, inflorescence and flower meristem alterations in *amp1-1* and *zpr3-1 zpr4-1* were identified, consistent with a model in which AMP1 controls shoot meristem organization by limiting HD-ZIP III over-accumulation.

1.3 *amp1* and *zpr3 zpr4* have a synergistic effect on SAM malformation

In light of the phenotypic similarity of *amp1-1* and *zpr3-1 zpr4-1*, the level of genetic interaction between these mutant lines was analyzed. Firstly, the aphenotypic *zpr4-1* single mutant was crossed with *amp1-1*. The resulting *amp1-1 zpr4-1* line showed a significantly increased true leaf number and also an elevated SAM size compared to the *amp1-1* parental line (Figure 5A, B and C). Moreover, mutating one *ZPR3* allele in *amp1-1 zpr4-1* further enhanced these defects: the leaf number was nearly doubled in *amp1-1 zpr3-1*$^{+/-}$ *zpr4-1* seedlings (Figure 5A and B) and their SAMs increased four-fold in size in relation to *amp1* (Figure 5C), whereas *zpr3-1*$^{+/-}$ *zpr4-1* plants did not show any obvious alterations in these parameters (data not shown). At the adult stage, a promoting effect of *zpr4-1* and *zpr3-1*$^{+/-}$ *zpr4-1* on the inflorescence number of *amp1* plants was also observed (Figure 6B).

The triple homozygous mutant *amp1-1 zpr3-1 zpr4-1* developed a severely over-proliferating shoot meristem with a completely distorted leaf initiation pattern, which is neither present in *amp1-1* nor in *zpr3-1 zpr4-1* (Figure 5A). Consistent with the strong meristematic hypertrophy, *pWUS::GUS* activity was dramatically expanded in *amp1-1 zpr3-1 zpr4-1* and was present in multiple domains of the supersized SAM (Figure 5E). At the stage of floral transition triple mutant meristems showed multiple *pWUS::GUS* positive foci surrounded by small organ primordia (Figure 6A), highly reminiscent of *amp1-1 lamp1-2* meristems (Huang et al., 2015).

In conclusion, *ZPR3/ZPR4* and *AMP1* demonstrate a strong synergistic genetic interaction in the control of shoot meristem organization, potentially by independently affecting HD-ZIP III activity/homeostasis.

1.4 Limiting HD-ZIP III activity by ectopic expression of *ZPR3* partially suppresses the *amp1* mutant phenotype

Next the impact of depleted HD-ZIP III activity on the shoot meristem phenotype of *amp1* was analysed by crossing the mutant with the *ZPR3* overexpression line *35S::ZPR3*.

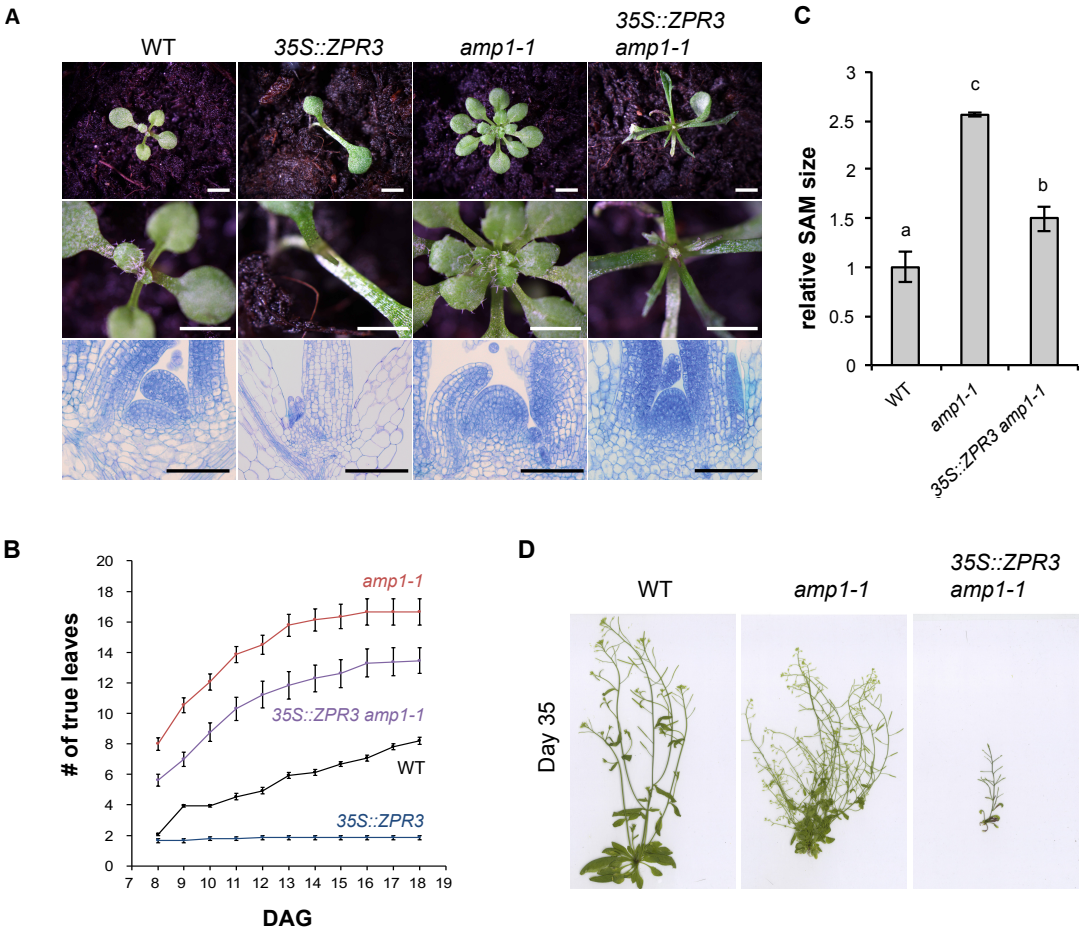

Figure 8. Limiting HD-ZIP III activity by ectopic ZPR3 expression partially suppresses *amp1* mutant phenotypes

(A) Phenotypes of 13-d-old wild type Col-0 (WT), *35S::ZPR3, amp1-1* and *35S::ZPR3 amp1-1* seedlings (upper and middle panel). Median longitudinal sections of SAMs from 7-d-old seedlings (lower panel). Scale bars: 2 mm (upper and middle panel), 50 µm (lower panel). (B) True leaf number quantification of the indicated genotypes from day 8 to day 18 (means ± SE of the mean; n ≥ 13). (C) Quantification of SAM area from median longitudinal sections of the indicated genotypes at 8 DAG (means ± SE of the mean; n ≥ 3). The SAM size was normalized to that of *amp1-1*. Different letters i.e., a, b and c over the error bars indicate significant differences at $p < 0.05$ levels as estimated by Duncan's multiple range test (DMRT). (D) Phenotypes of 35-d-old wild type Col-0 (WT), *amp1-1* and *35S::ZPR3 amp1-1* plants.

Approximately 30% of *35S::ZPR3* seedlings did not develop a shoot apical meristem but formed one radialized leaf-like organ between the cotyledons instead (Figure 8A). Those plants usually die off after a few days due to their inability to grow any further shoot organs. In the *amp1-1* background these severe *35S::ZPR3* plants still formed a functional SAM, however, the meristem size was significantly reduced compared to *amp1-1* (Figure 8A and C). *ZPR3* overexpression also significantly mitigated the increased leaf formation rate of *amp1-1* (Figure 8A and B). However, *35S::ZPR3 amp1-1* plants still produced more leaves than wild type, which showed polarity defects caused by reduced HD-ZIP III activity (Figure 8A). The suppressive effect of *35S::ZPR3* on *amp1-1* shoot meristem activity was even more pronounced in the adult growth phase. The elevated branching phenotype of *amp1-1* was completely abolished by *35S::ZPR3* (Figure 8D). Therefore, restricting HD-ZIP III function by overexpressing *ZPR3* can at least partially rescue AMP1-associated SAM phenotypes in different developmental stages.

1.5 Impact of AMP1 overexpression on *zpr3 zpr4*

To test whether ectopic expression of AMP1 can also conversely modulate the *zpr3 zpr4* phenotype, *35S::AMP1* was crossed with the double mutant. Although this line shows an approximately 20-times stronger *AMP1* expression compared to wild type (Poretska, 2016) it does not produce any obvious vegetative SAM phenotypes (Figure 9A), which is consistent with a recently reported *35S::AMP1-GFP* line (Shi et al., 2013b).

However, when brought into *zpr3-1 zpr4-1, 35S::AMP1* significantly reduced the size of the meristematic area compared to *zpr3-1 zpr4-1* without affecting the formation of the central protrusion (Figure 9A and C). Probably as a consequence, AMP1 overexpression also decreased the true leaf number only in the absence of ZPR3 and ZPR4 (Figure 9B). Thus, consistent with acting on the same regulatory module gain and loss of function alleles of ZPRs and AMP1 mutually affect each other's shoot meristem phenotypes.

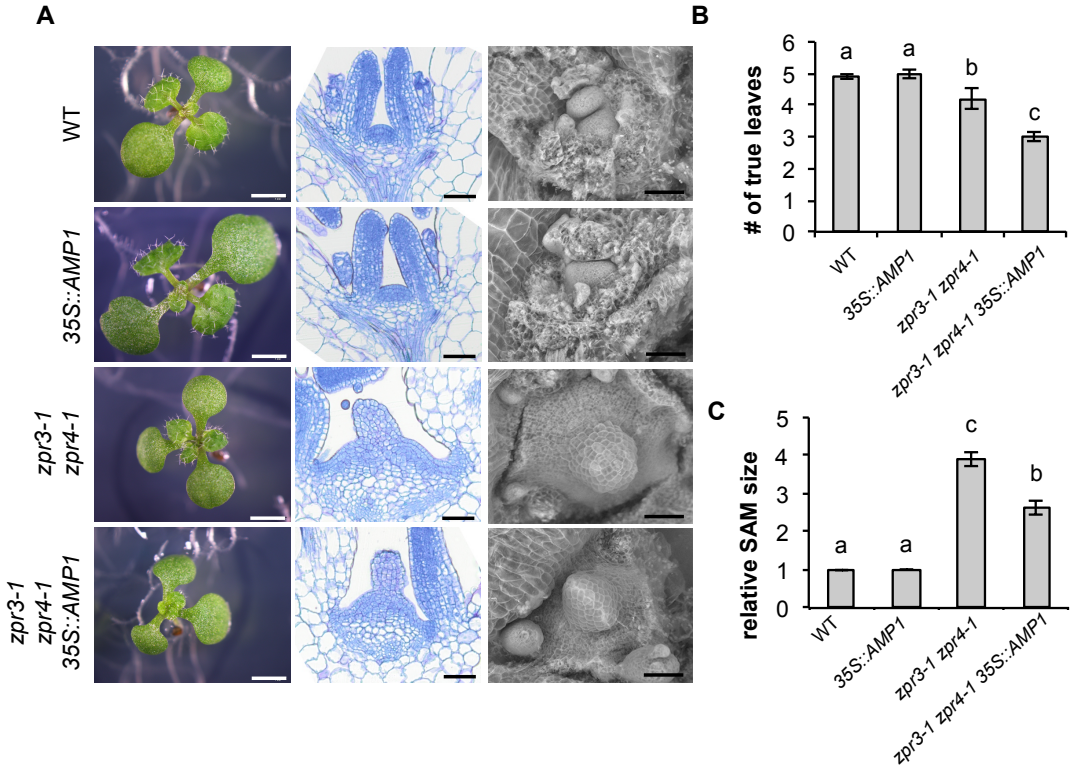

Figure 9. Impact of AMP1 ectopic expression on *zpr3-1 zpr4-1* mutant phenotypes

(A) Phenotypes of 12-d-old wild type Col-0 (WT), *35S::AMP1, zpr3-1 zpr4-1* and *zpr3-1 zpr4-1 35S::AMP1* seedlings (left panel). Median longitudinal sections of SAMs from 8-d-old seedlings (middle panel). Scanning electron micrographs of meristems from 8-d-old seedlings (right panel). Scale bars: 2 mm (left panel), 50 µm (middle and right panel). (B) True leaf number quantification of 12-d-old seedlings of the indicated genotypes (means ± SE of the mean; n ≥ 10). (C) SAM size quantification of the indicated genotypes at 8 DAG (means ± SE of the mean; n ≥ 6. The meristem size was normalized to that of wild-type Col-0. Different letters i.e., a, b and c over the error bars indicate significant differences at $p < 0.05$ levels as estimated by Duncan's multiple range test (DMRT).

1.6 HD-ZIP III protein accumulation but not distribution is altered in *amp1*

It has been previously shown that the miRNA165/166-mediated inhibition of HD-ZIP III translation is abolished in *amp1* and even more severely in *amp1 lamp1*, leading to an overall accumulation of HD-ZIP III proteins in these mutants (Li et al., 2013). The so far presented data of this thesis indicate that endogenous HD-ZIP III activity is indeed enhanced in *amp1* and contributes to the observed mutant defects in SAM organization and activity. The next aim was to refine how the loss of AMP1/LAMP1-dependent translational repression affects the tissue distribution of HD-ZIP III expression. This is of interest since the correct polar expression of these

transcription factors in adaxial and central domains is mainly determined by the activity of miRNA165/166.

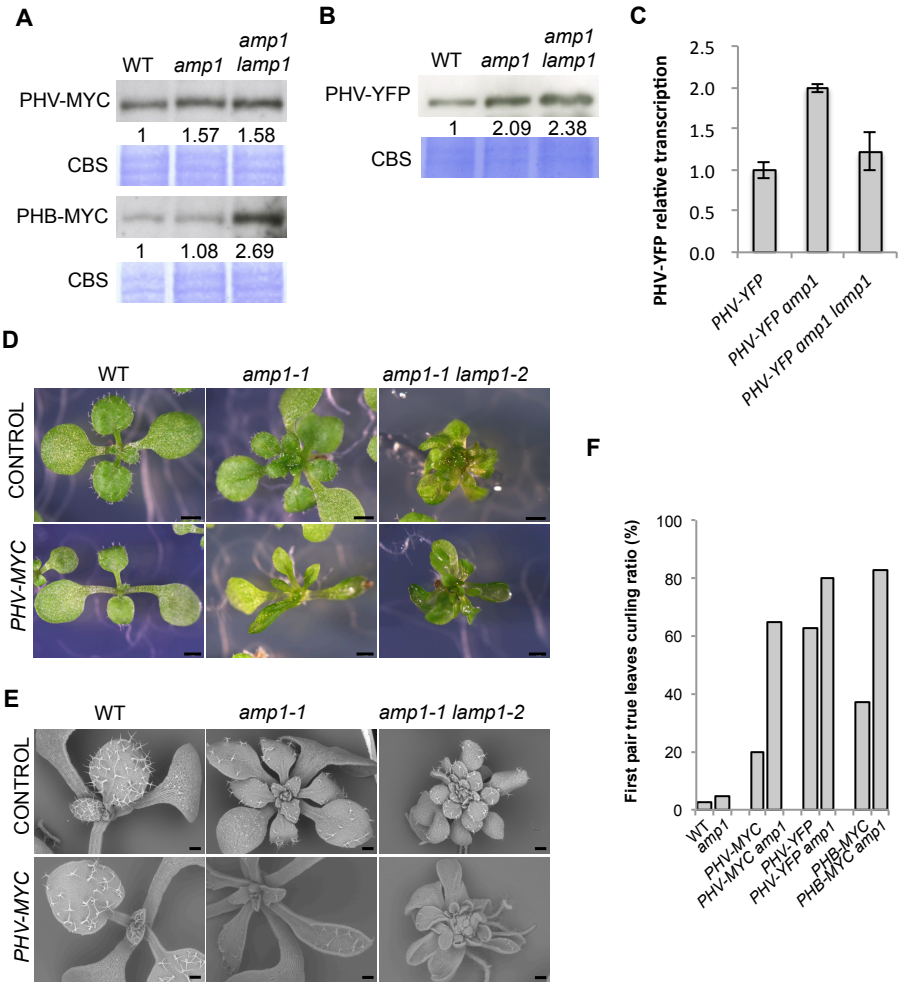

Figure 10. HD-ZIP III over-accumulation in *amp1* correlates with a higher tendency for leaf polarity defects

(A) Immunoblotting of protein extracts from 10-d-old *35S::PHV-MYC* and *35S::PHB-MYC* seedlings in the indicated genetic backgrounds. Autoradiogram: PHV-MYC and PHB-MYC detection using an anti-MYC antibody. Coomassie Blue staining (CBS) of the membrane is shown as a loading control. Normalized relative signal intensities are indicated. (B) Immunoblotting of protein extracts from 10-d-old *35S::PHV-YFP* seedlings in the indicated genetic backgrounds. Autoradiogram: PHV-YFP detection using an anti-GFP antibody. Coomassie Blue staining (CBS) of the membrane is shown as a loading control. Normalized relative signal intensities are indicated. (C) qPCR analysis of *PHV-YFP* expression in 10-d-old seedlings of the indicated genotypes. *UBC* was used as an internal control. The relative expression level of *PHV-YFP* was normalized to that of the wild-type background. The SE was calculated from three biological replicates. (D) *35S::PHV-MYC* in wild type Col-0 (WT), *amp1-1* and *amp1-1 lamp1-2* background, respectively. Phenotypes of 10-d-old *35S::PHV-MYC* seedlings in comparison with the respective control seedlings. Scale bars: 1 mm. (E) Scanning electron micrographs of the seedlings shown in D. Scale bars: 200 µm. (F) Upward curling ratio of the first pair of true leaves in 10-d-old seedlings of the indicated genotypes ($n \geq 20$).

To this end, *35S::PHV-MYC*, *35S::PHB-MYC* and *35S::PHV-YFP* lines were generated and crossed with *amp1-1* and *amp1-1 lamp1-2*. Consistent with published results (Li et al., 2013), overall protein levels of the tagged PHB and PHV versions were conclusively elevated in *amp1-1 lamp1-2*, whereas for *amp1* an increase could only be observed for the two PHV variants (Figure 10A and B). As previously described, the elevated protein abundance in *amp1-1 lamp1-2* is likely caused by the de-repression of the translation inhibition, since the transcription level in *amp1-1 lamp1-2* remained at a similar level to wild type (Figure 10C). On the other hand, this protein-specific increase was not observed in *amp1-1*, probably due to the remaining function of LAMP1 (Figure 10B and C). *HD-ZIP III* genes are master regulators of leaf adaxial identity and their elevated and/or ectopic expression leads in mild cases to upward curled leaves and in severe cases to trumpet-shaped adaxialized organs (McConnell et al., 2001; Emery et al., 2003). Accordingly, all three *PHV*/*PHB* overexpressing lines showed an increased ratio of upward curling leaves among the first pair of true leaves compared to wild type (Figure 10D-F). Notably, this effect was further promoted in the *amp1-1* mutant background (Figure 10D-F) and was fully penetrant in *amp1-1 lamp1-2* (Figure 10D and E). Thus, the observed over accumulation of HD-ZIP III proteins in *amp1* and *amp1 lamp1* correlates with advanced adaxialization of true leaves.

Next the spatial distribution of *PHV-YFP* was analysed in wild type, *amp1-1* and in *amp1-1 lamp1-2* leaves using confocal laser scanning microscopy. In wild type, although expressed under the 35S promoter, the PHV-YFP protein was only visible in the adaxial side of the leaf as expected based on the abaxial activity of miRNA 165/166 (Figure 11A). Notably, this adaxial localization of the PHV-YFP protein was not altered in *amp1-1* nor in *amp1-1 lamp1-2 (*Figure 11A) indicating that the miRNA165/166 triggered elimination of PHV expression is fully functional in these mutants. Meanwhile, in this analysis the fluorescence signal strength at the adaxial side of the mutant leaf sections was also not apparently enhanced compared to the wild type control. Due to the bigger meristem size in the mutants the PHV-YFP signal was clearly expanded in the SAM domain, however again the differences in signal strength in this area were only marginal between these genotypes. The tissue-distribution of the PHV-YFP reporter in primary roots was also analyzed.

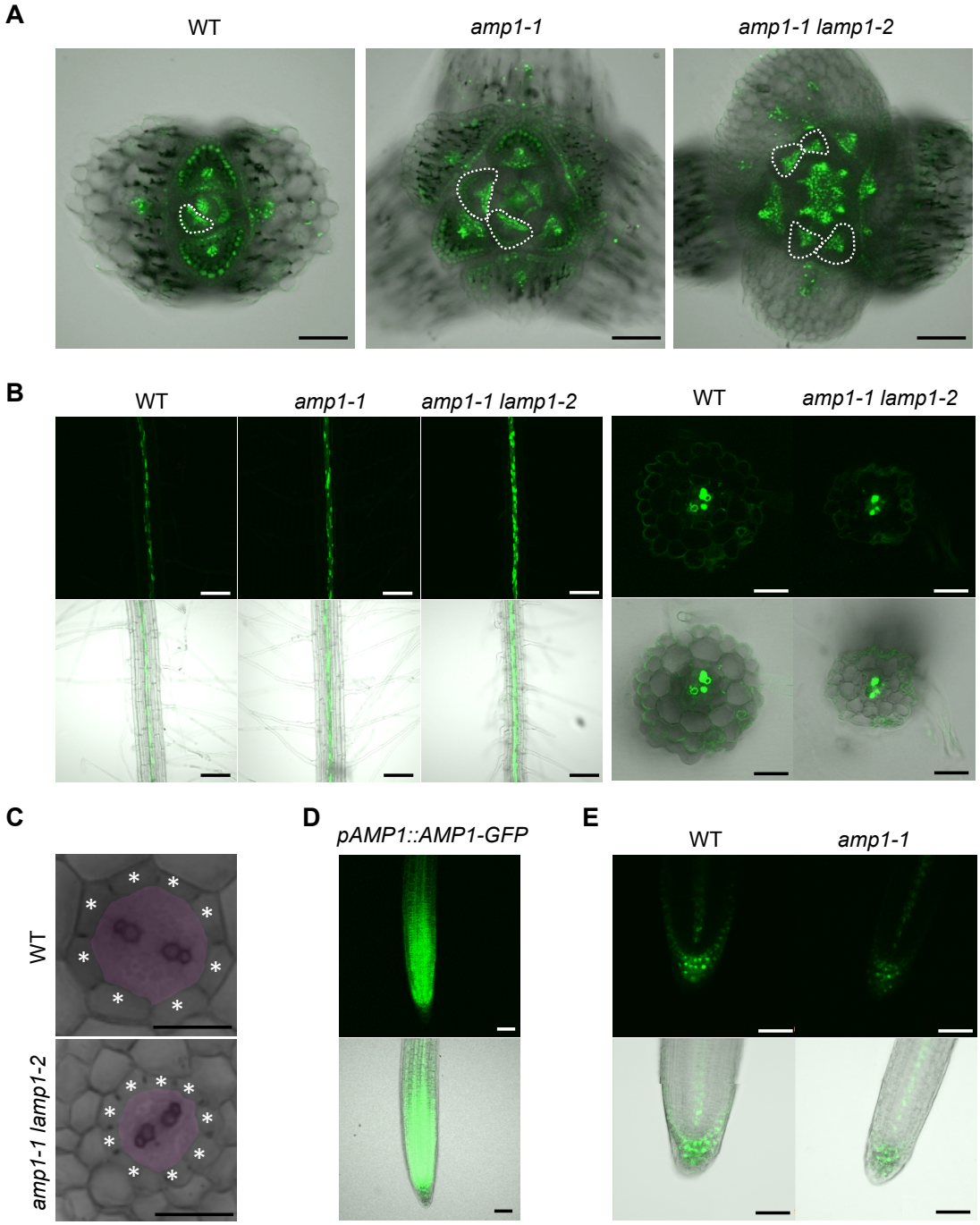

Figure 11. HD-ZIP III protein accumulation but not tissue distribution is affected in *amp1*

(A) Confocal images of shoot transverse vibratome sections prepared from 7-d-old *35S::PHV-YFP* seedlings in the indicated genetic background. Scale bars: 200 µm. (B) Confocal images of roots from 10-d-old *35S::PHV-YFP* seedlings in the indicated genetic background (left) and root transverse vibratome sections prepared from 10-d-old *35S::PHV-YFP* seedlings in the indicated genetic background (right). Upper panel: YFP signal; lower panel: overlay. Scale bars: 100 µm (left); scale bars: 50 µm (right). (C) Magnified transverse sections of roots from 10-d-old *35S::PHV-YFP* seedlings in the indicated genetic background, vascular cylinder labeled in red. Asterisks mark the surrounding endodermis cell layer. Scale bars: 50 µm. (D) Confocal images of root tip from 10-d-old *pAMP1::AMP1-GFP* seedlings. Upper panel: YFP signal; lower panel: overlay. Scale bars: 50 µm. (E) Confocal images of root tips from 8-d-old *35S::PHV-YFP* seedlings in the indicated genetic background. Upper panel: YFP signal; lower panel: overlay. Scale bars: 50 µm.

In wild type, HD-ZIP III expression is confined to the vascular cylinder by the presence of miRNA 165/166 in the endodermis (Carlsbecker et al. 2010; Figure 11B). Similar to the leaf, PHV-YFP expression in *amp1-1* and *amp1-1 lamp1-2* was present in the same tissues as in wild type and did not show any expansion to areas of miRNA165/166 activity (Figure 11B).

However, in longitudinal optical sections the PHV-YFP signal intensity in the central domain was clearly stronger in *amp1-1* and even more enhanced in *amp1-1 lamp1-2* compared to the wild type control (Figure 11B). When analysed in transversal sections the PHV-YFP stayed restricted to procambial tissues in *amp1-1 lamp1-2* (Figure 11B). Moreover, the vascular cylinder of *amp1-1 lamp1-2* has a smaller diameter compared to wild type (Figure 11C). A similar pattern was observed in the root tip, where AMP1 is strongly expressed in the division zone of the root meristem (Vidaurre et al., 2007; Figure 11D). In both *amp1-1* and the wild-type background, the PHV-YFP signal was identically restricted to the vasculature and the root cap (Figure 11E). Thus the stronger PHV-YFP signal in *amp1-1* and *amp1-1 lamp1-2* roots is not the result of an expanded vascular cylinder nor due to ectopic expression outside the vascular tissues, but rather caused by stronger expression level of the reporter per cell. Taken together, absence of AMP1/LAMP1 did not change the miRNA-dependent polarized expression of PHV in leaves and roots but increased PHV expression areas in the shoot meristem and PHV expression strength in the vascular cylinder of the root.

2. AMP1 controls shoot stem cell pool activity in Arabidopsis by limiting the expression of the AP2/ERF transcription factor RAP2.6L

2.1 *RAP2.6L* expression is upregulated in *amp1*

To identify additional downstream components through which AMP1 controls shoot meristem organization and activity the recently published *amp1* transcriptome data were screened for genes known to function in SAM regulation (Poretska et al., 2016). In this analysis, the AP2/ERF transcription factor RAP2.6L, a key regulator of *de novo* shoot formation (Che et al., 2006) was found to be significantly upregulated in *amp1-13*. Since *amp1* shows ectopic OC formation in the shoot meristem periphery (Huang et al., 2015), the functional relationship between these two factors was further investigated.

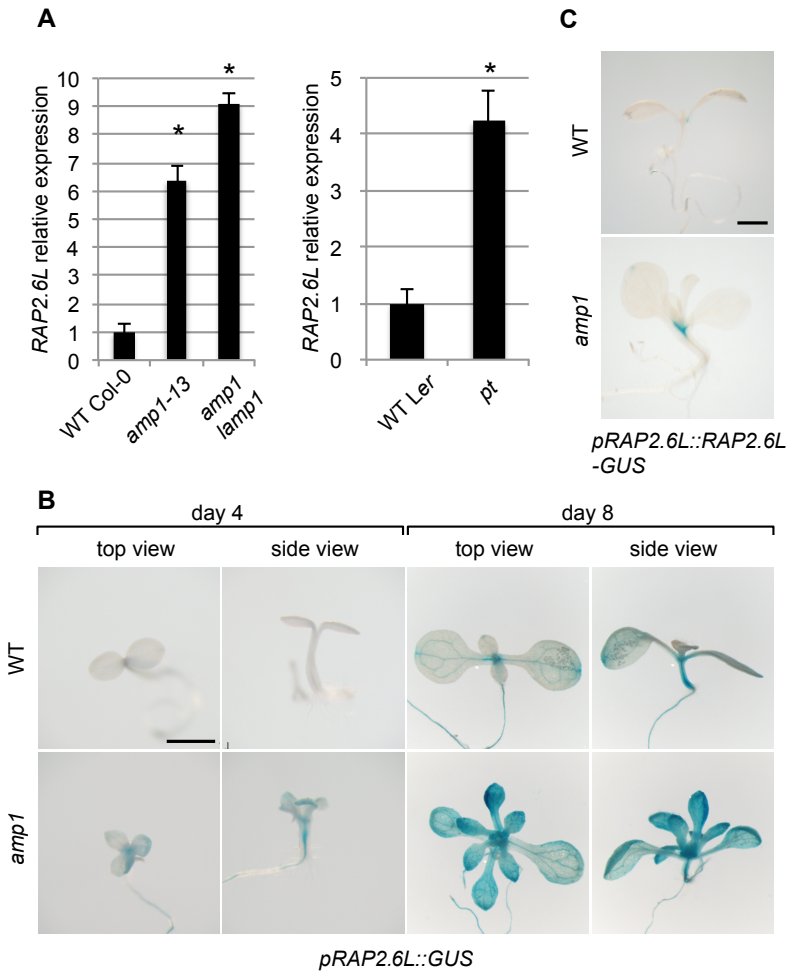

Figure 12. *RAP2.6L* expression is upregulated in *amp1*

(A) qPCR analysis of *RAP2.6L* expression in 8-d-old seedlings of the indicated lines. Fold changes compared to the respective wild-type (WT) are shown. The SE was calculated from three biological replicates after normalization to *UBC*. Asterisks indicate significant difference (Student's 2-tailed t-test; $p < 0.05$). (B) *pRAP2.6L::GUS* activity in wild-type Col-0 (WT) and *amp1-1* at 4 DAG and 8 DAG. Scale bar: 2 mm. (C) *pRAP2.6L::RAP2.6L-GUS* activity in wild-type Col-0 (WT) and *amp1-1* at 8 DAG. Scale bar: 1 mm.

Initially, the misexpression of *RAP2.6L* was verified by quantitative real-time PCR analysis in *amp1-13* (Col-0 background), *primordia timing* (*pt,* L*er* background) and *amp1-1 lamp1-2* (Col-0 background). Consistent with the microarray data, *RAP2.6L* was strongly upregulated in all three *amp1* alleles (Figure 12A). In contrast to *RAP2.6L*, none of its closest paralogs in the ERF-TF subfamily group X, including *RAP2.6 (At1g43160)*, *ERF112 (At2g33710), EBE (At5g61890)* and *ERF115 (At5g07310)* showed a comparable misexpression in *pt* (Figure 13A).

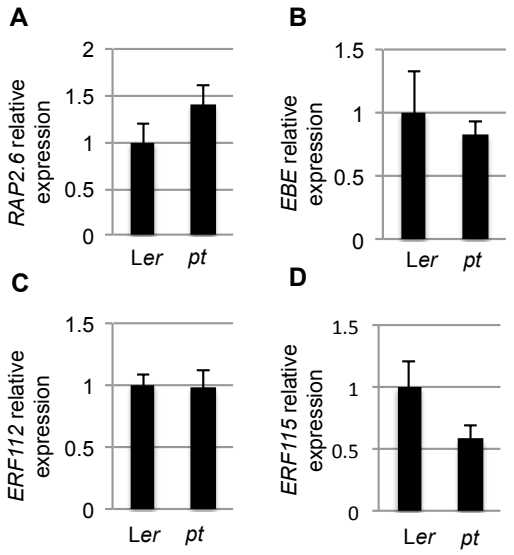

Figure 13. Expression analysis of ERF transcription factors closely related to *RAP2.6L*

(A-D) qPCR analysis of *RAP2.6* (A), *EBE* (B), *ERF112* (C) *and ERF115* (D) expression in 8-d-old seedlings of the indicated lines. The SE was calculated from three biological replicates. *UBC* was used as an internal control.

In order to further characterize the tissue-specific activation of *RAP2.6L* in *amp1*, the transcriptional GUS reporter *pRAP2.6L::GUS* was created. Similar to the previously reported *RAP2.6L promoter:GUS* line (Che et al., 2006), this reporter showed strong staining in the shoot apex, the hypocotyl and vascular tissues in 8-day-old seedlings (Figure 12B), with the only exception that the reported expression front in young leaf primordia connected to leaf maturation processes (Che et al., 2006) was not observed. Elimination of AMP1 function led to a prominent enhancement of *pRAP2.6L::GUS* activity. 4-day-old *amp1* seedlings showed strong staining in shoot apices and vascular tissues, while in the wild-type background the staining was barely visible (Figure 12B). Likewise, 8-day-old *amp1-1* seedlings demonstrated an overall enhanced staining, especially in young leaf primordia, where the staining was barely visible in the wild-type background (Figure 12B). To analyze the expression level of RAP2.6L protein in *amp1*, the translational reporter *pRAP2.6L::RAP2.6L-GUS* (Krishnaswamy et al., 2011) was crossed with *amp1-1*. Consistent with the increase at the transcription level, RAP2.6L protein expression in *amp1* was enhanced in and

around the shoot apex (Figure 12C).

To test whether the augmented *RAP2.6L* expression is caused by the high endogenous cytokinin levels in *amp1* (Nogué et al., 2000b), the response of *pRAP2.6L::GUS* activity to cytokinin was tested by short- and long-term *trans*-zeatin treatments. As shown in Figure 14, none of these treatments affected the *pRAP2.6L::GUS* staining pattern or intensity, neither in wild type nor in *amp1-1* (Figure 14), indicating that the pronounced *RAP2.6L* expression in *amp1* is not triggered by the accumulation of this hormone. Taken together, RAP2.6L shows enhanced and partially ectopic expression in *amp1* in a cytokinin-independent manner and this upregulation is most prominent in shoot tissues with high AMP1 expression levels such as young leaf primordia (Vidaurre et al., 2007).

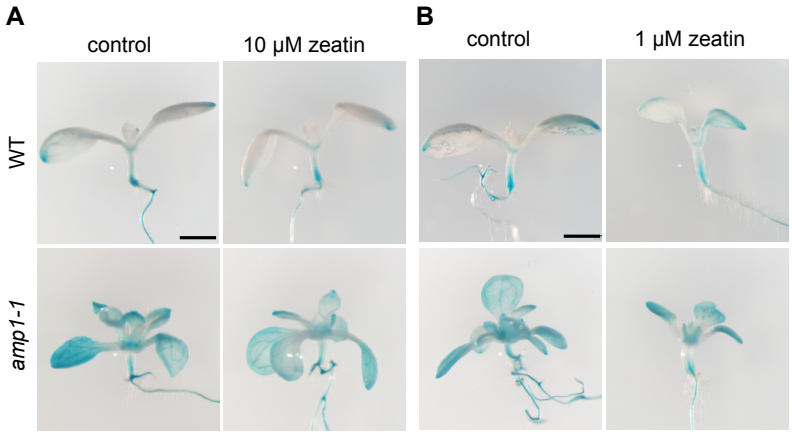

Figure 14. *RAP2.6L* expression is not affected by cytokinin

(A, B) *pRAP2.6L::GUS* activity in wild-type Col-0 (WT) and *amp1-1* seedlings. Seedlings were either grown on ½ MS medium for 8 days followed by 24h short-term treatment with 10 µM zeatin (A) or grown on ½ MS containing 1 µM zeatin (B) for 8 days (long-term treatment). Scale bars: 1 mm.

2.2 Overexpression of *RAP2.6L* causes *amp1*-related shoot phenotypes

To investigate whether the enhanced *RAP2.6L* expression contributes to the SAM phenotypes of *amp1*, the effect of RAP2.6L overexpression on shoot meristem activity was analyzed by using *35S::RAP2.6L (*named *RAP2.6L-OX* throughout this study*)* (Krishnaswamy et al., 2011). Like *amp1*, this line showed an increased true leaf formation rate, and this effect became apparent from day 20 on under short-day conditions (Figure 15A and B). Since the elevated leaf formation in *amp1* is associated with a hypertrophic SAM, the meristem architecture of *RAP2.6L-OX*

seedlings were assessed by scanning electron microscopy (SEM) and microscopic analysis of median longitudinal sections. *RAP2.6L-OX* seedlings not only displayed a larger SAM surface (Figure 15C) but also an increased apical-basal expansion of the SAM in median longitudinal sections (Figure 15D and E).

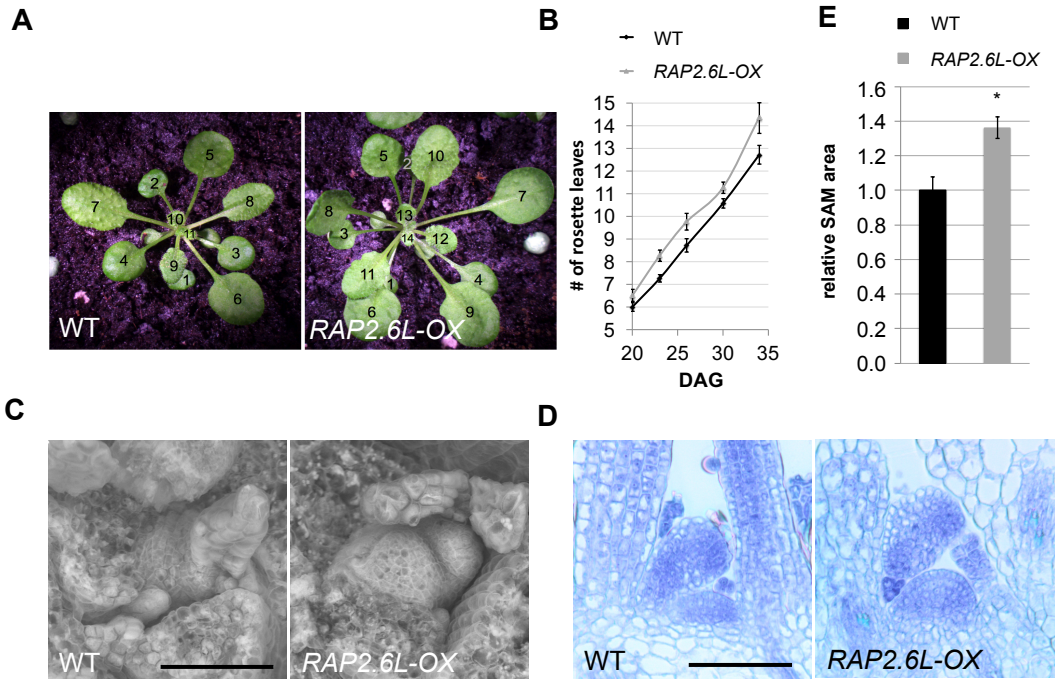

Figure 15. *RAP2.6L-OX* plants show *amp1*-related vegetative phenotypes

(A) Wild-type Col-0 (WT) and *RAP2.6L-OX* plants grown under short-day for 34 days. Leaves are numbered in the consecutive order of appearance. (B) Quantification of rosette leaves in wild-type Col-0 (WT) and *RAP2.6L-OX* plants at the indicated time points grown under short-day (means ± SE of the mean; n ≥ 8). (C) Scanning electron micrographs of SAM areas of wild-type Col-0 (WT) and *RAP2.6L-OX* seedlings grown under short-day for 18 days. (D) Median longitudinal SAM sections of wild-type Col-0 (WT) and *RAP2.6L-OX* seedlings grown under short-day for 18 days. (E) Quantification of SAM area from median longitudinal sections of wild-type Col-0 (WT) and *RAP2.6L-OX* seedlings. Normalized values (WT=1) are shown (means ± SE of the mean; n ≥ 3). Asterisk indicates significant difference ($p < 0.05$) as assessed by one-way ANOVA. Scale bars: 50 µm.

In previous studies, the ectopic SAM activity of *amp1* was also reflected by the enhanced expression of several SAM-related marker genes (Huang et al., 2015; Poretska et al., 2016). Along with the increased SAM size, an enlargement of the OC domain (*pWUS::GUS*; Figure 16) as well as of the stem cell pool (*pCLV3::GUS*; Figure 16) was observed in *RAP2.6L-OX*, to an extent resembling the early

developmental stages of weak *amp1* alleles (Huang et al., 2015). Moreover, as found in the faster forming leaves of *amp1* (Poretska et al., 2016), the expression area of the mitotic reporter *CYCLIN B1;1 (CYCB1;1)::GUS* also largely expanded in the shoot meristematic area and in young leaf primordia of *RAP2.6L-OX* plants (Figure 16). Additionally, the activity of *pKLU::GUS,* a reporter for the SAM boundary marker *CYP78A5/KLUH* (Wang et al., 2008), was also significantly broadened in *RAP2.6L-OX* (Figure 16). Notably, *CYP78A5/KLUH* had been repeatedly reported to be prominently upregulated in *amp1* (Helliwell et al., 2001; Griffiths et al., 2011; Poretska et al., 2016).

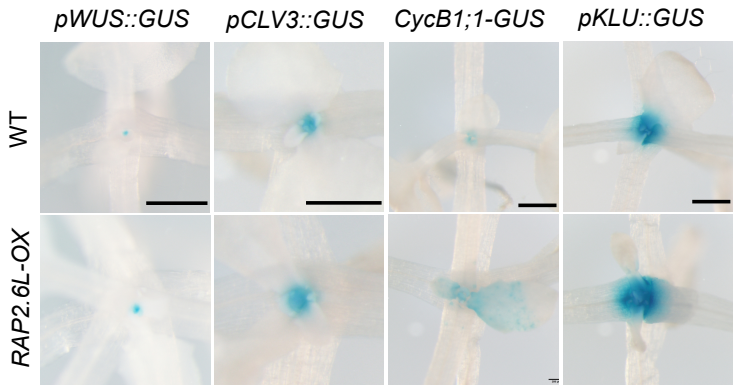

Figure 16. Comparison of GUS activities of indicated reporter lines in wild type and *RAP2.6L-OX* seedlings grown under short day

Except for *pWUS::GUS* (18 DAG) plants were analyzed at 15 DAG. Size bars: 500 µm.

As previously described (Krishnaswamy et al., 2011), overexpression of *RAP2.6L* also leads to a significant reduction in flowering time under long day conditions, which was also observed in *amp1* (Figure 17A). When grown under short day conditions (8 h light/ 16 h dark) under which wild-type plants show constant vegetative growth, both *RAP2.6L-OX* and *amp1* were able to initiate inflorescences at 20 to 27 days after germination (DAG) (Figure 17A and B). Moreover, both genotypes initiated abundant rosette and cauline branches, resulting in a similar compact inflorescence structure (Figure 17B and C). In conclusion, *RAP2.6L* overexpression lines partially phenocopy the growth alterations of *amp1*, especially its SAM defects, both in the vegetative and reproductive growth stage.

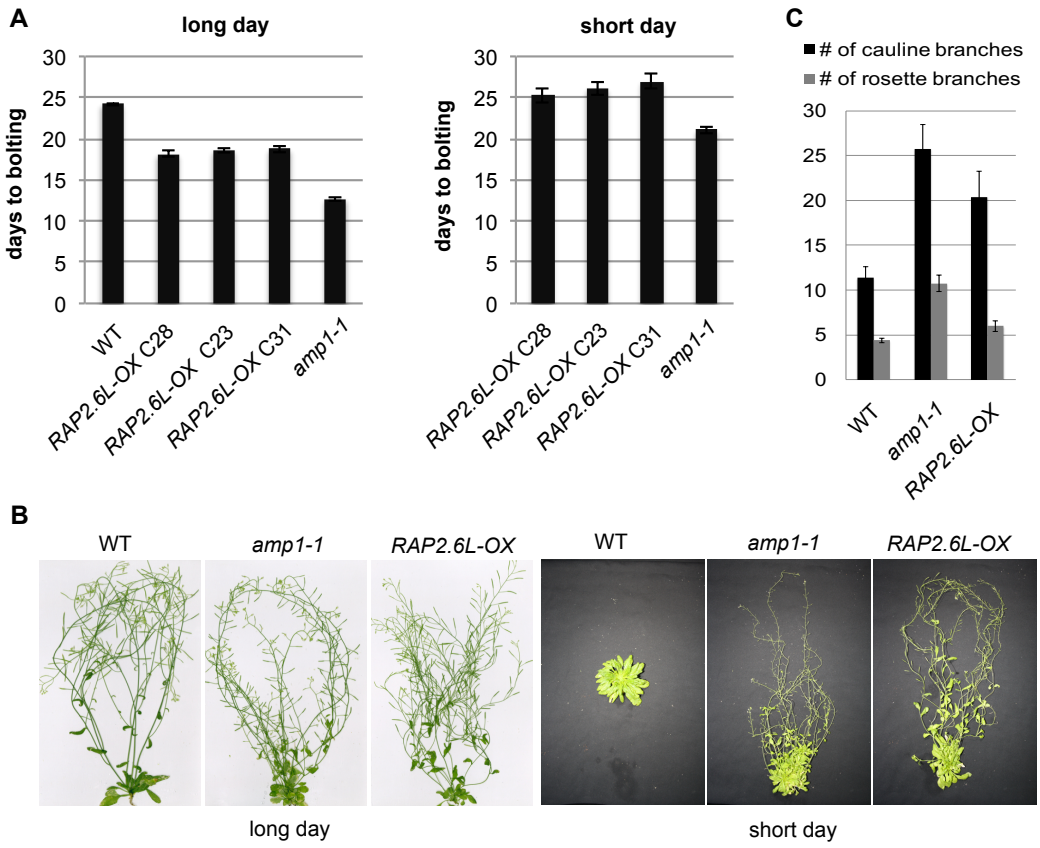

Figure 17. *RAP2.6L-OX* plants show *amp1*-related adult phenotypes

(A) Quantification of flowering time of indicated genotypes grown under long day (left panel) and short day (right panel). Graphs show means ± SE of the mean; n ≥ 15. (B) Comparison of wild-type Col-0 (WT), *amp1-1* and *RAP2.6L-OX* shoots grown under long day (70 DAG) or short-day (86 DAG). (C) Quantification of the rosette branch number and cauline branch number of 70-d-old wild-type Col-0 (WT), *amp1-1* and *RAP2.6L-OX* plants grown under long day (means ± SE of the mean; n ≥ 4).

2.3 Compromised RAP2.6L function suppresses the enhanced leaf formation rate of *amp1*

Based on the observations that *RAP2.6L* is upregulated in *amp1* and ectopic RAP2.6L expression leads to *amp1*-like shoot growth defects, it can be speculated that AMP1 controls SAM activity by restraining the spatio-temporal expression of RAP2.6L. To verify this assumption, the effect of RAP2.6L inactivation as well as inactivation of its closest paralogs was analyzed in wild type and *amp1*.

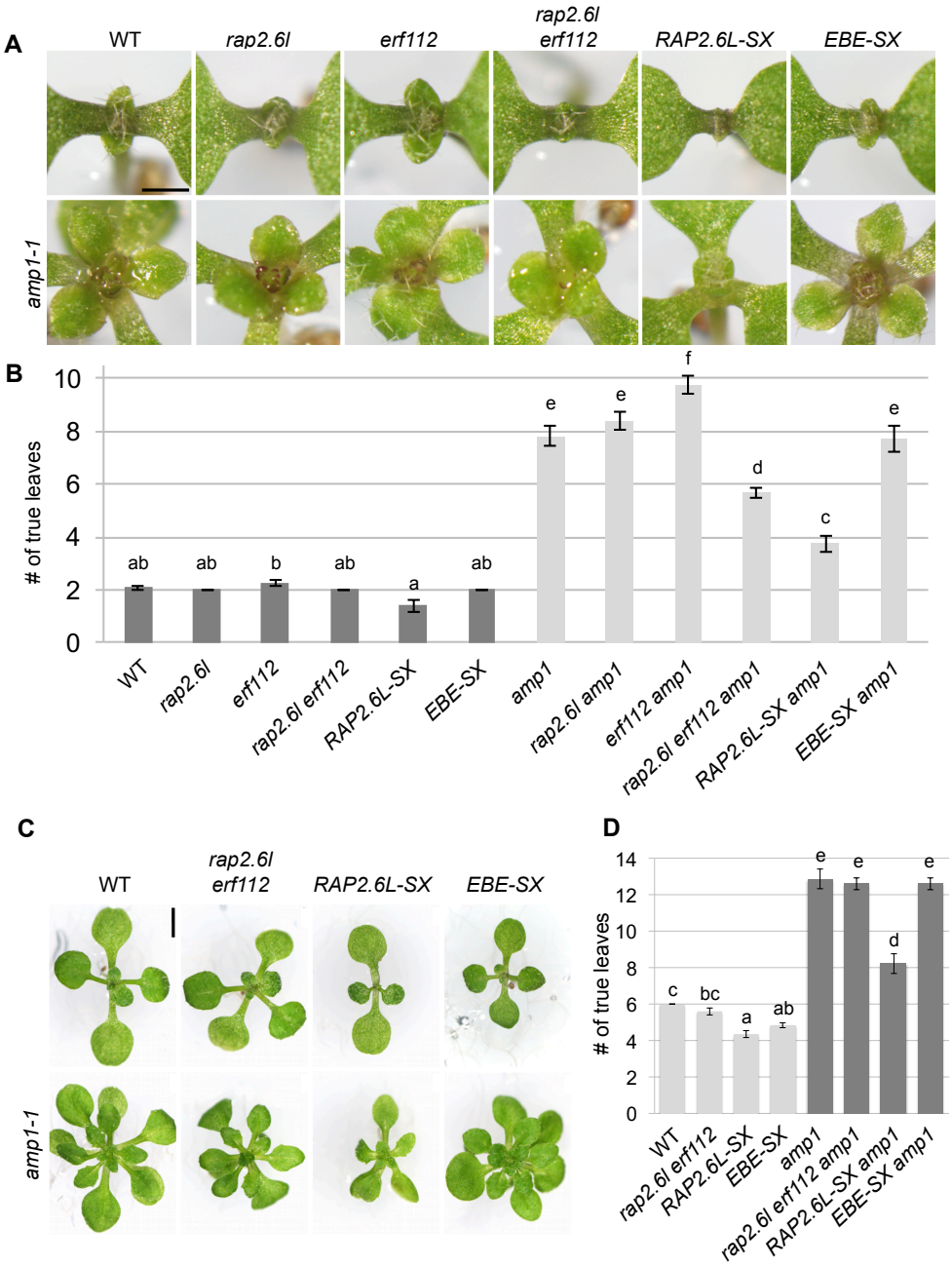

Figure 18. Compromised RAP2.6L function suppresses the enhanced leaf formation rate of *amp1*

(A) Shoot apices of wild-type Col-0 (WT), *rap2.6l-1, erf112-1, rap2.6l-1 erf112-1, RAP2.6L-SX* and *EBE-SX* seedlings at 7 DAG (upper panel). Shoot apices of the same lines in the *amp1-1* background at 7 DAG (lower panel). Scale bar: 500 µm. (B) Quantification of true leaf number of the indicated genotypes at 7 DAG (means ± SE of the mean; n ≥ 10). (C) Comparison of wild-type Col-0 (WT), *rap2.6l-1 erf112-1, RAP2.6L-SX* and *EBE-SX* seedlings at 12 DAG. Seedlings of the same lines in the *amp1-1* background at 12 DAG (lower panel). Scale bar: 2 mm. (D) Quantification of true leaf number of the indicated genotypes at 12 DAG (means ± SE of the mean; n ≥ 8).

To this end, available T-DNA insertion lines for *RAP2.6L*, *RAP2.6* and *ERF112* were used. In addition, the SRDX transcriptional repression domain and the *MYC* epitope tag were fused to the 35S-driven ORFs of RAP2.6L and EBE, resulting in the transgenic lines *RAP2.6L-SX* and *EBE-SX*, respectively. Except of a slightly retarded outgrowth of the first pair of true leaves in *rap2.6l*, the loss-of-function single mutants of *RAP2.6L*, *RAP2.6* and *ERF112* did not show a measurable impact on leaf formation neither in the wild-type nor *amp1* background (Figure 18A and B, 16A and B).

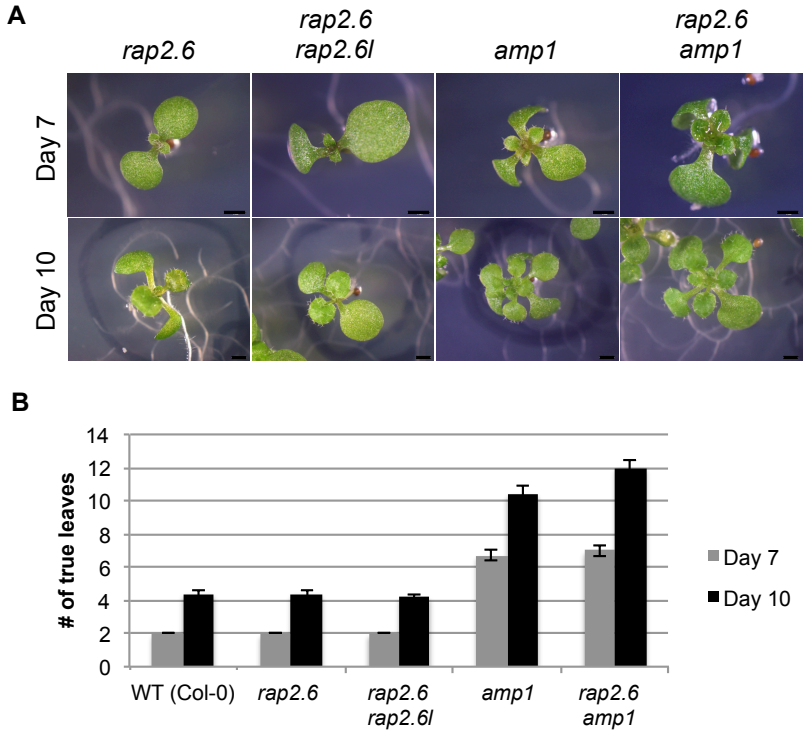

Figure 19. Effect of compromised *RAP2.6* function on leaf formation rate and shoot regeneration

(A) Comparison of *rap2.6-2, rap2.6-2 rap2.6l-1, amp1-1* and *rap2.6-2 amp1-1* seedlings at 7 DAG (upper panel) and 10 DAG (lower panel). Scale bars: 1 mm. (B) Quantification of true leaf number of wild-type Col-0, *rap2.6-2, rap2.6-2 rap2.6l-1, amp1-1* and *rap2.6-2 amp1-1* at 7 DAG and 10 DAG (means ± SE of the mean; n ≥ 10).

Whereas *rap2.6l rap2.6* was also aphenotypic in this respect (Figure 19A and B), a suppressive effect of *rap2.6l erf112* on the enhanced leaf formation rate of *amp1* was observed in 7-day-old seedlings (Figure 18A and B), which disappeared again in later developmental stages (Figure 18C and D). *RAP2.6L-SX* was even more potent in rescuing the enhanced leaf production of *amp1* at 7 DAG, and this effect persisted

during the vegetative growth phase. Notably, the relative suppression in leaf number by *RAP2.6L-SX* was stronger in *amp1* (7 DAG: 52%; 12 DAG: 36%) than in wild type (7 DAG: 32%; 12 DAG: 27%) supporting a specific genetic interaction rather than an independent effect (Figure 20).

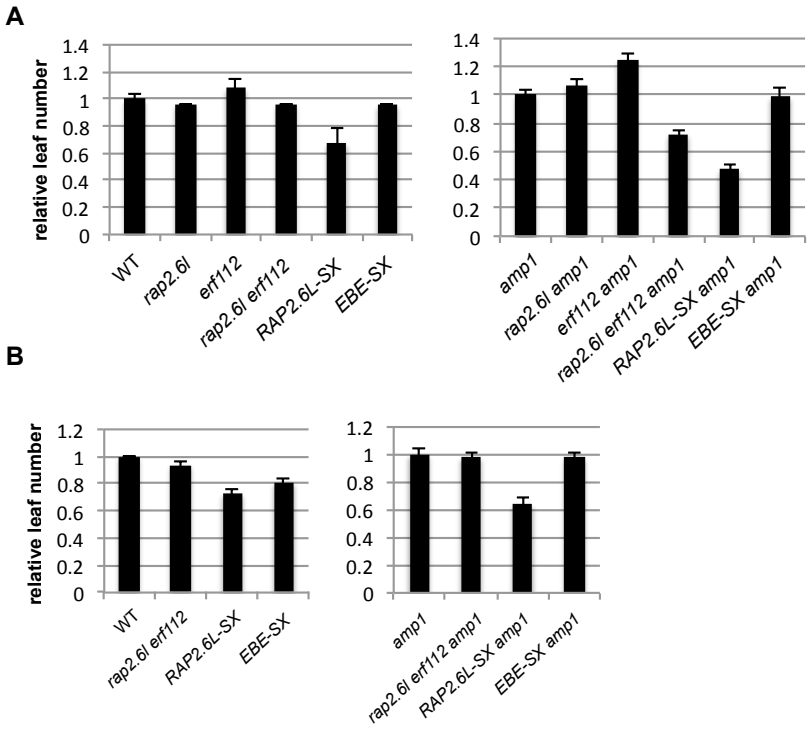

Figure 20. Effect of compromised *RAP2.6L* function on the leaf formation rate of *amp1*

(A, B) Normalized presentation of absolute leaf quantification data of indicated genotypes shown in Figure 7B (A, 7 DAG) and Figure 7D (B, 12 DAG). WT values (left graph) or *amp1-1* values (right graph) were set to 1.

Furthermore, although *EBE-SX* also affected the leaf formation rate in the wild-type background with increasing efficiency during development, its suppressive effect on *amp1* was only marginal (Figure 18A-D). Taken together, these data suggest that de-regulated *RAP2.6L* expression in *amp1* contributes to its shortened plastochron.

2.4 Compromised RAP2.6L function minimizes SAM over-proliferation in *amp1*

To investigate whether the SAM expansion phenotype of *amp1* is also specifically affected by the perturbation of RAP2.6L function, the SAM structures of these ERF transcription factor defective lines in the wild-type and *amp1* background were analyzed. SAM area determination in median longitudinal shoot sections revealed that except of *erf112*, all lines showed a slight but not significant reduction in meristem

size in the wild-type background (Figure 21A and B).

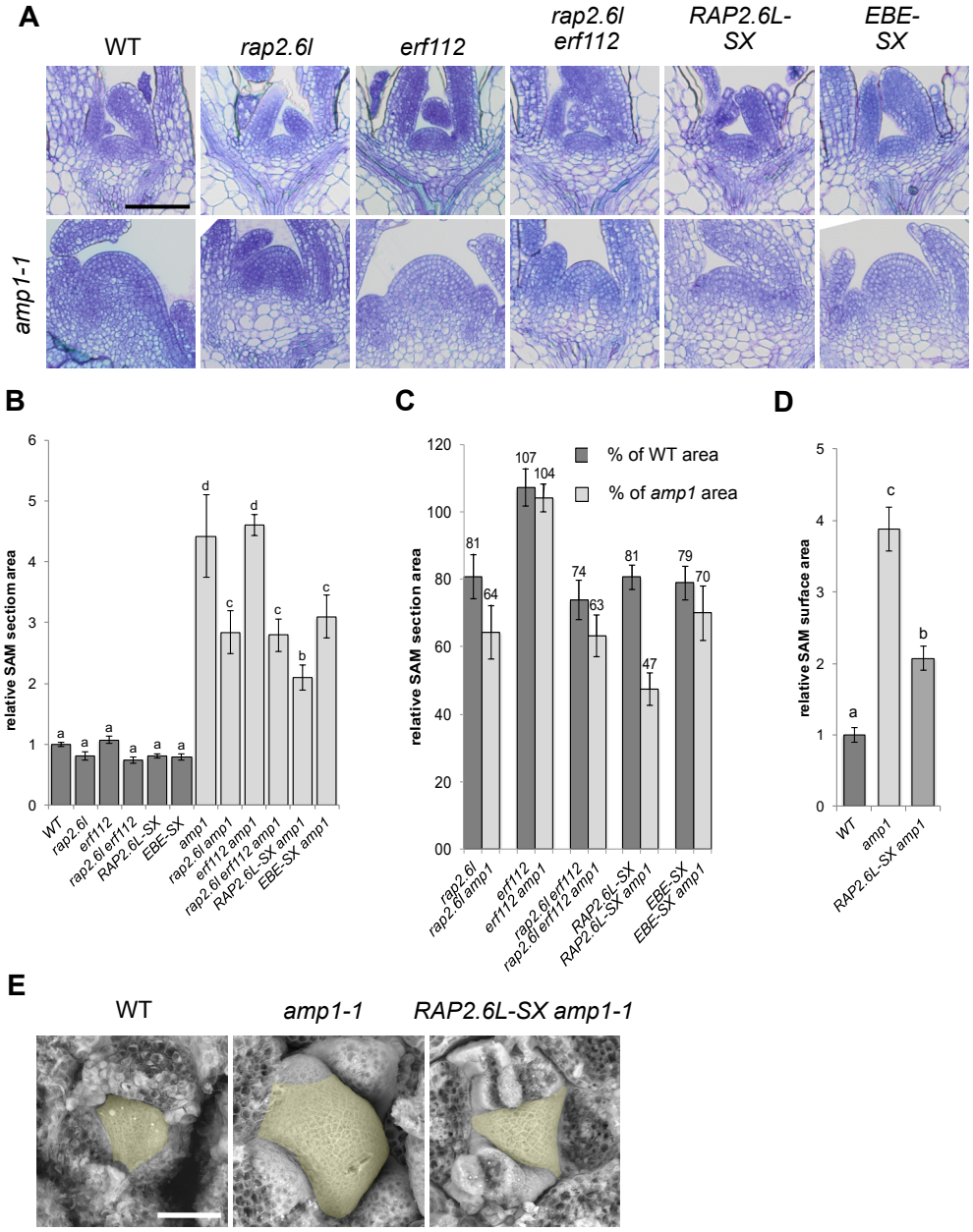

Figure 21. Compromised RAP2.6L function affects SAM size in *amp1*

(A) Median longitudinal SAM sections of wild-type Col-0 (WT), *rap2.6l-1, erf112-1, rap2.6l-1 erf112-1, RAP2.6L-SX* and *EBE-SX* at 7DAG. Median longitudinal SAM sections of the same lines in the *amp1-1* background at 7 DAG (lower panel). Size bars: 50 µm. (B) SAM area quantification from median longitudinal sections of the indicated genotypes at 7 DAG (means ± SE of the mean; n ≥ 4). The SAM areas were normalized to that of wild-type Col-0 (WT = 1). Different letters over the error bars indicate significant differences ($p < 0.05$) as estimated by Duncan's multiple range test. (C) Relative reduction of median SAM section areas by the indicated genotypes compared to wild-type Col-0 (WT) and *amp1-1* based on the data shown in (B). (D) SAM surface quantification from scanning electron micrographs of the indicated genotypes at 7 DAG (means ± SE of the mean; n ≥ 3). The SAM areas were normalized to that of wild-type Col-0 (WT = 1). (E) SAM scanning electron micrographs of wild-type Col-0 (WT), *amp1-1* and *RAP2.6L-SX amp1-1* seedlings. The SAM areas are highlighted in yellow. Size bar: 50 µm.

In contrast, the presence of *RAP2.6L-SX* reduced the SAM size in *amp1* by over 50%. Meanwhile, to a less pronounced extent, *rap2.6l*, *rap2.6l erf112* and *EBE-SX* also significantly suppressed the *amp1* SAM size, although *erf112* was again ineffective. The striking suppressive impact of *RAP2.6L-SX* on the meristematic overproliferation of *amp1* was also reflected in a clear reduction of the SAM surface area in SEM images, diminishing the visible area from around 400% to 200% compared to wild type (Figure 21D and E). Thus, perturbation of RAP2.6L function not only suppresses the increased true leaf production of *amp1* but also mitigates its abnormal SAM expansion phenotype.

2.5 RAP2.6L mediates the enhanced shoot regeneration capacity of *amp1*

RAP2.6L was originally described to be required for *de novo* shoot formation in tissue culture (Che et al., 2006) and *amp1* has been reported to show a higher shoot-regenerative capacity (Chaudhury et al., 1993) as well as ectopic shoot stem cell marker expression in the root (Poretska et al., 2016). To assess whether increased expression of *RAP2.6L* contributes to the elevated *de novo* SAM formation in *amp1*, we also analyzed the impact of RAP2.6L deficiency on this process. As previously shown (Che et al., 2006), *rap2.6l* displayed diminished regeneration of shoots from root explants (Figure 22A and B). Furthermore, *rap2.6l erf112* and *RAP2.6L-SX* showed an even stronger defect in this process, whereas *erf112* and *EBE-SX* were unaffected (Figure 22A and B). Intriguingly, *RAP2.6L* overexpression prominently promoted the shoot *de novo* formation capacity almost to the same extent as in *amp1-1*. Conversely, the presence of *RAP2.6L-SX* or *rap2.6l erf112* suppressed the elevated shoot regeneration of *amp1* to levels similar or even lower than wild type. Again, the effect of *rap2.6l*, *erf112* and *EBE-SX* were much more subtle in this respect. Together these findings provide evidence that the upregulated expression of RAP2.6L in *amp1* contributes to the enhanced shoot regeneration capacity of the mutant.

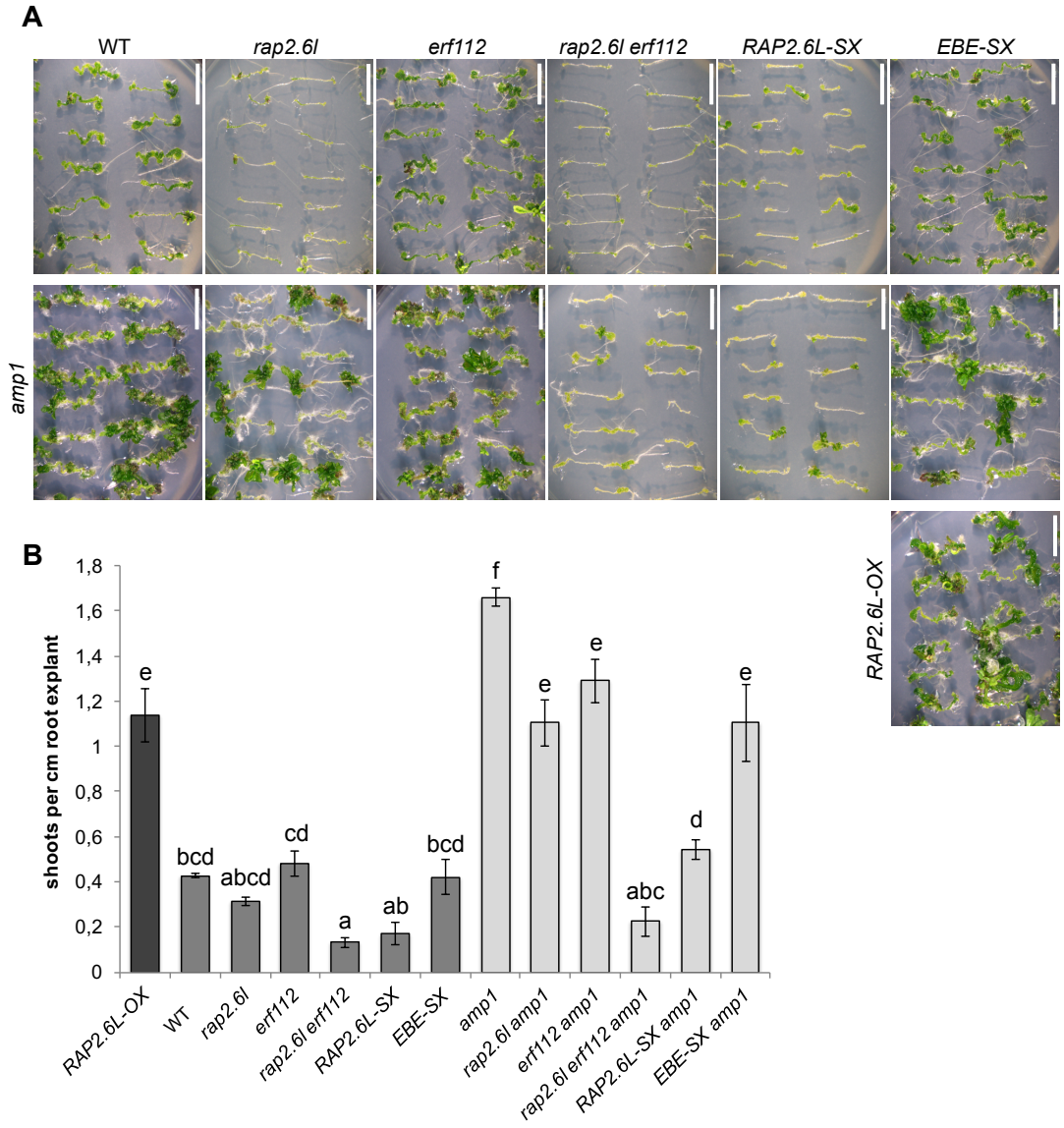

Figure 22. Compromised RAP2.6L function affects shoot regeneration in *amp1*

(A) Representative root explants of the indicated genotypes after 18 days on shoot induction medium. Scale bar: 10 mm. (B) Quantification of shoot regeneration of the indicated phenotypes. The regenerative capacity was calculated as number of shoots/cm root explant (means ± SE of the mean; n ≥ 30).

2.6 Mutants bearing miRNA-resistant versions of HD-ZIP III transcription factors show enhanced *RAP2.6L* expression similar to *amp1*

AMP1 has been shown to be required for the translational inhibition of miRNA targets (Li et al., 2013). Therefore, enhanced activity of a miRNA-controlled transcription factor regulating *RAP2.6L* expression might be causal for its overexpression in *amp1*. To substantiate this assumption, the Genevestigator

expression database was screened for genetic perturbations affecting *RAP2.6L* expression (Hruz et al., 2008). Interestingly, highly elevated *RAP2.6L* mRNA levels were identified in embryos of *dcl1*-15, a miRNA-biosynthesis deficient mutant (Willmann et al., 2011), consistent with the hypothesis that *RAP2.6L* expression is under control of a miRNA target (Figure 23A). Moreover, this analysis revealed that *RAP2.6L* transcript levels are also increased in *35S:GR-REV**, a line bearing a chemically inducible, miRNA-resistant version of REVOLUTA (Reinhart et al., 2013), suggesting that HD-ZIP III transcription factors might affect *RAP2.6L* expression (Figure 23B).

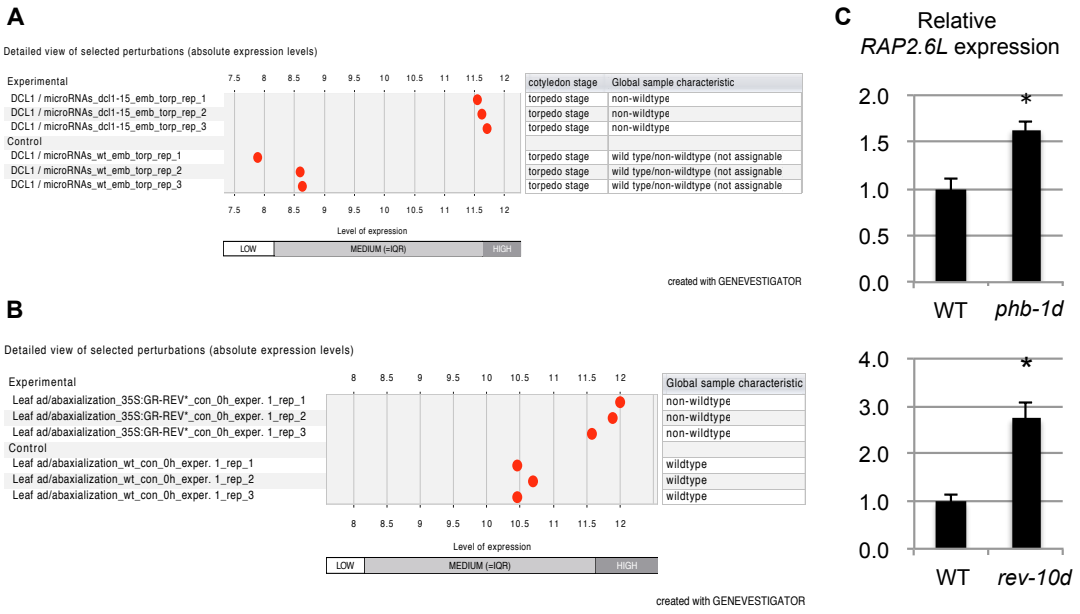

Figure 23. *RAP2.6L* expression is elevated in plant lines bearing miRNA resistant versions of HD-ZIP III transcription factors

RAP2.6L expression is increased in *dcl1* and *35S::GR-REV**. (A, B) Expression analysis of *RAP2.6L* in *dcl1* (A; Willmann et al., 2011) and *35S::GR-REV** (B; Reinhart et al., 2013) compared to the corresponding wild-type controls. Data were extracted from the Genevestigator database (Hruz et al., 2008). (C) qPCR analysis of *RAP2.6L* expression in 10-d-old seedlings of wild-type Ler (WT), *phb-1d* and *rev-10d*. Normalized means (WT = 1) are shown. The SE was calculated from three biological replicates after normalization to *UBC*. Asterisks indicate significant difference (Student's 2-tailed t-test; $p < 0.05$).

In line with this model, the mRNA levels of *RAP2.6L* were significantly upregulated in *phb-1d* and *rev-10d* (Figure 23C), mutants bearing miRNA-resistant versions of PHB and REV, respectively. Taken together, these data suggest an emerging regulatory module for the control of SAM organization, in which AMP1 constricts

stem cell pool homeostasis through limitation of *RAP2.6L* expression via translational control of HD-ZIP III activity.

IV. Discussion

Enhanced HD-ZIP III and RAP2.6L activities contribute to the defective SAM development of *amp1*

The putative carboxypeptidase AMP1 has been identified as a crucial determinant of radial SAM organization by suppression of stem cell identity in the morphogenetic zone (Huang et al., 2015). Absence of AMP1 causes disorganized growth patterns and uncoordinated hyperproliferative organ formation in the shoot. Furthermore, *amp1* mutants show a strong shoot regenerative capacity in tissue culture. However, compared to the detailed description of the *amp1* mutant phenotypes (Helliwell et al., 2001; Vidaurre et al., 2007; Huang et al., 2015), neither the biochemical function of AMP1 nor the regulatory network by which this enzyme controls SAM organization is known. Early studies attributed the SAM enlargement in *amp1* to its increased endogenous CK level, yet this had been shown to be rather a result of ectopic SAM activity than the cause (Huang et al., 2015). Likewise, AMP1 appears to act downstream or independent of WUS/CLV3 based on its genetic epistasis over WUS (Huang et al., 2015). A new avenue in understanding AMP1 function was opened by the discovery of the role of AMP1 in miRNA-related translation inhibition (Li et al., 2013). It was shown that knocking-out AMP1 function resulted in a general increase in miRNA-target protein abundance also affecting HD-ZIP III transcription factors, which are known as important SAM regulators. However, whether this function indeed evokes the *amp1* SAM phenotype is not known yet.

The presented work proposes two novel components of the AMP1 regulatory pathway. On the one hand it is demonstrated that AMP1 impacts on SAM structure and activity in an HD-ZIP III-dependent manner, which are key regulators of SAM radial organization. On the other hand evidence is provided that the SAM hypertrophy and enhanced shoot regeneration activity of *amp1* is at least partially driven by ectopic expression of the AP2/ERF transcription factor RAP2.6L. Moreover, preliminary data suggest that RAP2.6L induction in *amp1* is a consequence of the elevated HD-ZIP III activity in the mutant (Figure 21).

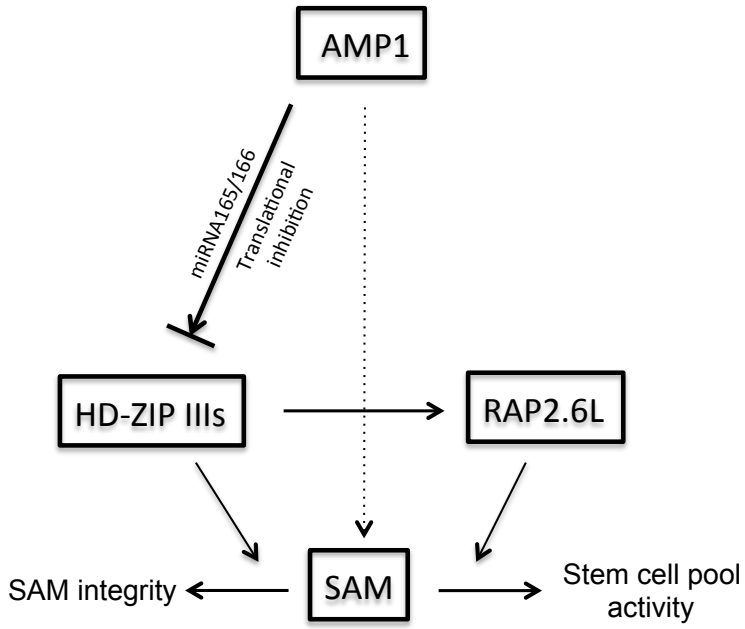

Figure 24. Working model of AMP1 controls SAM integrity and stem cell pool activity

AMP1 affects SAM organization in an HD-ZIP III-dependent manner

Loss of AMP1 function results in increased *ZPR3* expression in accordance with enhanced activity of the miRNA target family of HD-ZIP III proteins. Furthermore, general promotion of HD-ZIP III activity at the post-translational level by elimination of ZPR3/ZPR4 causes radial SAM patterning defects very similar to *amp1*. However whereas in *zpr3 zpr4* the enhanced HD-ZIP III activity is based on unimpeded dimerization of these transcription factors, in *amp1* it is postulated to result from increased protein accumulation due to inactivation of miRNA-dependent translation repression. In this context one would expect a similar or even higher phenotypic overlap between *amp1* and mutants bearing miRNA-resistant versions of HD-ZIP III members, however, this is not the case. Although gain-of-function alleles such *phb-D* develop a bigger embryonic meristem, obvious SAM splitting in the vegetative growth phase was not reported (McConnell et al., 2001). A potential explanation for the more severe SAM phenotype in *zpr3 zpr4* and *amp1* might be the simultaneous over-activation/accumulation of all HD-ZIP III members, whereas in the miRNA resistant mutants only one HD-ZIP III protein is misregulated. To proof this theory miRNA resistant versions of different HD-ZIP III proteins could be crossed and phenotypically characterized to assess whether they show a similar SAM hypertrophy

like *amp1*.

Such analysis might be complicated by the fact that HD-ZIP III members do not simply act redundantly but also have antagonistic roles in certain circumstances, especially in SAM development (Prigge et al., 2005). For instance, whereas *rev phb phv cna* seedlings do not form a functional SAM, *phb phv cna* triple mutants show a hypertrophic SAM and stem fasciation. Thus, the four HD-ZIP III act together in the process of embryonic shoot establishment, while in the seedling stage the promotive effect of REV on shoot stem cell specification is limited by the three other family members (Lee and Clark, 2015). An antagonistic function of REV and PHB/PHV/CNA is further substantiated by the analysis of overexpression lines of miRNA165 and miRNA166. Overexpression of miRNA165 suppresses all HD-ZIP III members and subsequently causes shoot meristem loss as in *rev phb phv cna* or *35S::ZPR3* (Zhou et al., 2007). In contrast, miRNA166 activation tagging lines such as *men-1* or *jabba-D* show reduced expression of *PHB/PHV/CNA* and normal or even enhanced expression of *REV* causing SAM hyperproliferation and ectopic OC formation as found in *amp1* (Kim et al., 2005; Williams et al., 2005). Based on these findings the observed SAM defects in *amp1* and *zpr3 zpr4* might be influenced by varying regulatory impact on the different HD-ZIP III members. However, this is not supported by previous studies, which indicated that ZPRs interact with all HD-ZIP III proteins to the same extent and in *amp1* all HD-ZIP III protein levels were upregulated in a comparable manner. Nevertheless, to fully exclude such a scenario one would have to test the genetic interaction between *amp1* and different combinations of HD-ZIP III loss-of-function mutants.

AMP1 limits PHV protein accumulation without controlling its tissue distribution

miRNA165/166 are known to define the spatial expression pattern of HD-ZIP IIIs in different organs, including the SAM and provasculature of the embryo, the adaxial side of the cotyledons (Zhu et al., 2011), the adaxial domain of true leaf primordia (Kidner and Martienssen, 2004) and the vascular cylinder of the roots (Carlsbecker et al., 2010). Based on the proposed function of AMP1 to mediate the translational inhibition of miRNA targets and the assumption that this mechanism contributes to the spatial restriction of HD-ZIP III proteins to adaxial/central domains one would expect ectopic expression of HD-ZIP IIIs in tissues where AMP1 and the relevant

miRNAs are present. The expression areas of miRNA165/166 and AMP1 overlap in the root endodermis cells and the abaxial side of leaf primordia (Vidaurre et al., 2007). However, surprisingly the tissue-specific expression pattern of PHV didn't seem to be changed neither in *amp1 nor amp1 lamp1*. The PHV-YFP signal was still only visible in the root vascular cylinder and the adaxial site of the leaf primordia, as in wild type (Figure 11). This finding implies that AMP1/LAMP1 do not significantly contribute to the miRNA-related control of the HD-ZIP III tissue distribution. One possible explanation is that the translation inhibition and the transcript cleavage activities of miRNA165/166 have different functions, and that the AMP1-dependent translation inhibition activity does not contribute to the abaxial/peripheral elimination of HD-ZIP III expression. This is supported by the absence of obvious leaf polarity phenotypes in *amp1* and *amp1 lamp1*, a hallmark of miRNA resistant HD-ZIP III mutants where expression expands to the whole organ.

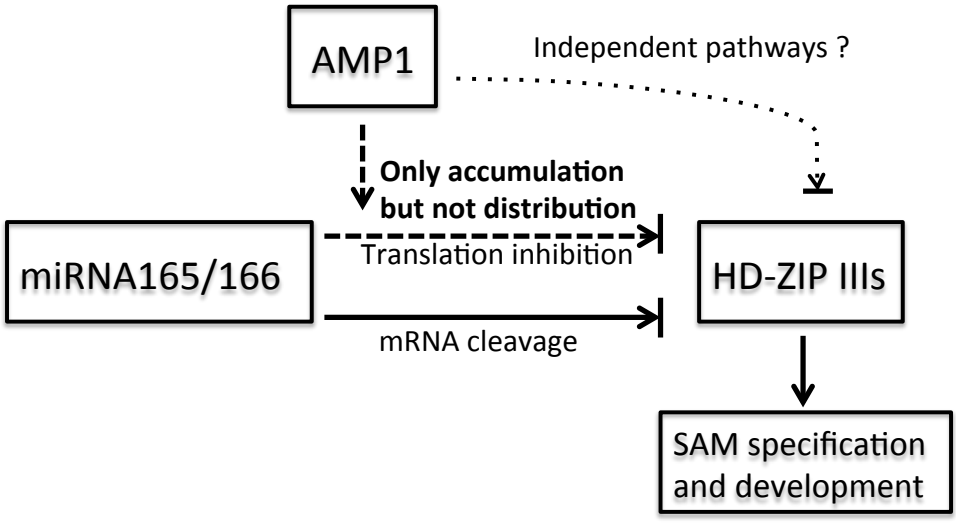

Figure 25. Current working model how AMP1 controls protein accumulation of HD-ZIP IIIs

In conclusion we propose a model in which miRNA165/166 locally restricts HD-ZIP III expression area mainly by mRNA cleavage, while the AMP1-involved translation inhibition only affects the accumulation but not the tissue distribution of HD-ZIP IIIs (Figure 25). Alternatively, AMP1 might regulate HD-ZIP III protein accumulation /activity also via a miRNA-independent pathway. To proof the existence of such a mechanism the expression level and tissue distribution of miRNA-resistant versions

of PHV should be compared between wild type and *amp1* in future studies to see whether the HD-ZIP III over accumulation in *amp1* is still obvious.

A further argument supporting a functional connection between AMP1 and the HD-ZIP III family is the finding that AMP1 transcription is under control of REV. AMP1 expression was strongly upregulated already 30 min after chemical induction of REV activity (Reinhart et al., 2013). Since our data suggest that AMP1 suppresses HD-ZIP III activity this might represent a negative feedback loop similar to the induction of the ZPR proteins. Thus, it would be interesting to analyze the phenotypic effect of uncoupling AMP1 expression from REV, e.g. by generating inducible AMP1 expression lines.

To further explore the mechanism by which AMP1 controls HD-ZIP III protein homeostasis and miRNA-dependent translation a better understanding of AMP1's biochemical function is also required. Using a chemical genetic approach, the small molecule hyperphyllin was identified, which evoked a wide spectrum of *amp1*-related responses (Poretska et al., 2016). Notably, hyperphyllin also triggered accumulation of HD-ZIP III proteins without apparent alteration in the transcription levels. Therefore, using hyperphyllin in proteomic approaches or for mutant screens might help to elucidate AMP1's biochemical function.

AMP1 controls stem cell pool activity by limiting the expression of the AP2/ERF transcription factor RAP2.6L

A role of RAP2.6L in the determination of shoot stem cell identity is supported by earlier studies. RAP2.6L had originally been identified as an essential component of shoot regeneration since its expression was strongly induced upon transfer of explants to shoot induction medium and its absence severely impaired shoot formation in tissue culture (Che et al., 2006). RAP2.6L is thus a crucial driver of trans-differentiation from root meristem-like callus to newly formed SAMs (Duclercq et al., 2011b). This function is also supported by the finding that upon wounding of inflorescence stems, RAP2.6L expression specifically increased at the lower side of the incision zone (Asahina et al., 2011), an area which under certain circumstances, such as shoot decapitation, gives rise to novel SAMs. Moreover, close homologs of RAP2.6L in the Xa group of the AP2/ERF transcription factor family were recently also shown to be involved in stem cell niche establishment and recovery.

Overexpression of EBE/ERF114 not only caused ectopic formation and enhanced outgrowth of axillary shoot meristems, but also increased the size and activity of the vegetative SAM (Mehrnia et al., 2013) similar to RAP2.6L overexpression described in this study. ERF115 on the other hand displays an analogous role in the root meristem. Together with the GRAS protein PHYTOCHROME A SIGNAL TRANSDUCTION1 (PAT1), it mediates stem cell niche recovery from differentiated cells in the wounding zone of excised root meristems and ubiquitous expression of the ERF115/PAT1 complex causes ectopic stem cell pool formation in the root (Heyman et al., 2016). ERF115 exerts its regenerative capacity at least partially by activating the AP2 transcription factor WIND1, a key player in wound-induced regeneration processes (Heyman et al., 2016; Iwase et al., 2011). Whether RAP2.6L also acts through WIND1 or other AP2/ERF proteins involved in shoot regeneration such as PHLETHORA (PLT) 3/5/7 or ESR1/DRN and ESR2/ DRNL has to be tested in future studies.

In the light of the emerging phenotypic similarities between RAP2.6L and EBE/ERF114 gain of function lines, the question arises whether AMP1 mainly acts through RAP2.6L or also other members of this ERF sub-family. Although among the tested homologs only RAP2.6L was significantly upregulated in *amp1*, we found that the *amp1* shoot defects were more strongly suppressed by *rap2.6l erf112* and *RAP2.6L-SX* than by *rap2.6l* alone, indicating functional redundancy between RAP2.6L and ERF112. In contrast, *EBE-SX* was much weaker (SAM size) or inefficient (leaf number, shoot regeneration) in suppressing *amp1*-related shoot phenotypes as compared to *RAP2.6L-SX*. Due to the phenotypic similarity of *rap2.6l* and *rap2.6l rap2.6* we also exclude a strong functional overlap between RAP2.6 and RAP2.6L. Based on these data it will be interesting to further investigate the role of ERF112 in shoot SCN replenishment and its potential interaction with AMP1 in this process.

Since AMP1 has been recently positioned in the miRNA-dependent control of translation we reasoned that the observed induction of RAP2.6L in *amp1* might be caused by over translation of miRNA targets affecting *RAP2.6L* expression, either directly or indirectly. Correspondingly, we found that miRNA-uncoupled expression of REV and PHB promotes *RAP2.6L* transcription indicating that HD-ZIP III proteins might represent such miRNA targets. HD-ZIP III TFs determine shoot meristem identity during embryogenesis (Smith and Long, 2010) and proper control of their

activity is important to maintain the radial symmetry of the SAM (Green et al., 2005; Kim et al., 2008; Williams et al., 2005) making it plausible that their enhanced translation in *amp1* (Li et al., 2013; Poretska et al., 2016) contribute to the ectopic SCN formation in this mutant. To further validate the direct impact of HD-ZIP III proteins on RAP2.6L transcription chromatin immunoprecipitation experiments with the generated PHV-YFP lines could be performed.

Since AMP1 affects the translation of a broad range of tested miRNA targets (Li et al., 2013) the HD-ZIP III/RAP2.6L regulatory cascade is most likely not the only avenue by which AMP1 affects SAM organization. This might be one reason, why ectopic *RAP2.6L* expression not fully mimics the *amp1* shoot phenotype. Moreover, the enhanced translation of HD-ZIP IIIs in *amp1* potentially misregulates other key determinants of SAM organization such as WUS, which has recently been shown to be under transcriptional control of REV/PHB/PHV in the process of shoot regeneration (Zhang et al., 2017). Nevertheless, the strong suppressive effect of RAP2.6L-SX on *amp1* overall SAM activity, shown in this study, compared to the obvious genetic epistasis of *amp1* over *wus* (Huang et al., 2015), supports a prominent role of RAP2.6L downstream of AMP1.

At the moment we can not fully exclude the existence of HD-ZIP III-independent modes of *RAP2.6L* activation in *amp1*. Whereas direct induction by the increased cytokinin levels in *amp1* appears rather unlikely, based on the unresponsiveness of *RAP2.6L* transcription towards exogenous cytokinin application (Figure 14; Che et al., 2006), induction might be caused by the enhanced JA response found in *amp1* (Poretska et al., 2016). *RAP2.6L* expression is promoted upon application of JA, a hormone synthesized upon wounding. Interestingly, wounding has been shown to be important for regeneration processes. However the underlying molecular mechanisms including the role of JA are not well understood (Ikeuchi et al., 2016). Whether the altered JA response in *amp1* is functionally relevant in respect to the SAM organization defect and the elevated *RAP2.6L* transcription levels are important future questions to be resolved.

Finally, it has to be clarified, how enhanced *RAP2.6L* expression in *amp1* triggers the expansion of SCN identity in the peripheral zone of the meristem as well as the enhanced ability for shoot regeneration in root explants. A potential downstream component is CUC2, a transcription factor required for embryonic SAM formation and shoot regeneration in tissue culture, whose expression has been shown to depend

on RAP2.6L (Che et al., 2006). Another valuable future research direction would be to test whether RAP2.6L feeds back on HD-ZIP III activity by physical interaction. It has been shown that the AP2/ERF transcription factors ESR1/DRN and ESR2/DRNL bind to HD-ZIP IIIs and that they cooperate in shoot patterning during embryogenesis (Chandler et al., 2007). It will be interesting to see whether RAP2.6L has a related competence to modulate HD-ZIP III function in the control of SAM development.

References

Aguilar-Martínez JA, Poza-Carrión C, Cubas P (2007) Arabidopsis BRANCHED1 acts as an integrator of branching signals within axillary buds. Plant Cell **19**: 458–472

Aida M, Beis D, Heidstra R, Willemsen V, Blilou I, Galinha C, Nussaume L, Noh Y-S, Amasino R, Scheres B (2004) The PLETHORA genes mediate patterning of the Arabidopsis root stem cell niche. Cell **119**: 109–120

Anastasiou E, Kenz S, Gerstung M, MacLean D, Timmer J, Fleck C, Lenhard M (2007) Control of plant organ size by KLUH/CYP78A5-dependent intercellular signaling. Developmental Cell **13**: 843–856

Asahina M, Azuma K, Pitaksaringkarn W, Yamazaki T, Mitsuda N, Ohme-Takagi M, Yamaguchi S, Kamiya Y, Okada K, Nishimura T (2011) Spatially selective hormonal control of RAP2. 6L and ANAC071 transcription factors involved in tissue reunion in Arabidopsis. Proc Natl Acad Sci USA **108**: 16128–16132

Atta R, Laurens L, Boucheron-Dubuisson E, Guivarc'h A, Carnero E, Giraudat-Pautot V, Rech P, Chriqui D (2009) Pluripotency of Arabidopsis xylem pericycle underlies shoot regeneration from root and hypocotyl explants grown in vitro. The Plant Journal **57**: 626–644

Banno H, Ikeda Y, Niu Q-W, Chua N-H (2001) Overexpression of Arabidopsis ESR1 induces initiation of shoot regeneration. Plant Cell **13**: 2609–2618

Barton MK (2010) Twenty years on: The inner workings of the shoot apical meristem, a developmental dynamo. Developmental Biology **341**: 95–113

Bařinka C, Rojas C, Slusher B, Pomper M (2012) Glutamate carboxypeptidase II in diagnosis and treatment of neurologic disorders and prostate cancer. Curr Med Chem **19**: 856–870

Bilsborough GD, Runions A, Barkoulas M, Jenkins HW, Hasson A, Galinha C, Laufs P, Hay A, Prusinkiewicz P, Tsiantis M (2011) Model for the regulation of Arabidopsis thaliana leaf margin development. Proc Natl Acad Sci USA **108**: 3424–3429

Bowman JL (2000) The YABBY gene family and abaxial cell fate. Current Opinion in Plant Biology **3**: 17–22

Brand U, Fletcher JC, Hobe M, Meyerowitz EM, Simon R (2000) Dependence of stem cell fate in Arabidopsis on a feedback loop regulated by CLV3 activity. Science **289**: 617–619

Brandt R, Salla-Martret M, Bou-Torrent J, Musielak T, Stahl M, Lanz C, Ott F, Schmid M, Greb T, Schwarz M, et al (2012) Genome-wide binding-site analysis of REVOLUTA reveals a link between leaf patterning and light-mediated growth responses. The Plant Journal **72**: 31–42

Brandt R, Xie Y, Musielak T, Graeff M, Stierhof Y-D, Huang H, Liu C-M, Wenkel S (2013) Control of stem cell homeostasis via interlocking microRNA and microProtein feedback loops. Mechanisms of Development **130**: 25–33

Bullock W (1987) XL1-Blue: a high efficiency plasmid transforming recA Escherichia coli strain with beta-galactosidase selection. Bio Tecchniques **5**: 376–379

Carlsbecker A, Lee J-Y, Roberts CJ, Dettmer J, Lehesranta S, Zhou J, Lindgren O, Moreno-Risueno MA, Vatén A, Thitamadee S, et al (2010) Cell signalling by microRNA165/6 directs gene dose-dependent root cell fate. Nature **465**: 316–321

Cary AJ, Che P, Howell SH (2002) Developmental events and shoot apical meristem gene expression patterns during shoot development in Arabidopsis thaliana. Plant J **32**: 867–877

Catterou M, Dubois F, Smets R, Vaniet S, Kichey T, Van Onckelen H, Sangwan Norreel BS, Sangwan RS (2002) hoc: an Arabidopsis mutant overproducing cytokinins and expressing high in vitro organogenic capacity. The Plant Journal **30**: 273–287

Chandler JW, Cole M, Flier A, Grewe B, Werr W (2007) The AP2 transcription factors DORNROSCHEN and DORNROSCHEN-LIKE redundantly control Arabidopsis embryo patterning via interaction with PHAVOLUTA. Development **134**: 1653–1662

Chatfield SP, Capron R, Severino A, Penttila P-A, Alfred S, Nahal H, Provart NJ (2013) Incipient stem cell niche conversion in tissue culture: using a systems approach to probe early events in WUSCHEL-dependent conversion of lateral root primordia into shoot meristems. Plant J **73**: 798–813

Chaudhury AM, Letham S, Craig S, Dennis ES (1993) amp1- a mutant with high cytokinin levels and altered embryonic pattern, faster vegetative growth, constitutive photomorphogenesis and precocious flowering. The Plant Journal **4**: 907–916

Che P, Gingerich DJ, Lall S, Howell SH (2002) Global and hormone-induced gene expression changes during shoot development in Arabidopsis. Plant Cell **14**: 2771–2785

Che P, Lall S, Nettleton D, Howell SH (2006) Gene expression programs during shoot, root, and callus development in Arabidopsis tissue culture. Plant Physiol **141**: 620–637

Chickarmane VS, Gordon SP, Tarr PT, Heisler MG, Meyerowitz EM (2012) Cytokinin signaling as a positional cue for patterning the apical-basal axis of the growing Arabidopsis shoot meristem. Proc Natl Acad Sci USA **109**: 4002–4007

Chin-Atkins AN, Craig S, Hocart CH, Dennis ES, Chaudhury AM (1996) Increased endogenous cytokinin in the Arabidopsis amp1 mutant corresponds with de-etiolation responses. Planta **198**: 549–556

Daum G, Medzihradszky A, Suzaki T, Lohmann JU (2014) A mechanistic framework for noncell autonomous stem cell induction in Arabidopsis. Proc Natl Acad Sci USA **111**: 14619–14624

De Klerk G, Arnholdt-Schmitt B, Lieberei R, Neumann K (1997) Regeneration of roots, shoots and embryos: physiological, biochemical and molecular aspects. Biologia plantarum **39**: 53–66

De Smet I, Chaerle P, Vanneste S, De Rycke R, Inzé D, Beeckman T (2004) An easy and versatile embedding method for transverse sections. Journal of microscopy **213**: 76–80

DiDonato RJ, Arbuckle E, Buker S, Sheets J, Tobar J, Totong R, Grisafi P, Fink GR, Celenza JL (2004) Arabidopsis ALF4 encodes a nuclear-localized protein required for lateral root formation. Plant J **37**: 340–353

Diener AC, Li H, Zhou W, Whoriskey WJ, Nes WD, Fink GR (2000) Sterol methyltransferase 1 controls the level of cholesterol in plants. Plant Cell **12**: 853–870

Duclercq J, Assoumou Ndong YP, Guerineau F, Sangwan RS, Catterou M (2011a) Arabidopsis shoot organogenesis is enhanced by an amino acid change in the ATHB15 transcription factor. Plant Biol (Stuttg) **13**: 317–324

Duclercq J, Sangwan-Norreel B, Catterou M, Sangwan RS (2011b) De novo shoot organogenesis: from art to science. Trends Plant Sci **16**: 597–606

Emery JF, Floyd SK, Alvarez J, Eshed Y, Hawker NP, Izhaki A, Baum SF, Bowman JL (2003) Radial patterning of Arabidopsis shoots by class III HD-ZIP and KANADI genes. Current Biology **13**: 1768–1774

Gaillochet C, Lohmann JU (2015) The never-ending story: from pluripotency to plant developmental plasticity. Development **142**: 2237–2249

Galinha C, Hofhuis H, Luijten M, Willemsen V, Blilou I, Heidstra R, Scheres B (2007) PLETHORA proteins as dose-dependent master regulators of Arabidopsis root development. Nature **449**: 1053–1057

Galli M, Gallavotti A (2016) Expanding the Regulatory Network for Meristem Size in Plants. Trends in Genetics **32**: 372–383

Goldshmidt A, Alvarez JP, Bowman JL, Eshed Y (2008) Signals derived from YABBY gene activities in organ primordia regulate growth and partitioning of Arabidopsis shoot apical meristems. Plant Cell **20**: 1217–1230

Gordon SP, Chickarmane VS, Ohno C, Meyerowitz EM (2009) Multiple feedback loops through cytokinin signaling control stem cell number within the Arabidopsis shoot meristem. Proc Natl Acad Sci USA **106**: 16529–16534

Gordon SP, Heisler MG, Reddy GV, Ohno C, Das P, Meyerowitz EM (2007) Pattern formation during de novo assembly of the Arabidopsis shoot meristem. Development **134**: 3539–3548

Graf P, Dolzblasz A, Würschum T, Lenhard M, Pfreundt U, Laux T (2010) MGOUN1 encodes an Arabidopsis type IB DNA topoisomerase required in stem cell regulation and to maintain developmentally regulated gene silencing. Plant Cell **22**: 716–728

Griffiths J, Barrero JM, Taylor J, Helliwell CA, Gubler F (2011) ALTERED MERISTEM PROGRAM 1 Is involved in Development of Seed Dormancy in Arabidopsis. PLoS ONE **6**: e20408

Grigg SP, Canales C, Hay A, Tsiantis M (2005) SERRATE coordinates shoot meristem function and leaf axial patterning in Arabidopsis. Nature **437**: 1022–1026

Gross-Hardt R, Lenhard M, Laux T (2002) WUSCHEL signaling functions in interregional communication during Arabidopsis ovule development. Genes Dev **16**: 1129–1138

Han P, Li Q, Zhu Y-X (2008) Mutation of Arabidopsis BARD1 causes meristem defects by failing to confine WUSCHEL expression to the organizing center. Plant Cell **20**: 1482–1493

Hasson A, Plessis A, Blein T, Adroher B, Grigg S, Tsiantis M, Boudaoud A, Damerval C, Laufs P (2011) Evolution and Diverse Roles of the CUP-SHAPED COTYLEDON Genes in Arabidopsis Leaf Development. Plant Cell **23**: 54–68

Heidstra R, Sabatini S (2014) Plant and animal stem cells: similar yet different. Nat Rev Mol Cell Biol **15**: 301–312

Hellens R, Mullineaux P, Klee H (2000) Technical focus: a guide to Agrobacterium binary Ti vectors. Trends Plant Sci **5**: 446–451

Helliwell CA, Chin-Atkins AN, Wilson IW, Chapple R, Dennis ES, Chaudhury A (2001) The Arabidopsis AMP1 gene encodes a putative glutamate carboxypeptidase. Plant Cell **13**: 2115–2125

Heyman J, Cools T, Canher B, Shavialenka S, Traas J, Vercauteren I, Van den Daele H, Persiau G, De Jaeger G, Sugimoto K, et al (2016) The heterodimeric transcription factor complex ERF115–PAT1 grants regeneration competence. Nat Plants **2**: 16165

Heyman J, Cools T, Vandenbussche F, Heyndrickx KS, Van Leene J, Vercauteren I, Vanderauwera S, Vandepoele K, De Jaeger G, Van Der Straeten D, et al (2013) ERF115 controls root quiescent center cell division and stem cell replenishment. Science **342**: 860–863

Horstman A, Willemsen V, Boutilier K, Heidstra R (2014) AINTEGUMENTA-LIKE proteins: hubs in a plethora of networks. Trends Plant Sci **19**: 146–157

Hruz T, Laule O, Szabo G, Wessendorp F, Bleuler S, Oertle L, Widmayer P, Gruissem W, Zimmermann P (2008) Genevestigator v3: a reference expression database for the meta-analysis of transcriptomes. Adv Bioinformatics **2008**: 420747

Huang T, Harrar Y, Lin C, Reinhart B, Newell NR, Talavera-Rauh F, Hokin SA, Barton MK, Kerstetter RA (2014) Arabidopsis KANADI1 Acts as a Transcriptional Repressor by Interacting with a Specific cis-Element and Regulates Auxin Biosynthesis, Transport, and Signaling in Opposition to HD-ZIP III Factors. Plant Cell **26**: 246–262

Huang W, Pitorre D, Poretska O, Marizzi C, Winter N, Poppenberger B, Sieberer T (2015) ALTERED MERISTEM PROGRAM1 suppresses ectopic stem cell niche formation in the shoot apical meristem in a largely cytokinin-independent manner. Plant Physiol **167**: 1471–1486

Husbands A, Aggarwal V, Ha T, Timmermans MC (2016) In Planta Single-Molecule Pull-down (SiMPull) Reveals Tetrameric Stoichiometry of HD-ZIP III:LITTLE ZIPPER Complexes. Plant Cell. doi: 10.1105/tpc.16.00289

Ikeda Y, Banno H, Niu Q-W, Howell SH, Chua N-H (2006) The ENHANCER OF SHOOT REGENERATION 2 gene in Arabidopsis regulates CUP-SHAPED COTYLEDON 1 at the transcriptional level and controls cotyledon development. Plant and Cell Physiology **47**: 1443–1456

Ikeuchi M, Ogawa Y, Iwase A, Sugimoto K (2016) Plant regeneration: cellular origins and molecular mechanisms. Development **143**: 1442–1451

Iwase A, Harashima H, Ikeuchi M, Rymen B, Ohnuma M, Komaki S, Morohashi K, Kurata T, Nakata M, Ohme-Takagi M, et al (2017) WIND1 Promotes Shoot Regeneration through Transcriptional Activation of ENHANCER OF SHOOT REGENERATION1 in Arabidopsis. Plant Cell **29**: 54–69

Iwase A, Mitsuda N, Koyama T, Hiratsu K, Kojima M, Arai T, Inoue Y, Seki M, Sakakibara H, Sugimoto K, et al (2011) The AP2/ERF Transcription Factor WIND1 Controls Cell Dedifferentiation in Arabidopsis. Current Biology **21**: 508–514

Jasinski S, Piazza P, Craft J, Hay A, Woolley L, Rieu I, Phillips A, Hedden P, Tsiantis M (2005) KNOX Action in Arabidopsis Is Mediated by Coordinate Regulation of Cytokinin and Gibberellin Activities. Current Biology **15**: 1560–1565

Kareem A, Durgaprasad K, Sugimoto K, Du Y, Pulianmackal AJ, Trivedi ZB, Abhayadev PV, Pinon V, Meyerowitz EM, Scheres B, et al (2015) PLETHORA Genes Control Regeneration by a Two-Step Mechanism. Curr Biol **25**: 1017–1030

Kawakatsu T, Taramino G, Itoh J-I, Allen J, Sato Y, Hong S-K, Yule R, Nagasawa N, Kojima M, Kusaba M, et al (2009) PLASTOCHRON3/GOLIATH encodes a glutamate carboxypeptidase required for proper development in rice. Plant J **58**: 1028–1040

Kidner CA, Martienssen RA (2004) Spatially restricted microRNA directs leaf polarity through ARGONAUTE1. Nature **428**: 81–84

Kim J, Jung J-H, Reyes JL, Kim Y-S, Kim S-Y, Chung K-S, Kim JA, Lee M, Lee Y, Narry Kim V, et al (2005) microRNA-directed cleavage of ATHB15 mRNA regulates vascular development in Arabidopsis inflorescence stems. The Plant Journal **42**: 84–94

Kim Y-S, Kim S-G, Lee M, Lee I, Park H-Y, Seo PJ, Jung J-H, Kwon E-J, Suh SW, Paek K-H, et al (2008) HD-ZIP III activity is modulated by competitive inhibitors via a feedback loop in Arabidopsis shoot apical meristem development. Plant Cell **20**: 920–933

Kinoshita A, Betsuyaku S, Osakabe Y, Mizuno S, Nagawa S, Stahl Y, Simon R, Yamaguchi-Shinozaki K, Fukuda H, Sawa S (2010) RPK2 is an essential receptor-like kinase that transmits the CLV3 signal in Arabidopsis. Development **137**: 3911–3920

Kirch T, Simon R, Grünewald M, Werr W (2003) The DORNROSCHEN/ENHANCER OF SHOOT REGENERATION1 gene of Arabidopsis acts in the control of meristem ccll fate and lateral organ development. Plant Cell **15**: 694–705

Klusák V, Bařinka C, Plechanovová A, Mlčochová P, Konvalinka J, Rulíšek L, Lubkowski J (2009) Reaction mechanism of glutamate carboxypeptidase II revealed by mutagenesis, X-ray crystallography, and computational methods. Biochemistry **48**: 4126–4138

Knauer S, Holt AL, Rubio-Somoza I, Tucker EJ, Hinze A, Pisch M, Javelle M, Timmermans MC, Tucker MR, Laux T (2013) A Protodermal miR394 Signal Defines a Region of Stem Cell Competence in the Arabidopsis Shoot Meristem. Developmental Cell **24**: 125–132

Kong J, Lau S, Jürgens G (2015) Twin Plants from Supernumerary Egg Cells in Arabidopsis. Current Biology **25**: 225–230

Krishnaswamy S, Verma S, Rahman MH, Kav NN (2011) Functional characterization of four APETALA2-family genes (RAP2. 6, RAP2. 6L, DREB19 and DREB26) in Arabidopsis. Plant Mol Biol **75**: 107–127

Kurakawa T, Ueda N, Maekawa M, Kobayashi K, Kojima M, Nagato Y, Sakakibara H, Kyozuka J (2007) Direct control of shoot meristem activity by a cytokinin-activating enzyme. Nature **445**: 652–655

Kwon CS, Chen C, Wagner D (2005) WUSCHEL is a primary target for transcriptional regulation by SPLAYED in dynamic control of stem cell fate in Arabidopsis. Genes Dev **19**: 992–1003

Lee B-H (2009) Ecotype-dependent genetic regulation of bolting time in the Arabidopsis mutants with increased number of leaves. J Microbiol Biotechnol **19**: 542–546

Lee C, Clark SE (2015) A WUSCHEL-Independent Stem Cell Specification Pathway Is Repressed by PHB, PHV and CNA in Arabidopsis. PLoS ONE **10**: e0126006

Leibfried A, To JPC, Busch W, Stehling S, Kehle A, Demar M, Kieber JJ, Lohmann JU (2005) WUSCHEL controls meristem function by direct regulation of cytokinin-inducible response regulators. Nature **438**: 1172–1175

Li H, Xu L, Wang H, Yuan Z, Cao X, Yang Z, Zhang D, Xu Y, Huang H (2005) The Putative RNA-dependent RNA polymerase RDR6 acts synergistically with ASYMMETRIC LEAVES1 and 2 to repress BREVIPEDICELLUS and MicroRNA165/166 in Arabidopsis leaf development. Plant Cell **17**: 2157–2171

Li S, Liu L, Zhuang X, Yu Y, Liu X, Cui X, Ji L, Pan Z, Cao X, Mo B, et al (2013) MicroRNAs Inhibit the Translation of Target mRNAs on the Endoplasmic Reticulum in Arabidopsis. Cell **153**: 562–574

Li T, Wu X-Y, Li H, Song J-H, Liu J-Y (2016) A Dual-Function Transcription Factor, AtYY1, Is a Novel Negative Regulator of the Arabidopsis ABA Response Network. Molecular Plant **9**: 650–661

Lindsay DL, Sawhney VK, Bonham-Smith PC (2006) Cytokinin-induced changes in CLAVATA1 and WUSCHEL expression temporally coincide with altered floral development in Arabidopsis. Plant Science **170**: 1111–1117

Liu P, Sun F, Gao R, Dong H (2012) RAP2.6L overexpression delays waterlogging induced premature senescence by increasing stomatal closure more than antioxidant enzyme activity. Plant Mol Biol **79**: 609–622

Liu W-Z, Kong D-D, Gu X-X, Gao H-B, Wang J-Z, Xia M, Gao Q, Tian L-L, Xu Z-H, Bao F, et al (2013) Cytokinins can act as suppressors of nitric oxide in Arabidopsis. Proc Natl Acad Sci USA **110**: 1548–1553

Lu P, Porat R, Nadeau J, O'Neill S (1996) Identification of a meristem L1 layer-specific gene in Arabidopsis that is expressed during embryonic pattern formation and defines a new class of homeobox genes. Plant Cell

Lynn K, Fernandez A, Aida M, Sedbrook J, Tasaka M, Masson P, Barton MK (1999) The PINHEAD/ZWILLE gene acts pleiotropically in Arabidopsis development and has overlapping functions with the ARGONAUTE1 gene. Development **126**: 469–481

Magnani E, Barton MK (2011) A per-ARNT-sim-like sensor domain uniquely regulates the activity of the homeodomain leucine zipper transcription factor REVOLUTA in Arabidopsis. Plant Cell **23**: 567–582

Mallory AC, Reinhart BJ, Jones-Rhoades MW, Tang G, Zamore PD, Barton MK, Bartel DP (2004) MicroRNA control of PHABULOSA in leaf development: importance of pairing to the microRNA 5' region. EMBO J **23**: 3356–3364

Marsch-Martinez N, Greco R, Becker JD, Dixit S, Bergervoet JHW, Karaba A, de Folter S, Pereira A (2006) BOLITA, an Arabidopsis AP2/ERF-like transcription factor that affects cell expansion and proliferation/differentiation pathways. Plant Mol Biol **62**: 825–843

Mayer KF, Schoof H, Haecker A, Lenhard M, Jurgens G, Laux T (1998) Role of WUSCHEL in regulating stem cell fate in the Arabidopsis shoot meristem. Cell **95**: 805–815

McConnell J, Barton M (1998) Leaf polarity and meristem formation in Arabidopsis. Development **125**: 2935–2942

McConnell JR, Emery J, Eshed Y, Bao N, Bowman J, Barton MK (2001) Role of PHABULOSA and PHAVOLUTA in determining radial patterning in shoots. Nature **411**: 709–713

Mehrnia M, Balazadeh S, Zanor M-I, Mueller-Roeber B (2013) EBE, an AP2/ERF transcription factor highly expressed in proliferating cells, affects shoot architecture in Arabidopsis. Plant Physiol **162**: 842–857

Merelo P, Ram H, Pia Caggiano M, Ohno C, Ott F, Straub D, Graeff M, Cho SK, Yang SW, Wenkel S, et al (2016) Regulation of MIR165/166 by class II and

class III homeodomain leucine zipper proteins establishes leaf polarity. Proc Natl Acad Sci USA **113**: 11973–11978

Meyerowitz EM (1997) Genetic control of cell division patterns in developing plants. Cell **88**: 299–308

Mordhorst AP, Voerman KJ, Hartog MV, Meijer EA, van Went J, Koornneef M, de Vries SC (1998) Somatic embryogenesis in Arabidopsis thaliana is facilitated by mutations in genes repressing meristematic cell divisions. Genetics **149**: 549–563

Mudunkothge JS, Krizek BA (2012) Three Arabidopsis AIL/PLT genes act in combination to regulate shoot apical meristem function. Plant J **71**: 108–121

Mukherjee K (2006) MEKHLA, a Novel Domain with Similarity to PAS Domains, Is Fused to Plant Homeodomain-Leucine Zipper III Proteins. Plant Physiol **140**: 1142–1150

Müller R, Bleckmann A, Simon R (2008) The receptor kinase CORYNE of Arabidopsis transmits the stem cell-limiting signal CLAVATA3 independently of CLAVATA1. Plant Cell **20**: 934–946

Nakano T, Suzuki K, Fujimura T, Shinshi H (2006) Genome-wide analysis of the ERF gene family in Arabidopsis and rice. Plant Physiol **140**: 411–432

Navrátil M, Ptáček J, Šácha P, Starková J, Lubkowski J, Bařinka C, Konvalinka J (2014) Structural and biochemical characterization of the folyl-poly-γ-l-glutamate hydrolyzing activity of human glutamate carboxypeptidase II. FEBS J **281**: 3228–3242

Nimchuk ZL, Zhou Y, Tarr PT, Peterson BA, Meyerowitz EM (2015) Plant stem cell maintenance by transcriptional cross-regulation of related receptor kinases. Development **142**: 1043–1049

Nogué F, Grandjean O, Craig S, Dennis S, Chaudhury M (2000a) Higher levels of cell proliferation rate and cyclin CycD3 expression in the Arabidopsis amp1 mutant. Plant growth regulation **32**: 275–283

Nogué N, Hocart H, Letham DS, Dennis ES, Chaudhury AM (2000b) Cytokinin synthesis is higher in the Arabidopsis amp1 mutant. Plant growth regulation **32**: 267–273

O'Keefe DS, Su SL, Bacich DJ, Horiguchi Y, Luo Y, Powell CT, Zandvliet D, Russell PJ, Molloy PL, Nowak NJ, et al (1998) Mapping, genomic organization and promoter analysis of the human prostate-specific membrane antigen gene. Biochim Biophys Acta **1443**: 113–127

Pandey GK, Grant JJ, Cheong YH, Kim BG, Li L, Luan S (2005) ABR1, an APETALA2-domain transcription factor that functions as a repressor of ABA response in Arabidopsis. Plant Physiol **139**: 1185–1193

Parizot B, Laplaze L, Ricaud L, Boucheron-Dubuisson E, Bayle V, Bonke M, De Smet I, Poethig SR, Helariutta Y, Haseloff J, et al (2008) Diarch symmetry of the vascular bundle in Arabidopsis root encompasses the pericycle and is reflected in distich lateral root initiation. Plant Physiol **146**: 140–148

Pitaksaringkarn W, Ishiguro S, Asahina M, Satoh S (2014) ARF6 and ARF8 contribute to tissue reunion in incised Arabidopsis inflorescence stems. Plant Biotechnology **31**: 49-53

Poppenberger B, Rozhon W, Khan M, Husar S, Adam G, Luschnig C, Fujioka S, Sieberer T (2011) CESTA, a positive regulator of brassinosteroid biosynthesis. EMBO J **30**: 1149–1161

Poretska O (2016) Temporal control of leaf formation in Arabidopsis: an integrative approach towards a better understanding of the emerging regulatory network. (Dissertation) University of Vienna

Poretska O, Yang S, Pitorre D, Rozhon W, Zwerger K, Uribe MC, May S, McCourt P, Poppenberger B, Sieberer T (2016) The Small Molecule Hyperphyllin Enhances Leaf Formation Rate and Mimics Shoot Meristem Integrity Defects Associated with AMP1 Deficiency. Plant Physiol **171**: 1277–1290

Prigge MJ, Otsuga D, Alonso JM, Ecker JR, Drews GN, Clark SE (2005) Class III homeodomain-leucine zipper gene family members have overlapping, antagonistic, and distinct roles in Arabidopsis development. Plant Cell **17**: 61–76

Reinhardt D, Frenz M, Mandel T, Kuhlemeier C (2003) Microsurgical and laser ablation analysis of interactions between the zones and layers of the tomato shoot apical meristem. Development **130**: 4073–4083

Reinhart BJ, Liu T, Newell NR, Magnani E, Huang T, Kerstetter R, Michaels S, Barton MK (2013) Establishing a Framework for the Ad/Abaxial Regulatory Network of Arabidopsis: Ascertaining Targets of Class III HOMEODOMAIN LEUCINE ZIPPER and KANADI Regulation. Plant Cell **25**: 3228–3249

Rhoades MW, Reinhart BJ, Lim LP, Burge CB, Bartel B, Bartel DP (2002) Prediction of plant microRNA targets. Cell **110**: 513–520

Robinson MB, Blakely RD, Couto R, Coyle JT (1987) Hydrolysis of the brain dipeptide N-acetyl-L-aspartyl-L-glutamate. Identification and characterization of a novel N-acetylated alpha-linked acidic dipeptidase activity from rat brain. J Biol Chem **262**: 14498 – 14506

Rozhon W, Mayerhofer J, Petutschnig E, Fujioka S, Jonak C (2010) ASKθ, a group-III Arabidopsis GSK3, functions in the brassinosteroid signalling pathway. The Plant Journal **62**: 215–223

Saibo NJM, Vriezen WH, De Grauwe L, Azmi A, Prinsen E, Van Der Straeten D (2007) A comparative analysis of the Arabidopsis mutant amp1-1 and a novel weak amp1 allele reveals new functions of the AMP1 protein. Planta **225**: 831–842

Sarojam R, Sappl PG, Goldshmidt A, Efroni I, Floyd SK, Eshed Y, Bowman JL (2010) Differentiating Arabidopsis shoots from leaves by combined YABBY activities. Plant Cell **22**: 2113–2130

Schoof H, Lenhard M, Haecker A, Mayer KF, Jurgens G, Laux T (2000) The stem cell population of Arabidopsis shoot meristems in maintained by a regulatory loop between the CLAVATA and WUSCHEL genes. Cell **100**: 635–644

Schuster C, Gaillochet C, Medzihradszky A, Busch W, Daum G, Krebs M, Kehle A, Lohmann JU (2014) A regulatory framework for shoot stem cell control integrating metabolic, transcriptional, and phytohormone signals. Developmental Cell **28**: 438–449

Sessa G, Steindler C, Morelli G, Ruberti I (1998) The Arabidopsis Athb-8, -9 and -14 genes are members of a small gene family coding for highly related HD-ZIP proteins. Plant Mol Biol **38**: 609–622

Shi B, Zhang C, Tian C, Wang J, Wang Q, Xu T, Xu Y, Ohno C, Sablowski R, Heisler MG, et al (2016) Two-Step Regulation of a Meristematic Cell Population Acting in Shoot Branching in Arabidopsis. PLoS Genet **12**: e1006168

Shi H, Ye T, Wang Y, Chan Z (2013a) Arabidopsis ALTERED MERISTEM PROGRAM 1 negatively modulates plant responses to abscisic acid and dehydration stress. Plant Physiol Biochem **67**: 209–216

Shi Y, Wang Z, Meng P, Tian S, Zhang X, Yang S (2013b) The glutamate carboxypeptidase AMP1 mediates abscisic acid and abiotic stress responses in Arabidopsis. New Phytol **199**: 135–150

Skoog F, Miller C (1957) Chemical regulation of growth and organ formation in plant tissues cultured in vitro. Symposia of the Society for Experimental Biology **11**: 118–130

Smith ZR, Long JA (2010) Control of Arabidopsis apical-basal embryo polarity by antagonistic transcription factors. Nature **464**: 423–426

Soyars CL, James SR, Nimchuk ZL (2016) Ready, aim, shoot: stem cell regulation of the shoot apical meristem. Current Opinion in Plant Biology **29**: 163–168

Sugimoto K, Jiao Y, Meyerowitz EM (2010) Arabidopsis regeneration from multiple tissues occurs via a root development pathway. Developmental Cell **18**: 463–471

Suzaki T, Kim CS, Takeda N, Szczyglowski K, Kawaguchi M (2013) TRICOT encodes an AMP1-related carboxypeptidase that regulates root nodule development and shoot apical meristem maintenance in Lotus japonicus. Development **140**: 353–361

Suzuki M, Latshaw S, Sato Y, Settles AM, Koch KE, Hannah LC, Kojima M, Sakakibara H, McCarty DR (2008) The Maize Viviparous8 locus, encoding a putative ALTERED MERISTEM PROGRAM1-like peptidase, regulates abscisic acid accumulation and coordinates embryo and endosperm development. Plant Physiol **146**: 1193–1206

Takada S, Takada N, Yoshida A (2013) ATML1 promotes epidermal cell differentiation in Arabidopsis shoots. Development **140**: 1919–1923

Takeda S, Tadele Z, Hofmann I, Probst AV, Angelis KJ, Kaya H, Araki T, Mengiste T, Mittelsten Scheid O, Shibahara K-I, et al (2004) BRU1, a novel link between responses to DNA damage and epigenetic gene silencing in Arabidopsis. Genes Dev **18**: 782–793

The Arabidopsis Genome Initiative (2000) Analysis of the genome sequence of the flowering plant Arabidopsis thaliana. Nature **408**: 796–815

To JPC, Haberer G, Ferreira FJ, Deruère J, Mason MG, Schaller GE, Alonso JM, Ecker JR, Kieber JJ (2004) Type-A Arabidopsis response regulators are partially redundant negative regulators of cytokinin signaling. Plant Cell **16**: 658–671

Vernon DM, Hannon MJ, Le M, Forsthoefel NR (2001) An expanded role for the TWN1 gene in embryogenesis: defects in cotyledon pattern and morphology in the twn1 mutant of Arabidopsis (Brassicaceae). Am J Bot **88**: 570–582

Vidaurre DP, Ploense S, Krogan NT, Berleth T (2007) AMP1 and MP antagonistically regulate embryo and meristem development in Arabidopsis. Development **134**: 2561–2567

Wang J-W, Schwab R, Czech B, Mica E, Weigel D (2008) Dual effects of miR156-targeted SPL genes and CYP78A5/KLUH on plastochron length and organ size in Arabidopsis thaliana. Plant Cell **20**: 1231–1243

Wenkel S, Emery J, Hou B-H, Evans MMS, Barton MK (2007) A feedback regulatory module formed by LITTLE ZIPPER and HD-ZIP III genes. Plant Cell **19**: 3379–3390

Williams L (2005) Regulation of Arabidopsis shoot apical meristem and lateral organ formation by microRNA miR166g and its AtHD-ZIP target genes. Development **132**: 3657–3668

Willmann MR, Mehalick AJ, Packer RL, Jenik PD (2011) MicroRNAs regulate the timing of embryo maturation in Arabidopsis. Plant Physiol **155**: 1871–1884

Xu L, Xu Y, Dong A, Sun Y, Pi L, Xu Y, Huang H (2003) Novel as1 and as2 defects in leaf adaxial-abaxial polarity reveal the requirement for ASYMMETRIC LEAVES1 and 2 and ERECTA functions in specifying leaf adaxial identity. Development **130**: 4097–4107

Yadav RK, Perales M, Gruel J, Girke T, Jönsson H, Reddy GV (2011) WUSCHEL protein movement mediates stem cell homeostasis in the Arabidopsis shoot apex. Genes Dev **25**: 2025–2030

Yadav RK, Perales M, Gruel J, Ohno C, Heisler M, Girke T, Jönsson H, Reddy GV (2013) Plant stem cell maintenance involves direct transcriptional repression of differentiation program. Mol Syst Biol **9**: 1–13

Yanai O, Shani E, Dolezal K, Tarkowski P, Sablowski R, Sandberg G, Samach A, Ori N (2005) Arabidopsis KNOXI Proteins Activate Cytokinin Biosynthesis. Current Biology **15**: 1566–1571

Yao Y, Dong C-H, Yi Y, Li X, Zhang X, Liu J (2014) Regulatory function of AMP1 in ABA biosynthesis and drought resistance in arabidopsis. J Plant Biol **57**: 117–126

Zhang T-Q, Lian H, Zhou C-M, Xu L, Jiao Y, Wang J-W (2017) A Two-Step Model for de novo Activation of WUSCHEL during Plant Shoot Regeneration. Plant Cell. doi: 10.1105/tpc.16.00863

Zhou Y, Liu X, Engstrom EM, Nimchuk ZL, Pruneda-Paz JL, Tarr PT, Yan A, Kay SA, Meyerowitz EM (2015) Control of plant stem cell function by conserved interacting transcriptional regulators. Nature **517**: 377–380

Zhu H, Hu F, Wang R, Zhou X, Sze S-H, Liou LW, Barefoot A, Dickman M, Zhang X (2011) Arabidopsis Argonaute10 Specifically Sequesters miR166/165 to Regulate Shoot Apical Meristem Development. Cell **145**: 242–256

Acknowledgements

Firstly, I would like to express my sincerest gratitude to my mentor Dr. Tobias Sieberer, for giving me the opportunity to work in his lab, for his encouraging advices and inspiring criticisms. His patient guidance during my PhD study opened a gate for me to continue my career as a researcher in molecular plant biology.

Equally important for me, I would like to thank my supervisor Prof. Dr. Brigitte Poppenberger for the helpful scientific discussion and valuable suggestions in my research topic.

I am greatly obliged to Prof. Dr. Kay Schneitz for chairing the examination committee and Prof. Dr. Ramón Angel Torres Ruiz for being the examiner in my examination committee.

I am deeply grateful for the help of all my colleagues in the lab, especially Olena Poretska, for her enthusiastic advices during the early times in my PhD study.

I would like to thank Irene Ziegler and other technical staff in my lab for always kindly providing technical support and Christina Duffner, for helping with my administration matters.

Many thanks to China Scholarship Council for providing financial support during my study and TUM graduate school for supporting me in the international exchanges.

My deepest thanks belong to my dearest grandma, my beloved parents, my soul mate Tingting Chen and all my family members, their unconditioned love is always the warmest harbor for me.

Saiqi